Development and Application of a Hydrological Cycle Model as Part of the GREB Climate Model

Christian Stassen

Supervisor: Dr Dietmar Dommenget
Co-supervisor: Prof Michael Reeder

A thesis submitted for the degree of
Doctor of Philosophy
at Monash University in February 2020

School of Earth, Atmosphere and Environment
Faculty of Science
Melbourne, Australia

Copyright

Abstract

The hydrological cycle is one of the most important features of the Earth's climate system and influences the climate in many ways. In order to understand how the climate may change into the future, a thorough understanding of the hydrological cycle is required. Yet, it remains one of the least understood natural cycles. Most of our understanding of changes of the global hydrological cycle with climate change are based on coupled general circulation models (CGCMs). CGCMs evaluated by the Intergovernmental Panel on Climate Change (IPCC) for the fifth assessment report are among the most complex simulations of the climate system. However, it is far from trivial to understand even simple aspects of the climate system using CGCMs, as several processes interact with each other. The present thesis introduces a simple hydrological cycle model for the Globally Resolved Energy Balance (GREB) model, investigates the performance and shows applications of the new hydrological cycle model.

Starting from a rudimentary hydrological cycle model included in the GREB model, three new models are developed: precipitation, evaporation and horizontal transport of water vapour. Precipitation is modelled based on the actual simulated specific and relative humidity in GREB and the prescribed boundary condition of vertical velocity. The evaporation bulk formula is slightly refined by considering differences in the sensitivity to winds between land and oceans, and by improving the estimates of the wind magnitudes. Horizontal transport of water vapour is improved by approximating moisture convergence by vertical velocity. The hydrological cycle model is fitted against observations and reanalysis data sets. The new hydrological cycle model is evaluated against the Coupled Model Intercomparison Project phase 5 (CMIP5) model simulations, reduction in correction terms and by three different sensitivity experiments (annual cycle, El

Nino-Southern Oscillation and climate change). It is shown that the skill of the hydrological cycle model in the GREB model is now within the range of more complex CMIP5 CGCMs and capable of simulating key features of the climate system within the range of uncertainty of CMIP5 model simulations.

The new GREB model is applied to achieve a more conceptual understanding of the projected changes of precipitation, which is difficult if only based on CGCMs. CMIP5 simulations suggest a fairly complex pattern of global precipitation changes, with regions of reduced and enhanced precipitation. A simple deconstruction of the CMIP5 ensemble mean projections is described. In a series of sensitivity experiments the GREB model is forced with four different CMIP5 ensemble mean changes in: surface temperature, evaporation and the vertical atmospheric velocities mean and its standard deviation. The resulting response in the precipitation of the GREB model is very close to the CMIP5 ensemble mean response, suggesting that the precipitation changes can be well represented by a linear combination of these four forcings. The results further provide good insights into the drivers of precipitation change. The GREB model suggests that not one forcing alone can be seen as the main driver, but only the combination of all four changes results in the complex response pattern. However, the dominant forcings are the changes in the large-scale circulation, rather than the pure thermodynamic warming effect. Here, it is interesting to note that changes in high-frequency atmospheric variability of vertical air motion (weather), that are partly independent of the changes in the mean circulation, have a control on the pattern of the time-mean global precipitation changes.

The simple deconstruction approach developed provides a powerful basis on which the hydrological cycles of CGCM simulations can be analysed and was applied to get a more quantitative understanding of precipitation biases in CMIP5 models. To achieve this, the GREB precipitation equation is fitted to observations and CMIP5 model data output using the least-squares method. The fitting parameters for the CMIP5 models are compared against the observed precipitation parameter set. The values of the fitting constants are used as an indication of how CMIP5 model precipitation reacts to changes in the boundary conditions. The results of the fitting indicate that CMIP5 models are overly sensitive to the vertical mean velocity, which is confirmed by other studies but show too little sensitivity to atmospheric variability of vertical air motion (weather).

Although precipitation in CMIP5 models reacts too sensitive to the mean circulation the conceptual deconstruction highlights the importance of moisture transports to the total precipitation bias independent of the mean vertical velocity.

In the last chapter the precipitation trend reversal for the southern hemisphere is discussed. The chapter is mainly based on analysis by Sniderman et al. (2019) who found that the initial drying in the southern hemisphere subtropics might be a transient rather than equilibrium response to a warmer climate. The outcome of all previous chapters: the new hydrological cycle model, the conceptual deconstruction analysis, and the uncertainties in CMIP5 tuned parameters are applied and it is found that the GREB model with observed precipitation parameter set is unable to reproduce the precipitation trend reversal. Instead the GREB model shows a strong drying in the southern hemisphere subtropics driven mostly by a strong decrease in atmospheric vertical velocity circulation. Only an increase in evaporation and a decrease of vertical mean velocity are leading to an increase in precipitation but are not strong enough to offset the drying precipitation trend. However, these findings are changing when the precipitation parameter uncertainties are considered. CMIP5 models are overly sensitive to mean vertical velocity and less sensitive to the circulation variability which leads to reduce the importance of the strong negative trend of vertical velocity variability and makes the wettening through the mean circulation more pronounced. Using the CMIP5 fitted precipitation parameter set precipitation in GREB is plateauing in the twenty-third century. The results highlight the importance of considering the model precipitation parameter biases.

Publications during enrolment

Stassen, C., Dommenget, D., and Loveday, N.: A hydrological cycle model for the Glob- ally Resolved Energy Balance (GREB) model v1.0, Geoscientific Model Development, 12, 425–440, 2019.

Stassen, C., Dommenget, D., and Chadwick, R.: Conceptual Deconstruction of the Simulated Precipitation Response to Climate Change, Climate Dynamics, accepted (pending minor revisions), 2020.

Dommenget, D., Nice, K., Bayr, T., Kasang, D., **Stassen, C.**, & Rezny, M.: The Monash Simple Climate Model experiments (MSCM-DB v1. 0): an interactive database of mean climate, climate change, and scenario simulations. Geoscientific Model Development, 12, 2155-2179, 2019.

Declaration

This thesis contains no material which has been accepted for the award of any other degree or diploma at any university or equivalent institution and, to the best of my knowledge and belief, this thesis contains no material previously published or written by another person, except where due reference is made in the text of the thesis. This thesis includes two original articles, one of which is published in a peer-reviewed journal while the other has been submitted for review to a peer-reviewed journal. The ideas, development and writing up of all the papers in the thesis were the principal responsibility of myself, the candidate, working under the supervision of Dr. Dietmar Dommenget and Prof. Michael Reeder. The published and submitted works constitute the majority of Chapters 2 and 3, with minor modifications to the introductions, figure and section numbers, and discussion sections in order to create continuity in the presentation of this thesis.

Chapter	Publication Title	Status	Nature and extend of candidate's contribution
2	A Hydrological Cycle Model for the Globally Resolved Energy Balance (GREB) model v1.0	Published	Methodology, analysis and writing (80%)
3	Conceptual Deconstruction of the Simulated Precipitation Response to Climate Change	Accepted (minor revisions received)	Methodology, analysis and writing (80%)

The undersigned hereby certify that the above declaration correctly reflects the nature and extent of the student and co-authors contributions to this work.

_____

Candidate: Christian Stassen

Date: 12/02/2020

_____

Supervisor: Dr. Dietmar Dommenget

Date: 12/02/2020

Acknowledgements

Without the support of many people I could not have taken on this PhD project, let alone finished it. Firstly, I must thank Dr. Dietmar Dommenget. It was Dietmar's ideas that let to the simple climate model GREB and Dietmar's idea that led to this project. Dietmar's curious personality for the climate system is infectious and I appreciate the time and effort he put in to mentor me during this project. Prof. Michael Reeder has been a great co-supervisor and always there to give me a hand with professional advice. Dr. Duncan Ackerley, who in my first year has been a great 'unofficial' supervisor always there to assist me with PhD problems.

I am grateful for my colleagues, post-graduate students and researchers who made Monash a great place to study. A special thanks to Mathias Zeller, Sonja Neske and David Hoffmann who started this PhD journey at the same time and made moving to the other side of the planet so much easier. I also want to thank you for all the games of Curve Fever that lead to a nice distraction in the sometimes-busy research life.

I would like to thank all the staff at Monash University, Silvana Katragadda, Christine Hi, Emily Tran, Yuzhou Lin and Robert Oakley, Sook Chor and Ada Han who supported me with all the admin work that a PhD brings along.

A big thank you to my family, Mama, Papa, Laura, Oma, Xara and my friends in Germany, Etienne, Becky, Julius, Geli, Patrick and Isa.

And last but not least I want to thank my partner Sarah, who supported me throughout my PhD, especially in the last few weeks when I was busy bringing this project to an end.

Contents

List of Figures

List of Tables

Chapter 1

Introduction

1.1 The Hydrological Cycle and Climate Change

The hydrological cycle is one of the most important features of the Earth's climate system and influences the climate in many ways. Forced mainly by the heating of the sun water is evaporated over ocean and land, transported in the atmosphere by winds and falls out as precipitation over oceans and land. Precipitation over land might be stored in form of snow, soil moisture or glaciers. Most precipitation falls over oceans directly closing the water cycle, while excess rain over land forms rivers which ultimately return water to the ocean (Trenberth et al., 2007). The global cycle of water (solid, liquid and gaseous) is illustrated in Fig. 1.1.

The hydrological cycle is important beyond the pure exchange of moisture and plays an important role in the exchange of heat between the Earth's surface and atmosphere which in turn modifies the dynamics and thermodynamics of the climate system. For example, evapotranspiration cools the Earth's surface and increases moisture content of the atmosphere. Water vapour in the atmosphere acts as a greenhouse gas, clouds alter the radiation budget and the latent heat released by condensation affects atmospheric dynamics (Chahine, 1992). It is therefore evident that looking at the energy budget of the climate system means looking at the hydrological cycle.

Accordingly, in order to understand how the climate may change into the future, a
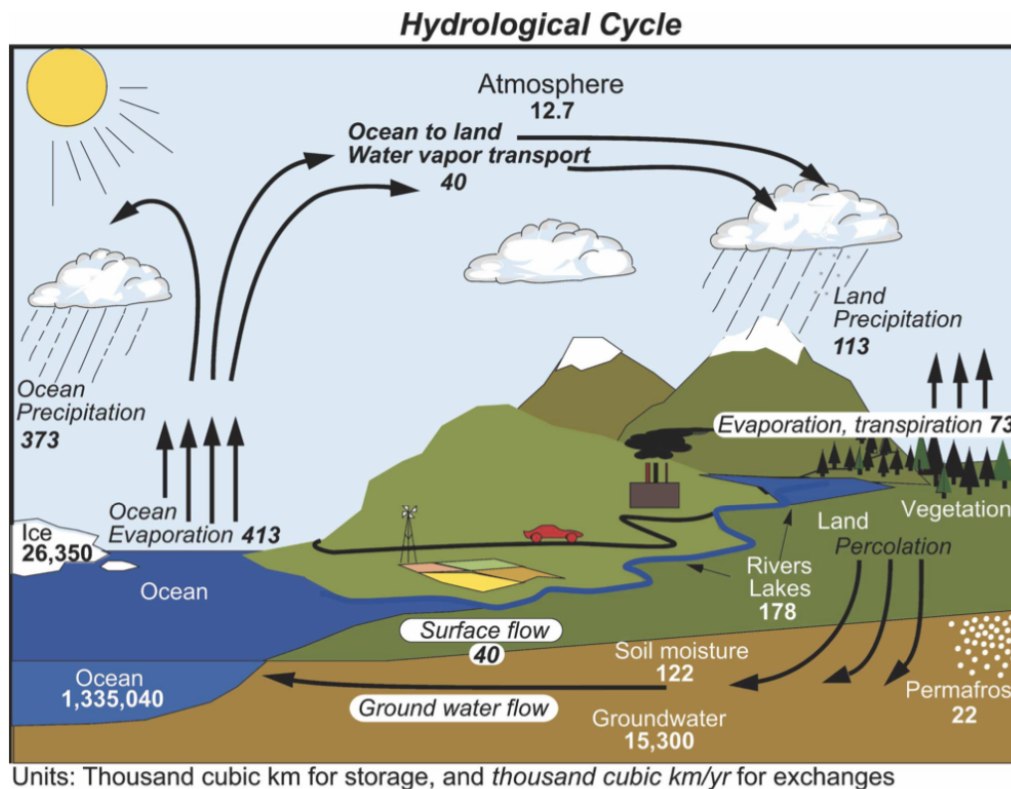
Figure 1.1: *The hydrological cycle. Estimates of the main water reservoirs, given in plain font in $10^3 km^3$, and the flow of moisture through the system, given in slant font ($10^3 km^3 yr^1$), equivalent to Eg ($10^{18}g$) yr^1. Taken from ([Trenberth et al., 2007](#)).*

thorough understanding of the hydrological cycle is required ([Roderick et al., 2014](#)). One topic that deserves urgent and systematic attention is the response of the hydrological cycle (specifically precipitation) to climate change ([Donat et al., 2016](#)). The response in precipitation predicted by global climate models is not uniform. The equatorial Pacific and the high-latitudes are likely to receive an increase in annual mean precipitation, while many subtropical dry regions are likely to see even less precipitation with climate change (Fig. [1.2](#)). While, for the projection of surface temperature changes most models agree on the sign and global pattern, this is not the case for projections of precipitation changes. Currently, two main hypotheses exist concerning how precipitation is predicted to change. One is known as the 'wet get wetter' hypothesis which is the intensification of the hydrological cycle (see [Chou and Neelin, 2004](#); [Held and Soden, 2006](#); [Chou et al., 2009](#)). The other is the 'warmer get wetter' hypothesis caused by deviations of sea surface temperature and thus influencing tropical cyclones ([Ma et al., 2012](#)). Precipitation projections are one of the most important considerations under climate change as any change in rainfall may have a major impact on human health, agriculture,
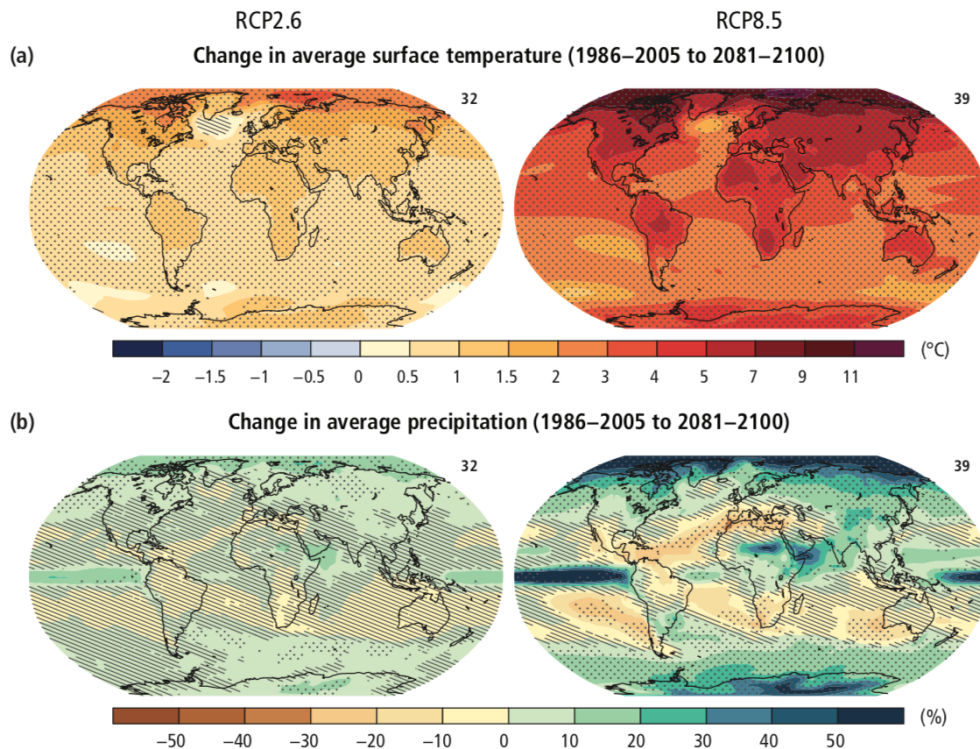
Figure 1.2: *Change in average surface temperature (a) and change in average precipitation (b) based on multi-model mean projections for 2081–2100 relative to 1986–2005 under the RCP2.6 (left) and RCP8.5 (right) scenarios. The number of models used to calculate the multi-model mean is indicated in the upper right corner of each panel. Stippling (i.e., dots) shows regions where the projected change is large compared to natural internal variability and where at least 90% of models agree on the sign of change. Hatching (i.e., diagonal lines) shows regions where the projected change is less than one standard deviation of the natural internal variability. Taken from (Pachauri et al., 2014).*

economics, ecosystems, water resources and tourism (Parry et al., 2004; Patz et al., 2005; Dai, 2011).

Despite its importance, there is little consensus on the observed or expected changes in spatial patterns of precipitation due to climate change (Donat et al., 2016). Climate models simulate an increase in global mean precipitation of 1-3% per degree of warming whereas the total amount of water vapour increases at a rate of 7% per degree of warming, consistent with the Clausius-Clapeyron relation. This increase (7% per degree of warming) in water vapour under a global warming scenario is consistently found in climate models and observations (Roderick et al., 2014). The slower increase in global mean precipitation is dictated by energy constraints rather than moisture availability (Allen and Ingram, 2002; Kramer and Soden, 2016). That is, as water vapour increases, the atmosphere becomes less effective in radiating away heat generated by condensation to support an increase of precipitation by 7%.

Nevertheless, some observational studies contradict this muted response in precipitation and suggest that water vapour and precipitation have increased at about the same rate (7% per degree of warming) over the past two decades (Wentz et al., 2007). However, given the large inter annual variability of precipitation Lambert et al. (2008) showed that at any given 20 year observation period an increase of more than 1-3% per degree of warming of global mean precipitation can be found and the slow increase of global precipitation can only be seen on a century long time series. Newer studies also suggest that the wet-get-wetter and warm get warmer paradigm do not fully explain changes in precipitation (He and Soden, 2016). While wet-get-wetter is a good first order explanation it fails to explain the response over some land regions (He and Soden, 2016; Byrne and O'Gorman, 2015).

Projections of climate change are primarily based on Coupled General Circulation Models (CGCMs). CGCMs evaluated by the Intergovernmental Panel on Climate Change (IPCC) for the fifth assessment report (AR5), provide the best possible and most complex simulations of the climate system. However, it is far from trivial to understand even simple aspects of the climate system because several processes interact with each other (e.g. ice-albedo feedback, Curry et al., 1995; Dommenget and Flöter, 2011). Simplified models, for example the Earth system models of intermediate complexity (Petoukhov et al., 2005) or the Globally Resolved Energy Balance (GREB) model (Dommenget and Flöter, 2011) are capable of simulating the large-scale features of the climate system and climate change in temperature and rainfall (e.g. arctic winter amplification; see Dommenget and Flöter, 2011). They provide a framework to conceptually understand the hydrological response to climate change and help to develop hypotheses about the processes involved. However, these models are simplified tools compared to more complex CGCMs and all results must be evaluated against observations and/or more complex and realistic CGCMs (Dommenget and Flöter, 2011).

Nonetheless, there is an increasing interest in a more conceptual understanding how the rainfall distribution and pattern are changing with climate change. Rainfall is generated by a multitude of different systems (e.g. midlatitude cyclones, tropical convection), which makes it one of the most complex processes in the climate system to model and thus to forecast. Yet many aspects of the changes seen in complex CGCMs can be found in idealized models such as the omega and humidity based model by Pendergrass and

Gerber (2016) or the simple enhanced advection model by Chadwick et al. (2016).

Although the agreement of large scale precipitation projections has improved from the 4th Assessment Report (AR4) to the fifth assessment report (AR5) (Collins et al., 2013) and climate models agree more over land (Knutti and Sedláček, 2013) substantial regional differences still remain (Fig. 1.2) (Collins et al., 2013) in climate change simulations for precipitation. Over large areas, especially in the tropics, climate models do not even agree on the sign of precipitation change. This does not come by surprise considering the large differences in existing observational and re-analysis data sets (Fig. 1.3) which are used to improve climate models.
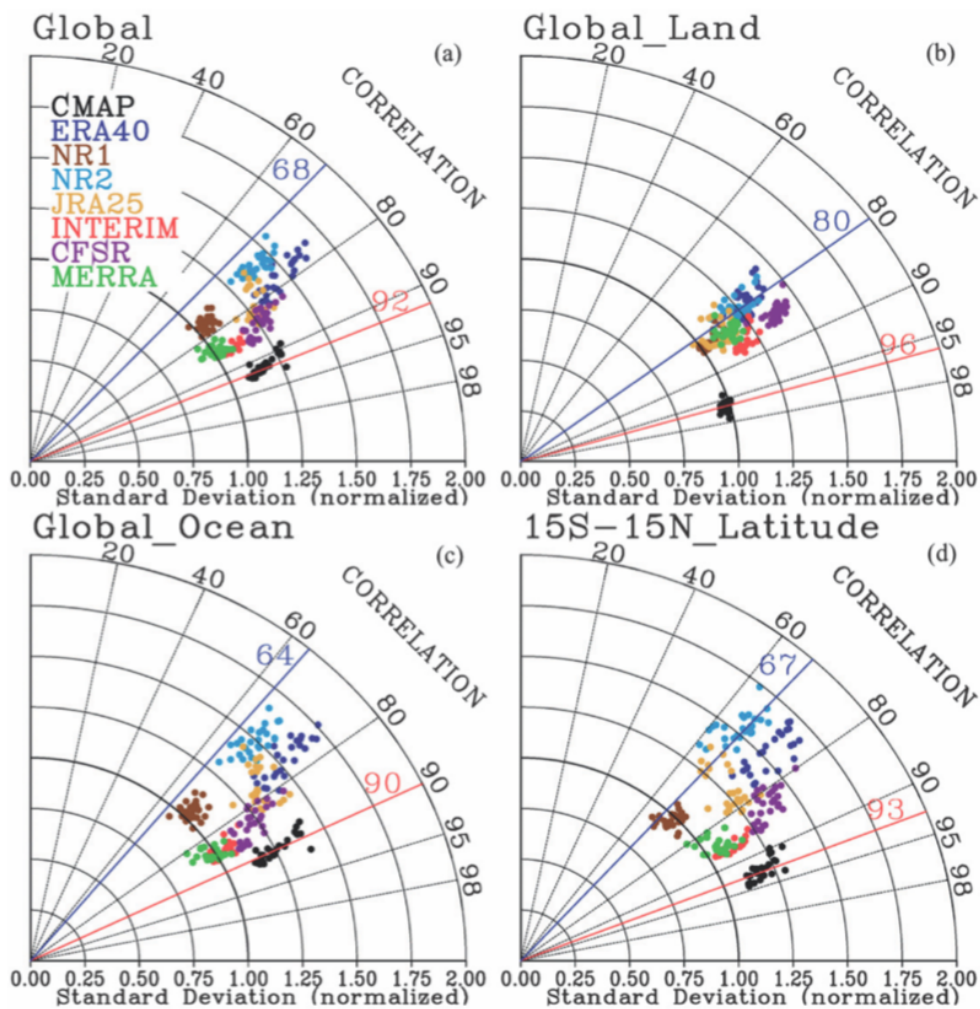
Figure 1.3: *Taylor diagrams of annual mean precipitation from reanalyses using GPCP as a reference and CMAP as an additional observing reference the regional statistics for the (a) globe, (b) land, (c) ocean, and (d) tropics. The red and blue lines show limits of expected high and low correlation as determined by comparing GPCP and CMAP observations. Taken from (Bosilovich et al., 2011).*

As pointed out by Marotzke et al. (2017) the global water cycle with all its sub

processes (evaporation, rainfall, etc.) remains one of the least understood natural cycles. This leads to uncertainty in predicting changes in the hydrological cycle associated with climate change. To reduce these uncertainties, we must build the best models we can. Both a substantial increase in climate model resolution (Marotzke et al., 2017) and also a more conceptual understanding of the hydrological cycle, are needed to identify where uncertainties lie.

1.2   The Globally Resolved Energy Balance model

The aim of the Globally Resolved Energy Balance (GREB) model is to provide the simplest possible representation of the climate system, that can still simulate the main features of the regional and seasonal evolution of surface temperature. The GREB model allows to: reduce the complexity of the climate system, a stepwise deconstruction of the climate change surface temperature response, to avoid mean state climate biases and to gain a conceptual understanding of the climate system. It was first developed by Dommenget and Flöter (2011).

     The GREB model is a three layer (land and ocean surface, atmosphere and deep ocean) global climate model on a $3.75^o \times 3.75^o$ horizontal latitude-longitude grid. The GREB model simulates the thermal (long-wave) and solar (short-wave) radiation, heat transport in the atmosphere by isotropic diffusion and advection with the mean winds, the hydrological cycle (evaporation, precipitation and water vapour transport), a simple ice/snow albedo feedback and heat uptake in the sub-surface ocean. The process simulated within the GREB model are illustrated in Fig. 1.4. Each process is represented through strongly simplified equations. The main prognostic variable in GREB is surface temperature which follows the tendency equation:

$$\gamma \frac{dT_{surf}}{dt} = F_{solar} + F_{thermal} + F_{latent} + F_{sense} + F_{ocean} + F_{correct} \tag{1.1}$$

with the heat capacity γ. The temperature is forced by solar radiation, F_{solar}, the net thermal radiation, $F_{thermal}$, the latent heat taken up through evaporation of water, F_{latent}, sensible heat exchange between the surface and the atmosphere, F_{sense} and heat exchange with the subsurface ocean, F_{ocean}. The last term, $F_{correct}$, is an artificial correction term of the tendency equation of surface temperature. The correction term

corrects the GREB model to have a climatological surface temperature as observed.
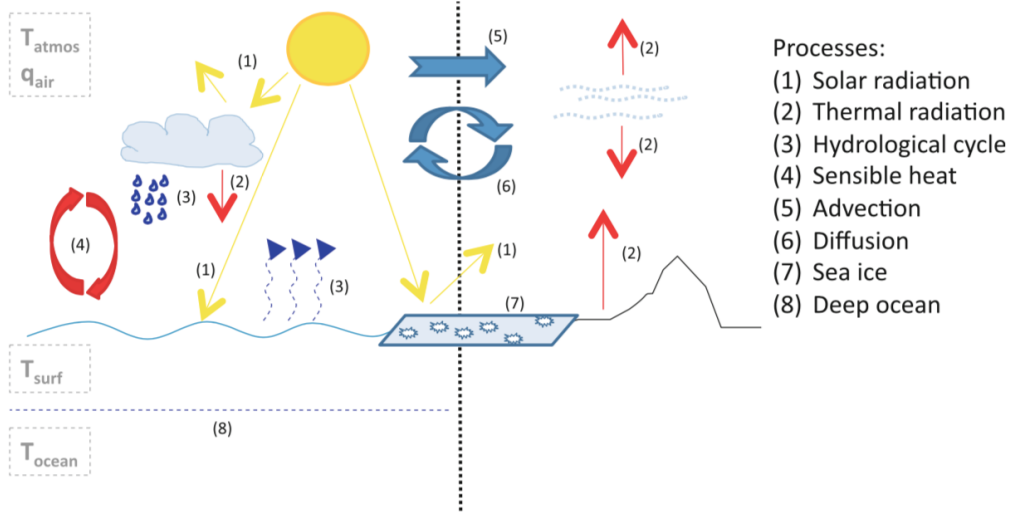
Figure 1.4: *A sketch of the physical processes considered in the GREB model. Taken from (Dommenget and Flöter, 2011).*

Radiation

The daily cycle of incoming solar radiation is not resolved, instead the 24 hours mean incoming solar radiation at the surface is used:

$$F_{solar} = (1 - \alpha_{clouds}) \cdot (1 - \alpha_{surf}) \cdot S_0 \cdot r(\lambda, t_{Julian}) \tag{1.2}$$

with the 24 h mean top of the atmosphere solar constant, S_0, as function of latitude, λ, and Julian day of year, t_{Julian}. Not all top of the atmosphere solar radiation reaches the surface. Some is reflected by clouds, α_{clouds}, some is reflected by the surface, α_{surf}. The cloud albedo, α_{clouds} is a given seasonally varying boundary condition (Fig. 1.6) and the surface albedo, α_{surf} is a linear function of the surface temperature near the freezing point to simulate snow and ice cover and constant otherwise (Fig. 1.5).

The GREB model calculates thermal radiation using the black body emission for the surface and the atmosphere. The net thermal radiation is due to outgoing radiation from the surface and incoming radiation from the atmosphere.

$$F_{thermal} = -\sigma T_{surf}^4 + \epsilon_{atmos} \sigma T_{atmos-rad}^4 \tag{1.3}$$

For the atmosphere the thermal radiation depends on the atmospheric temperature and
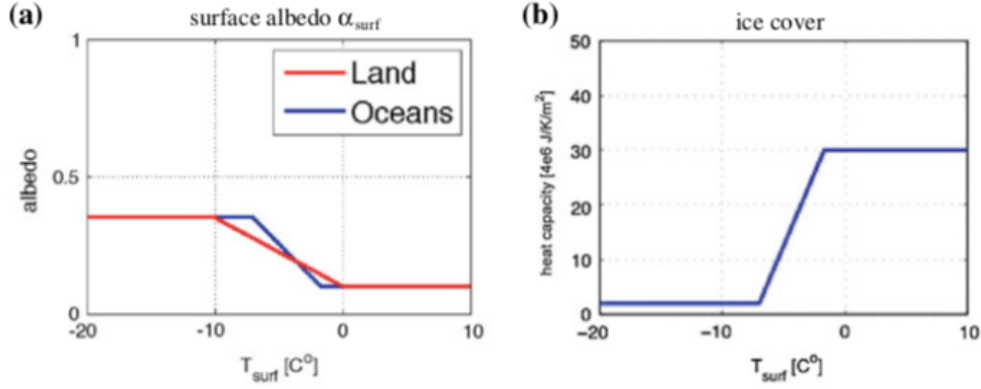
Figure 1.5: *The parameterization of the surface albedo α_{surf} (a). The surface layer heat capacity as function of surface temperature (b). Taken from (Dommenget and Flöter, 2011).*

the concentration of greenhouse gases, CO_2 and water vapour, and the cloud cover. The effective emissivity ϵ_{atmos} is a function of CO_2 concentration, the vertically integrated water vapour amount $viwv_{atmos}$ and the cloud cover. The emissivity follows a log-function to consider a saturation of greenhouse gases and considers three spectral bands (CO_2 and water vapour, only CO_2 and only water vapour absorption). The emissivity without clouds is

$$
\begin{aligned}
\epsilon_0 = {} & pe_4 \cdot log[pe_1 \cdot CO_2^{topo} + pe_2 \cdot viwv_{atmos} + pe_3] \\
& + pe_5 \cdot log[pe_1 \cdot CO_2^{topo} + pe_3] \\
& + pe_6 \cdot log[pe_2 \cdot viwv_{atmos} + pe_3] + pe_7
\end{aligned}
\tag{1.4}
$$

with fitting parameters pe_{1-7}, CO_2 concentration scaled by height, $CO_2^{topo} = e^{\frac{-z_{topo}}{z_{atmos}}}$, the topographic height z_{topo} and atmospheric scaling height $z_{atmos} = 8400$ m. Using the scaling by topographic height mimics a thinner atmosphere that has less CO2.

When the cloud cover, CLD, is considered the following equation is used:

$$
\epsilon_{atmos} = \frac{pe_8 - CLD}{pe_9} \cdot (\epsilon_0 - pe_{10}) + pe_{10}
\tag{1.5}
$$

The cloud cover in GREB is a seasonally varying externally prescribed boundary condition and therefore, is not responding dynamically to changes in the GREB model (Fig. 1.6).

(a) topography [m]

(b) glacier mask

(c) NCEP T$_{surf}$ [°C]

(d) NCEP atmosphshericwater vapor [kg/m^2]

(e) NCEP 850hPa winds [m/s]

(f) ISCCP cloud cover [%]

(g) NCEP soil moisture[%]

(h) WOCE ocean mixed layer depth [m]
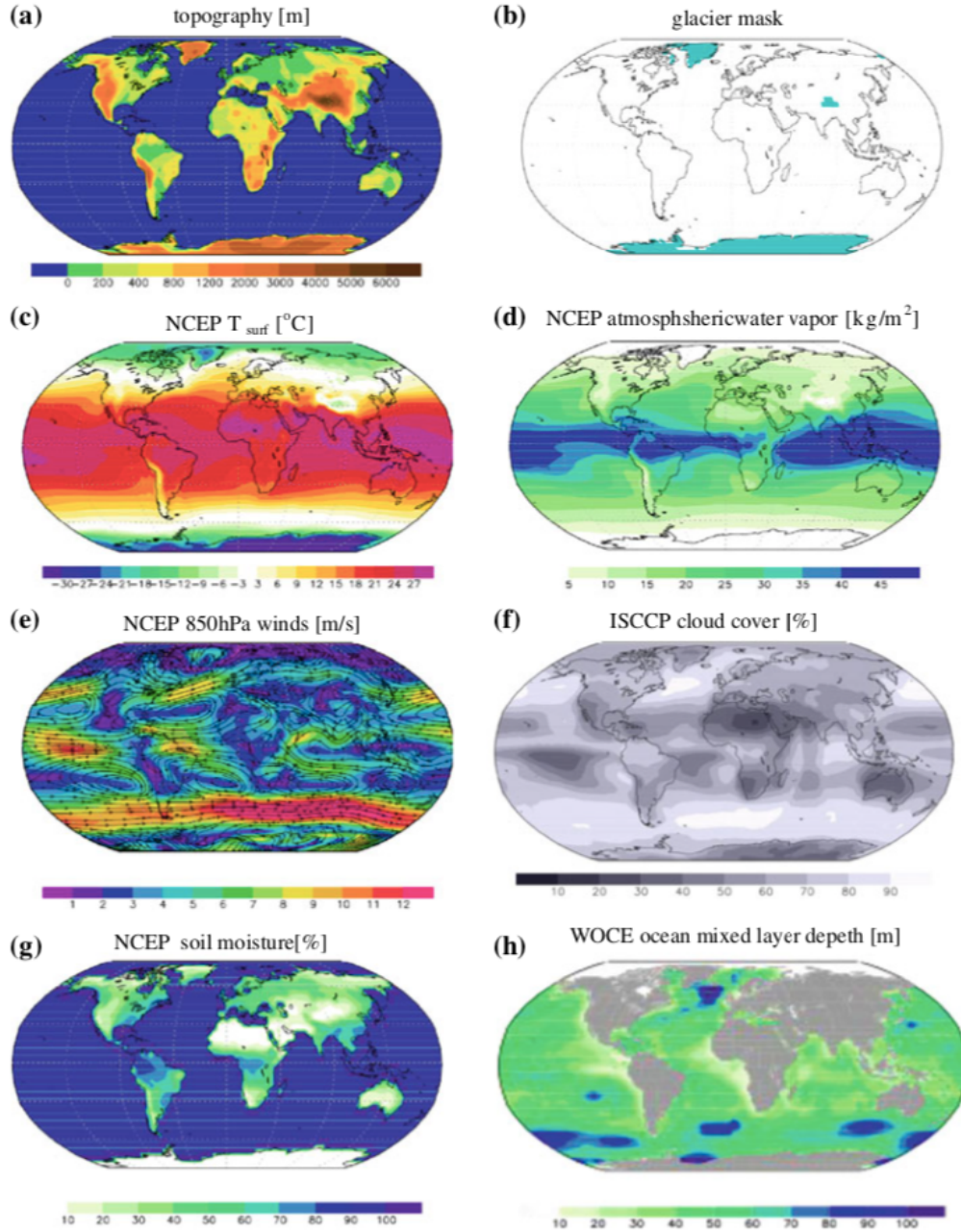
Figure 1.6: *GREB mean state climate boundary conditions: topography (a), glacier mask (b), surface temperature (c), vertically integrated water vapour (d), horizontal winds (e), cloud cover (f), soil moisture (g), and mixing layer depth (h). Taken from (Dommenget and Flöter, 2011).*

Hydrological Cycle

The hydrological cycle in GREB includes the evaporation of water vapour at the surface (land and ocean), Δq_{eva}, the transport of water vapour in the atmosphere through diffusion, $\kappa \cdot \nabla^2 q$ and advection, $\vec{u} \cdot \nabla q$, and precipitation, Δq_{precip}. The latent heat fluxes associated with the hydrological cycle are central to the climate system and therefore also

considered in the GREB model. This leads to the specific humidity tendency equation in the GREB model:

$$\frac{dq}{dt} = \Delta q_{eva} + \Delta q_{precip} + \kappa \cdot \nabla^2 q - \vec{u} \cdot \nabla q + \Delta q_{correct} \tag{1.6}$$

Evaporation is calculated using a Bulk formula approach

$$\Delta q_{eva} = \rho_{air} \cdot c_w \cdot |\vec{u_*}| \cdot \theta_{soil} \cdot (q - q_{sat}) \tag{1.7}$$

and depends on the saturation deficit, $(q - q_{sat})$, the soil moisture, θ_{soil}, the wind speed, $|\vec{u_*}|$, and the constant parameters of density of air, ρ_{air} and a transfer coefficient, c_w. The soil moisture field is a seasonally prescribed boundary condition (Fig. 1.6). The saturation specific humidity in GREB is taken from James (1995)

$$q_{sat} = e^{\frac{-z_{topo}}{z_{atmos}}} \cdot 3.75 \cdot 10^{-3} \cdot e^{17.08085 \frac{T_{surf} - 273.15}{T_{surf} - 38.975}} \tag{1.8}$$

Precipitation in the GREB model follows a simplified life time approached assuming a mean residence of water vapour in the atmosphere of 14 days.

$$\Delta q_{precip} = r_{precip} \cdot q \tag{1.9}$$

with the decorrelation coefficient $r_{precip} = -0.1/24$ h.

Atmospheric circulation

While the input boundary conditions for the GREB model include the typical CGCM constraints, such as, incoming sun light, topography, land-sea mask, CO_2 concentrations etc. other, often dynamical variables in CGCMs, are externally prescribed in the GREB model. The atmospheric circulation in the GREB model is a seasonally varying externally prescribed boundary condition (Fig. 1.6) and does therefore not respond to external forcings. The mean horizontal winds, $\vec{u}$ are taken from the National Centres for Environmental Prediction (NCEP) reanalysis data from 1950 to 2008 (Kalnay et al., 1996). The atmospheric diffusion mimics a typical weather system, which are assumed to be the main source of diffusion, with a lifetime of about one week. This leads to an isotropic diffusion coefficient, $\kappa = 8 \times 10^5 m^2/s$.

Flux corrections and limitations

The tendency equation of surface temperature, deep ocean temperature and specific humidity are flux corrected, $F_{correct}$ and $q_{correct}$, towards reanalysis data. The correction terms force the GREB model to maintain a mean climate state as observed. Thus, the GREB model is conceptually very different from the CGCM simulations in the Coupled Model Inter-comparison Project phase 5 (CMIP5), as atmospheric circulations, cloud cover and changes to soil moisture are not simulated but prescribed as external boundary conditions in the model. This leads to some parts of the hydrological cycle not being simulated in the GREB hydrological cycle model (i.e. runoff). The effect of ocean circulation on the atmosphere is represented only through the sea surface temperature but is not explicitly simulated. Additionally, the GREB model has no internal variability, as atmospheric fluid dynamics (e.g. weather systems) are not explicitly simulated. Subsequently, the model will converge to its equilibrium points (all tendency equations converge to zero), if all boundary conditions are constant. The control climate or response to forcings can therefore be estimated from a single year.

Performance

The purpose of the GREB model is a simple representation of the climate system, that can still simulate the main features of the regional and seasonal evolution of surface temperature. The tendency equations of the model (i.e. tendency equation of specific humidity) are solved with a time step of 12 h. For the atmospheric transport equations, a shorter time step of 0.5 h is used. This is necessary for the model to remain numerically stable. With its three layer (land and ocean surface, atmosphere and deep ocean) $3.75^o \times 3.75^o$ horizontal latitude-longitude grid the GREB model simulates one year in about one second real-time on a standard computer. It therefore provides a quick and easy tool to test conceptual ideas of the climate system and climate change.

1.3 Research Aims

This work looks at the hydrological cycle in general and focuses especially on precipitation. Although large improvements have been made in modelling the hydrological cycle in CGCMs over the recent years, precipitation still inhibits uncertainties in climate

models. This limits our understanding on how the hydrological cycle will respond to a warmer climate and a more conceptual understanding of the hydrological cycle is needed to help address these uncertainties. Therefore, the aims of this research are:

1. Can the large-scale features of the hydrological cycle be simulated on a monthly time scale (evaporation, advection and rainfall) in the simplified model GREB with a skill comparable to CGCMs?

2. How do the climate boundary conditions (temperature, evaporation, mean circulation and circulation variability) for precipitation change with climate change and can we quantify their role in changing precipitation.

3. What processes cause large uncertainties in precipitation in CMIP5 simulations?

1.4 Thesis Outline

The simplicity and fast performance of the GREB model makes it a perfect tool for this study. However, before the GREB model can be used the rudimentary hydrological cycle needs to be improved. In chapter 2 we describe the development of the new hydrological cycle model in GREB to address the first research question. This chapter is based on Stassen et al. (2019). The development and improvement of the three parts of the hydrological cycle model (precipitation, evaporation and water vapour transport) are described and, three different sensitivity experiments are performed to validate and evaluate the new model.

In chapter 3 the new model is applied to gain a deeper understanding of the precipitation response to climate change to answer research question 2. To achieve this the climate change response is separated into four forcings (surface temperature changes, evaporation changes, mean circulation changes and circulation variability changes) and the response of the GREB model to each forcing is evaluated. The method is validated by comparing the super imposed response of the four forcings to the CMIP5 ensemble mean response. This chapter is based on Stassen et al. (2020).

Chapter 4 applies a similar deconstruction used in chapter 3 to investigate the origin of biases in precipitation in CMIP5 models to address research question 3.

In the last chapter, chapter 5, the precipitation reversal is discussed. This is a trend

in the southern hemisphere simulated by climate models where the initial reduction in precipitation is reversed and more rain is falling with climate change in the southern hemisphere subtropics.

Chapter 2

New Hydrological Cycle Model

2.1 Preface

This chapter describes the development of the hydrological cycle model for the Globally Resolved Energy Balance (GREB) model. Starting from a rudimentary hydrological cycle model included in the GREB model, we develop three new models: precipitation, evaporation and horizontal transport of water vapour. Precipitation is modelled based on the actual simulated specific and relative humidity in GREB and the prescribed boundary condition of vertical velocity. The evaporation bulk formula is slightly refined by considering differences in the sensitivity to winds between land and oceans, and by improving the estimates of the wind magnitudes. Horizontal transport of water vapour is improved by approximating moisture convergence by vertical velocity. The new parameterisations are fitted against the Global Precipitation Climatology Project (GPCP) data set and reanalysis data sets (ERA-Interim). The new hydrological cycle model is evaluated against the Coupled Model Intercomparison Project phase 5 (CMIP5) model simulations, reduction in correction terms and by three different sensitivity experiments (annual cycle, El Nino-Southern Oscillation and climate change). The skill of the hydrological cycle model in the GREB model is now within the range of more complex CMIP5 coupled general circulation models and capable of simulating key features of the climate system within the range of uncertainty of CMIP5 model simulations. The results illustrate that the new

GREB model's hydrological cycle is a useful model to study the climate's hydrological response to external forcings and also to study inter-model differences or biases.

2.2   Introduction

The simple Globally Resolved Energy Balance (GREB) model was originally developed to simulate the globally resolved surface temperature and in particular its response to a CO2 forcing (Dommenget and Flöter, 2011). The GREB code computes about one model year per second on a standard personal computer. It therefore is a relatively fast tool, which allows conducting sensitivity studies to external forcing within minutes to hours (Dommenget and Flöter, 2011). The hydrological cycle in the GREB model was only needed as a zero-order estimate to model the latent heat in the energy balance and the atmospheric water vapour levels.

This chapter introduces a simple hydrological cycle model for the GREB model. The aim of this hydrological cycle model is to present a simple and fast model for studies of the large-scale climate in precipitation, its response to climate variability (e.g. El Nino or climate change) and external forcings. We improve three separate parameterisations in the model: precipitation, evaporation and the circulation of water vapour. The model is based on the dynamical variables (surface temperature, atmospheric temperature and humidity) in the GREB model and on the boundary conditions of the GREB model (horizontal and vertical winds).

The following section presents the data sets used, the original GREB model and the methods. In Section 2.4, the new parameterisations of the hydrological cycle model in the GREB model are described. Section 2.5 presents three different sensitivity experiments to test the new hydrological cycle model. Finally, we give a discussion and summary of the results.

2.3   Data and Methods

The original GREB model has been described in chapter 1.2 and here only the new developments are discussed. The observed hydrological cycle in terms of the annual mean and its seasonal cycle (DJF minus JJA) for precipitation, evaporation and moisture circulation are shown in Figures 2.2a and 2.3a. The global pattern of observed precipitation
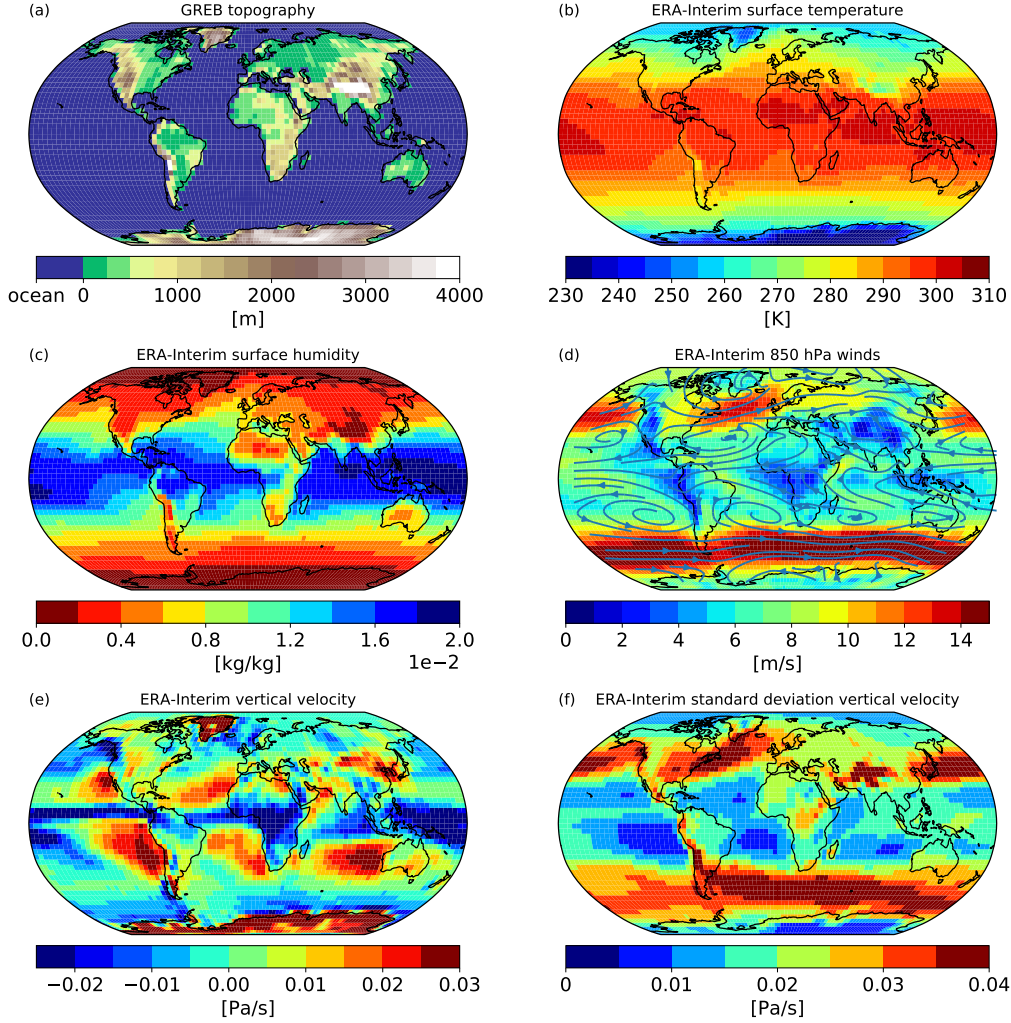
Figure 2.1: *GREB mean state boundary conditions and reference climatologies: topography (a), surface temperature (b), surface humidity (c), 850 hPa wind direction (streamline) and strength (shading) (d), vertical velocity omega (e) and the daily standard deviation of vertical velocity omega (f).*

is marked by the ITCZ, its seasonal cycle and by the storm tracks of the midlatitudes. The evaporation is strongest over subtropical oceans and has a complex seasonal cycle with generally more evaporation in the warm season over land. The horizontal moisture transport (Figures 2.2c and 2.3c) is dominated by large scale convergence and divergence zones over the oceans and their seasonal shift.

Model simulations, pre-industrial (pi-Control) and Representative Concentration Pathway 8.5 (RCP8.5), from the CMIP5 database are used for comparison (Taylor et al., 2012). All data sets are regridded to a horizontal resolution of $3.75^o \times 3.75^o$ to match the GREB model grid. See Table 2.1 for a complete list of models used. The original GREB hydrological cycle model, which is the starting point for this study, is shortly presented below. All variables and parameters are listed and explained in Table 2.2. The
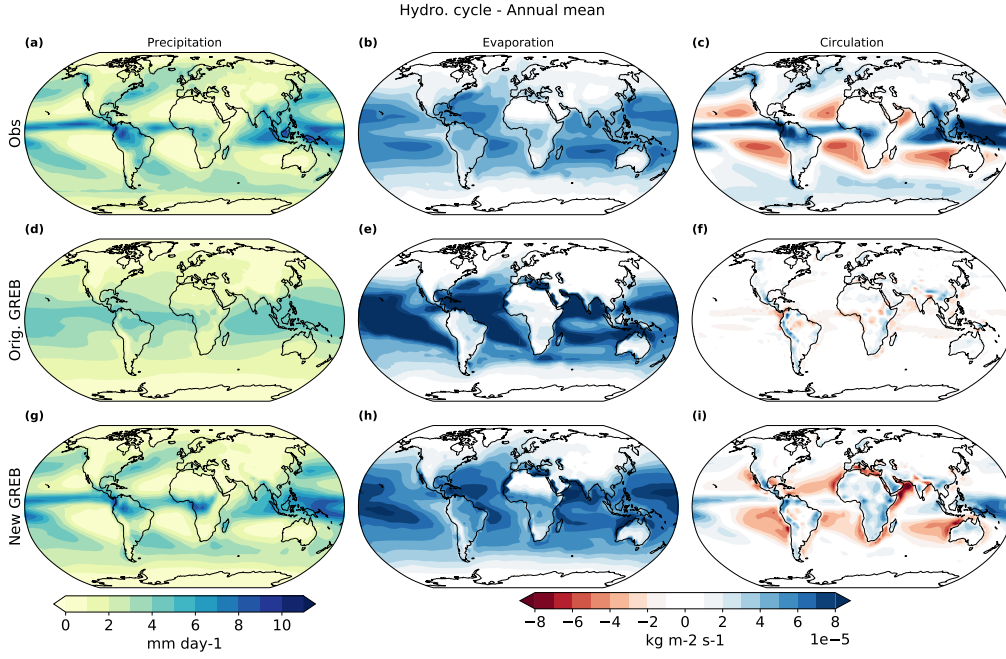
Figure 2.2: *The decomposition of the hydrological cycle into its parts precipitation in mm/day (left column), evaporation (middle column) and circulation in kg/m2/s (right column) in observations (upper row), the original GREB model (middle row) and the new GREB model (lower row) for the annual mean.*
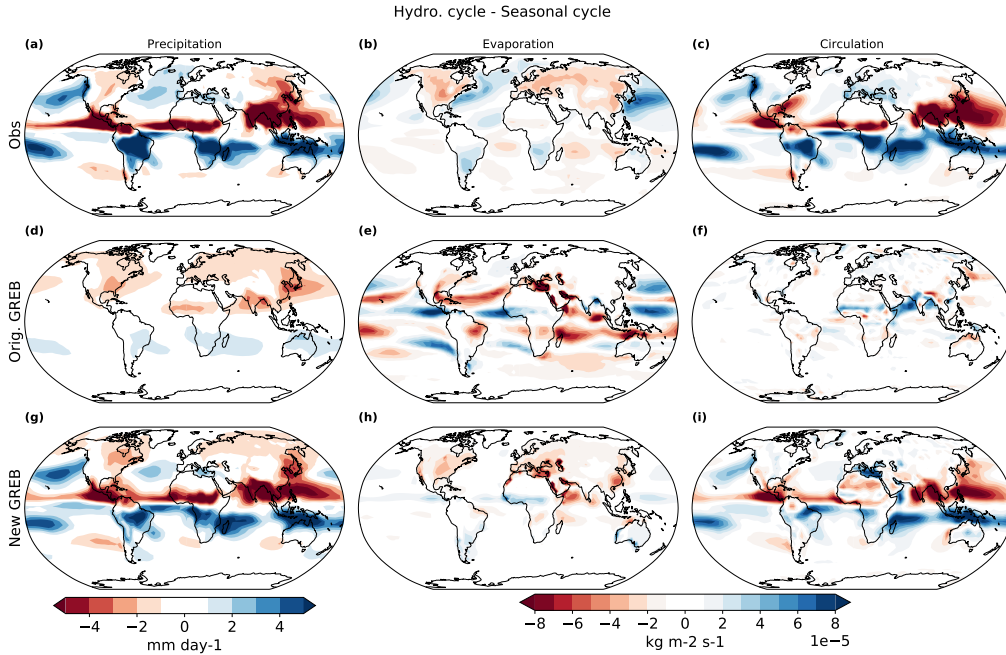
Figure 2.3: *As Fig. 2.2 but for the seasonal cycle (DJF minus JJA). The decomposition of the hydrological cycle into its parts precipitation in mm/day (left column), evaporation (middle column) and circulation in kg/m2/s (right column) in observations (upper row), the original GREB model (middle row) and the new GREB model (lower row) for the seasonal cycle.*

precipitation is proportional to the specific humidity

$$\Delta q_{precip} = r_{precip} \cdot q_{air} \qquad (2.1)$$

with Eq. (2.1), which corresponds to an autoregressive model with a decorrelation (recirculation) time of about 14 days (Dommenget and Flöter, 2011). Evaporation, Δq_{eva}, in the original GREB model is calculated using an extended bulk formula:

$$\Delta q_{eva} = \rho_{air} \cdot c_w \cdot |u_* + c_{turb}| \cdot \theta_{soil} \cdot (q_{air} - q_{sat}) \cdot \frac{1}{r_{qviwv}} \tag{2.2}$$

The bulk formula depends on the saturation deficit $(q_{air} - q_{sat})$, the wind speed u_*, with a turbulent wind factor c_{turb}, the density of air ρ_{air}, the transfer coefficient c_w, and a linear regression factor, r_{qviwv}, which links surface humidity to the vertically integrated water vapour column (Dommenget and Flöter, 2011; Rapti, 2005). The saturation water vapour pressure is calculated after (Dommenget and Flöter, 2011; James, 1995):

$$q_{sat} = e^{\frac{z_{topo}}{z_{atmos}} \cdot 3.75 \cdot 10^{-3}} \cdot e^{17.08085 \cdot \frac{T_{surf} - 273.15}{T_{surf} - 38.975}} \tag{2.3}$$

Together, this leads to the complete tendency equation of specific humidity in GREB

$$\frac{dq_{air}}{dt} = \Delta q_{eva} + \Delta q_{precip} + \kappa \cdot \nabla^2 q_{air} - \vec{u} \cdot \nabla q_{air} + \Delta q_{correct} \tag{2.4}$$

with the diffusion term $\kappa \cdot \nabla^2 q_{air}$, the advection term $\vec{u} \cdot \nabla q_{air}$ and the flux correction term $\Delta q_{correct}$. The simulated annual mean and seasonal cycle for precipitation, evaporation and mean horizontal moisture transport are shown in Figures 2.2 and 2.3 for the original GREB model as discussed above. The diffusion term is only one-fifth of the magnitude of the advection term in hlthe global average (not shown) but is more important in some locations and therefore not ignored in the GREB model. The original GREB model simulated some of the main features of the regional differences in the precipitation and evaporation, but many important details are missing (e.g. ITCZ, subtropical dry regions or extratropical storm tracks). However, horizontal moisture transport is not simulated well by the original GREB model.

Table 2.2: *List of variables used in the GREB model.*

Variable	Dimension	Description
c_{eva}	constant	Evaporation efficiency
$c_{eva-temp}$	constant	Temperature scaling of evaporation

Continued on next page

Table 2.2 – *Continued from previous page*

Variable	Dimension	Description
c_{turb}	constant	Turbulent wind offset for evaporation
c_q	constant	Precipitation parameter for specific humidity
c_{rq}	constant	Precipitation parameter for relative humidity
c_ω	constant	Precipitation parameter for ω
$c_{\omega std}$	constant	Precipitation parameter for standard deviation of ω
f	constant	Convergence scaling parameter
g	constant	Gravitational acceleration
q_{air}	x, y, t	Atmospheric humidity
q_{sat}	x, y, t	Saturation pressure
$q_{sat-skin}$	x, y, t	Saturation pressure with temperature offset
r_{precip}	constant	Mean lifetime of water vapour
r_{qviwv}	constant	Regression between atmospheric humidity and vertically integrated water vapour
rq	x, y, t	Relative humidity
Tsurf	x, y, t	Surface temperature
$|u_*|$	x, y, t	Absolute wind climatology
u	x, y, t	Horizontal wind climatology
z_{atmos}	constant	Scaling height of atmosphere
z_{topo}	constant	Topographic height
z_{vapour}	constant	Scaling height of water vapour
Θ_{soil}	x, y, t	Surface wetness fraction
ρ_{air}	constant	Density of air
ωstd	x, y, t	Standard deviation of vertical wind climatology
q_{eva}	x, y, t	Mass flux for the atmospheric humidity by evaporation
q_{precip}	x, y, t	Mass flux for the atmospheric humidity by precipitation
$q_{correct}$	x, y, t	Mass flux correction of specific humidity
$q_{cor-circul}$	x, y, t	Mass flux correction due to circulation
$q_{cor-evapo}$	x, y, t	Mass flux correction due to evaporation
$q_{cor-precip}$	x, y, t	Mass flux correction due to precipitation

Continued on next page

Table 2.2 – *Continued from previous page*

Variable	Dimension	Description
$q_{precip-GREB}$	x, y, t	Precipitation change in GREB
$q_{precip-OBS}$	x, y, t	Precipitation change in observations
t	constant	Model integration time step
dt_{crcl}	constant	Model integration time step for circulation
κ	constant	Isotropic diffusion coefficient
ω	x, y, t	Vertical velocity in pressure coordinates

The seasonally varying flux correction term, $\Delta q_{correct}$, is calculated as the residual between the tendencies without flux corrections and observed tendencies:

$$\Delta q_{correct} = \left.\frac{dq_{air}}{dt}\right|_{obs} - \Delta q_{eva} + \Delta q_{precip} + \kappa \cdot \nabla^2 q_{air} - \vec{u} \cdot \nabla q_{air} \qquad (2.5)$$

This effectively corrects the GREB model to have a climatological specific humidity as observed. The flux correction term $\Delta q_{correct}$ can help to evaluate the improvements in the hydrological cycle model. The better the model the smaller the correction term should be in Eq. (2.5). We can therefore split the flux correction into three diagnostic terms

$$\Delta q_{correct} = \Delta q_{cor-precip} + \Delta q_{cor-evapo} + \Delta q_{circul} \qquad (2.6)$$

With each term on the right-hand side representing the fraction of the flux corrections attributed to precipitation, evaporation and circulation biases, respectively. Each term is estimated as the difference between the observed and the GREB model tendencies of the humidity resulting from precipitation, evaporation and circulation biases:

$$\Delta q_{cor-precip} = \Delta q_{precip-OBS} - \Delta q_{precip-GREB} \qquad (2.7)$$

$$\Delta q_{cor-evapo} = \Delta q_{evapo-OBS} - \Delta q_{evapo-GREB} \qquad (2.8)$$

$$\Delta q_{cor-circul} = \Delta q_{circul-OBS} - \Delta q_{circul-GREB} \qquad (2.9)$$

with the GREB model tendencies of the humidity resulting from circulation, $\Delta q_{circul-GREB}$,

Table 2.1: *List of CMIP5 models used for developing the hydrological cycle model.*

Models		
ACCESS1-0	ACCESS1-3	bcc-csm1-1
bcc-csm1-1-m	BNU-ESM	CCSM4
CESM1-BGC	CESM1-CAM5	CESM1-FASTCHEM
CESM1-WACCM	CMCC-CM	CMCC-CM5
CSIRO-Mk3-6-0	CanESM2	EC-EARTH
FGOALS-g2	FGOALS-s2	FIO-ESM
GFDL-CM3	GFDL-ESM2G	GFDL-ESM2M
GISS-E2-H-CC	GISS-E2-H-R	HadGEM2-CC
HadGEM2-ES	inmcm4	MIROC-ESM-CHEM
MIROC-ESM	MIROC4h	MIROC5
MPI-ESM-LR	MPI-ESM-MR	MPI-ESM-P
MRI-CGCM3	NorESM1-M	NorESM1-ME

defined as:

$$\Delta q_{circul-GREB} = \kappa \cdot \nabla^2 q_{air} - \vec{u} \cdot \nabla q_{air} \qquad (2.10)$$

The observed humidity tendencies resulting from circulation, $\Delta q_{circul-GREB}$, are defined by the residual of the total humidity tendency minus the precipitation and evaporation tendencies. By construction, all three flux correction terms (evaporation, precipitation and circulation) sum up to the total flux correction term.

2.4   Hydrological Cycle Model Development

The development of the new hydrological cycle model of the GREB model is based on the existing zero-order hydrological cycle model of the GREB model. The following section outlines the development of each of the three models and discusses how the change in the reference climatologies from NCEP to ERA-interim has affected the model. All variables are summarised in Tab. 2.2.

2.4.1   Precipitation

The original GREB precipitation model captures some large-scale aspects of the mean and seasonal cycle of observed precipitation, such as more precipitation in the tropics and during warm seasons over land (Figures 2.2 and 2.3). It has however, substantial differences from the observed precipitation, as it cannot capture the high rainfall in the

ITCZ, the enhanced precipitation over the midlatitudes storm track regions and misses many aspects of the seasonal cycle. The root mean square error for the annual mean of the original GREB model precipitation parameterisation is $1.46 \ \mathrm{mm \ day}^{-1}$.

The new parameterisation of precipitation in the GREB model is assumed to be proportional to q_{air}, as in the original GREB model. We further assume that relative humidity, rq, and upward air motion, ω, increase rainfall. The latter is assumed to be a function of the mean and the standard deviation of the daily mean variation, ω_{mean} and ω_{std}, respectively. The new precipitation parameterisation is:

$$\Delta q_{precip} = r_{precip} \cdot q_{air} \cdot (c_q + c_{rq} \cdot rq + c_\omega \cdot \omega_{mean} + c_{\omega std} \cdot \omega_{std}) \qquad (2.11)$$

The model parameters, r_{precip}, c_q, c_{rq}, c_ω and $c_{\omega std}$ are fitted to minimise the root mean square error (RMSE) between observations and GREB simulated precipitation. As training period the monthly mean climatologies of precipitation and the precursors (e.g. relative humidity) are used. Thus, the GREB model is trained for the mean climate. For validation of the precipitation parameters three sensitivity experiments were designed (see chapter 2.5). The resulting mean precipitation and its seasonal cycle are shown in Figures 2.2g and 2.3g. The model is evaluated in a Taylor diagram in Figures 2.4a and b against observations. The new GREB precipitation model is now very close to the observed precipitation patterns in both the mean and annual cycle. It is actually closer to the observed precipitation than any CMIP5 model (Figures 2.4a and 2.4d). We further test the different elements of the precipitation model by only considering a subset of the variables in Eq. (2.11), setting the other terms to zero and fitting the parameterisations for these reduced models. This allows us to estimate the effect of each term in the equation, see Figures 2.4a and 2.4b and Figure 2.5.

Relative humidity (rq) is widely used in climate models as a predictor for precipitation (Petoukhov et al., 1999, 2005; Wang and Myask, 2000; Weaver et al., 2001). In the GREB model it increases precipitation mainly over humid regions such as the Amazons Basin (Figure 2.5c) and amplifies the seasonal cycle (Figure 2.5d). The overall pattern of rainfall with high precipitation in the tropics and decreasing towards higher latitudes is not changed. Including rq gives some moderate improvement relative to the original GREB model (Figure 2.4a comparing marker '0' to marker 'b').

The mean vertical air motion (ω_{mean}) provides a substantial improvement of the
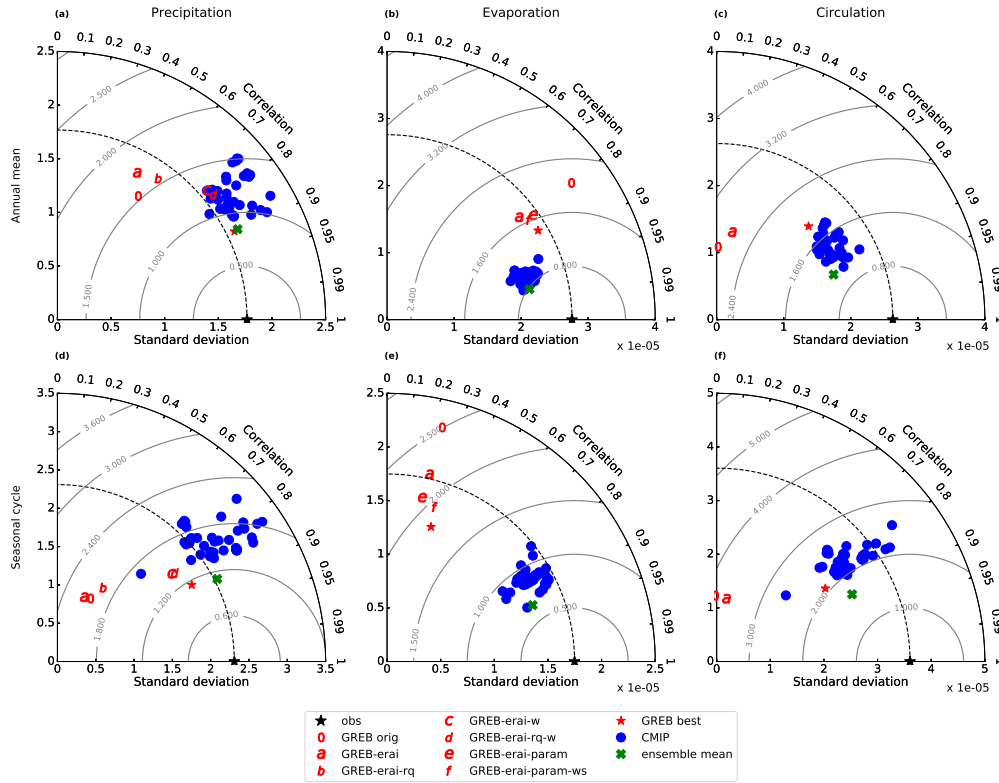
Figure 2.4: *Precipitation (left column), evaporation (middle column) and circulation (right column) in the annual mean (top row) and seasonal cycle (bottom row) in mm/day in a Taylor diagram against observations from GPCP and ERA-Interim. Red colours indicate different GREB parametrisations with 0 being the original and * the best parametrisation. Blue dots are pi-Control CMIP5 models and the green cross indicates the ensemble mean of all CMIP5 models.*

precipitation model (Figures 2.4a and d comparing marker '0' to 'c'). Ascending air masses in the ITCZ lead to increased precipitation, whereas descending air masses (i.e. in the subtropics) supress precipitation. It creates a sharper and more realistic gradient in precipitation than the original GREB model (compare Figures 2.2d & 2.5e). With the addition of ω_{mean}, GREB is in the range of uncertainty of more complex CMIP5 models in the annual mean and the seasonal cycle (Figures 2.4a and d). The GREB precipitation model without ω_{std} has still fairly weak mean precipitation in the midlatitudes storm track regions (compare Figures 2.5g and 2.2g) and has a weak seasonal cycle with the wrong sign in these regions as well (compare Figures 2.5h and 2.2g). The transient pressure systems in these regions lead to large vertical motions (ω) on shorter, daily time scales that result into large precipitation, but have a near zero ω_{mean}. Thus, to capture the precipitation in regions with strong variability in ω, but weak ω_{mean}, we include ω_{std}. ω_{std} is calculated with a daily time resolution to capture daily changing weather and wind patterns. This mainly enhances rainfall in the midlatitudes and high latitudes (Figures
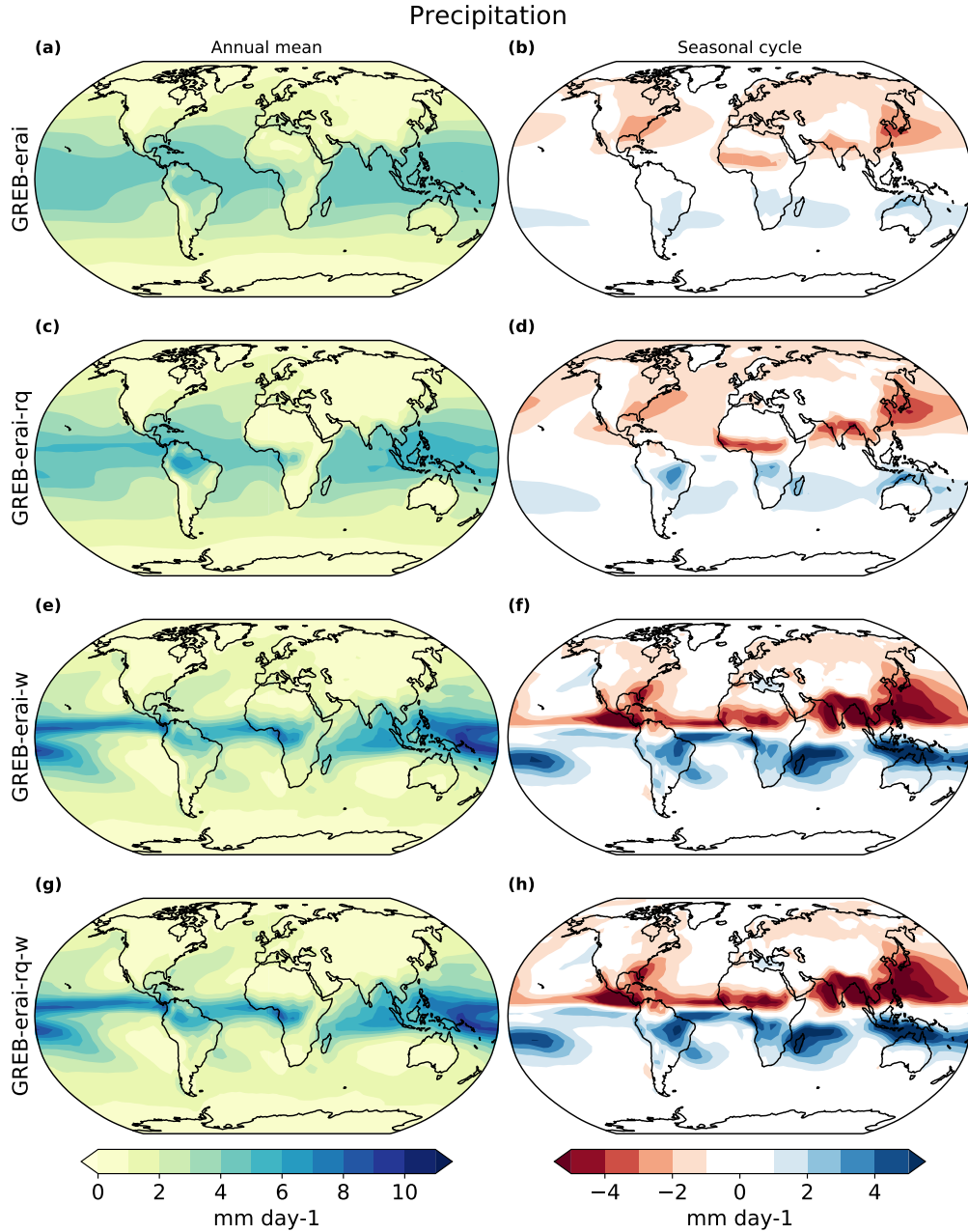
Precipitation

Figure 2.5: *Annual mean precipitation for four development steps of the GREB precipitation parametrisation (a, c, e, g) and their corresponding seasonal cycles (b, d, f, h) in mm/day. The first step was changing the specific humidity boundary climatology (a) and (b). Then subsequently more variables have been added to the precipitation parametrisation: adding only relative humidity (c, d), adding only omega (e, f), adding relative humidity and omega (g, h).*

2.2g and 2.3g) and is used to mimic precipitation in the storm tracks.

In summary, the new GREB precipitation model is significantly better than the original model. The RMSE is reduced by $0.65 \mathrm{~mm~day}^{-1}$ to $0.81 \mathrm{~mm~day}^{-1}$ in the annual mean and by $1 \mathrm{~mm~day}^{-1}$ in the seasonal cycle. GREB precipitation now has a comparable skill to more complex CGCMs and lies within the range of uncertainty of CMIP5 modelled

precipitation. Introducing the new precipitation parameterisation globally reduces the flux corrections of specific humidity caused by precipitation, see Figures 2.6c and 2.6d. The root mean square of the flux corrections caused by precipitation are reduced by more than 40%, indicating that the new parametrization has indeed improved the simulation of the hydrological cycle in the GREB model. Similar improvements are gained for the seasonal cycle (Figures 2.7c and 2.7d). The original GREB model showed large flux corrections, especially in the tropics where the ITCZ moves with seasons and in the midlatitudes. The pattern of the flux corrections of the new model still looks similar to the original model, but is only half as large in amplitude (Figures 2.6c & d and 2.7c & d).

2.4.2 Evaporation

In the original GREB model, evaporation is calculated using a widely used bulk formula approach (see Eq. (1) in Richter and Xie (2008)). This model does capture the main aspects of the regional differences in the annual mean evaporation in GREB, with enhanced evaporation over subtropical oceans and weaker evaporation over land (Figure 2.2e). The seasonal cycle (Figure 2.3e) is, however, very different from observed, and the land-sea differences are too strong.

For the new evaporation model, we retained the original bulk formula approach and included a few minor changes by considering land-sea differences, revised wind (u_*) estimates, scaled effectivity and skin temperature. The new evaporation model is:

$$\Delta q_{eva} = \frac{1}{r_{qviwv}} \cdot \rho_{air} \cdot c_{eva} \cdot c_w \cdot |u_* + c_{turb}| \cdot \theta_{soil} \cdot (q_{air} - q_{sat-skin}) \qquad (2.12)$$

The constant c_{eva} modifies the evaporation efficiency for a given mean wind speed, u_*. $q_{sat-skin}$ is an estimate of saturated humidity considering skin temperature. It is calculated using:

$$q_{sat-skin} = e^{\frac{z_{topo}}{z_{atmos}} \cdot 3.75 \cdot 10^{-3}} \cdot e^{17.08085 \cdot \frac{T_{surf} + c_{eva-temp} - 273.15}{T_{surf} + c_{eva-temp} - 38.975}} \qquad (2.13)$$

The parameter $c_{eva-temp}$ is a constant temperature offset to mimic skin temperature difference to T_{surf}. The parameters c_{eva}, $c_{eva-temp}$ and c_{turb} are fitted against observations for ocean and land points individually to minimise the RMSE. The values we estimated

Flux corrections - Annual mean
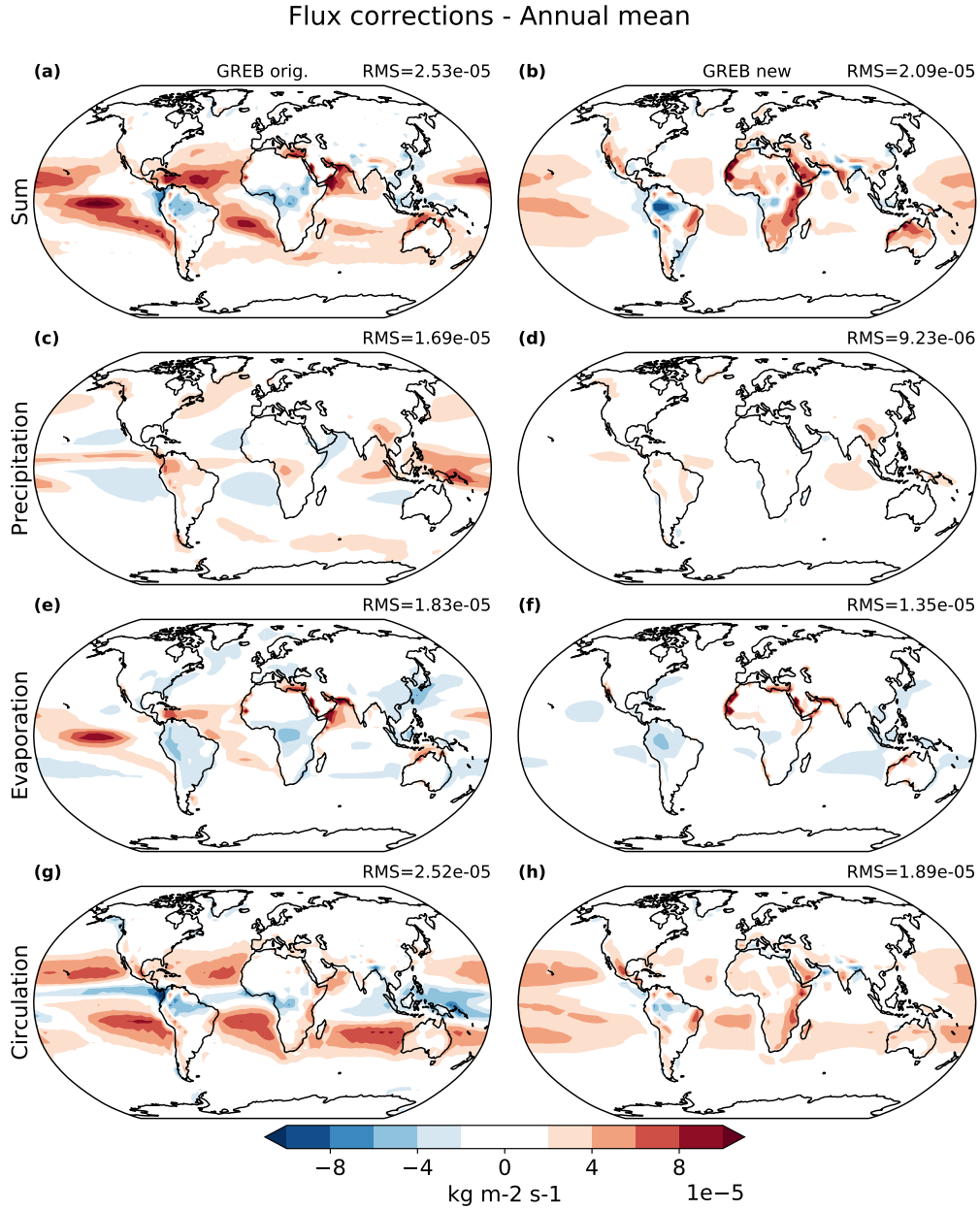
Figure 2.6: *Annual mean flux corrections of specific humidity for the original GREB model (a) and the improved GREB model (b). The flux corrections are then split into their contributions of precipitation (c, d), evaporation (e, f) and circulation (g, h) for the original GREB model (left column) and the improved GREB model (right column) in kg/m2/s. The top right shows the global root-mean-square (RMS).*

are:

$$c_{eva} = \begin{cases} 0.25 & \text{over land} \\ 0.58 & \text{over ocean} \end{cases} \tag{2.14}$$

Flux corrections - Seasonal cycle
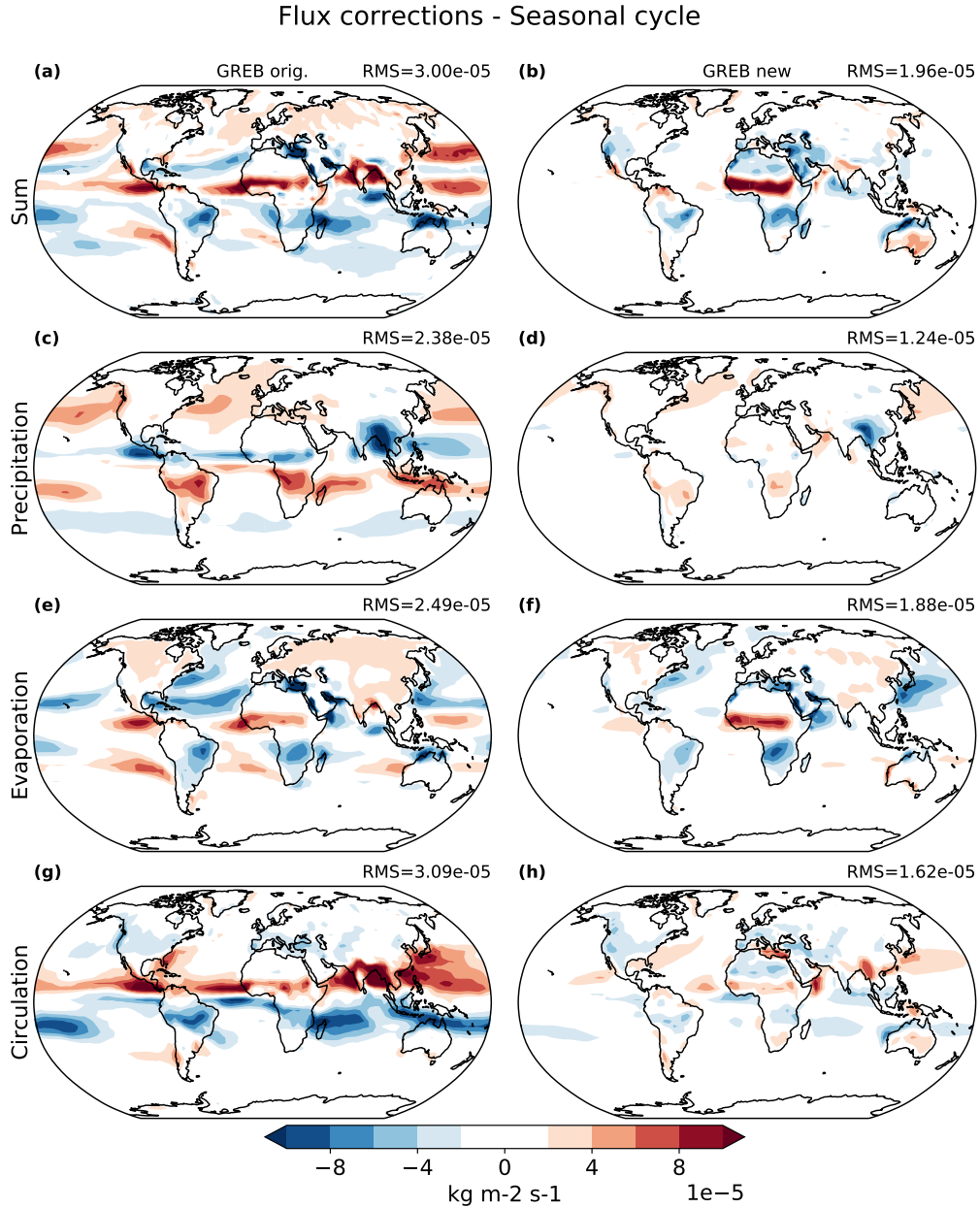
Figure 2.7: *As Fig. 2.6 but for the seasonal cycle (DJF minus JJA). Flux corrections of specific humidity for the original GREB model (a) and the improved GREB model (b). The flux corrections are then split into their contributions of precipitation (c, d), evaporation (e, f) and circulation (g, h) for the original GREB model (left column) and the improved GREB model (right column) in kg/m2/s. The top right shows the global root-mean-square (RMS).*

$$c_{eva-temp} = \begin{cases} 5K & \text{over land} \\ 1K & \text{over ocean} \end{cases} \tag{2.15}$$

$$c_{turb} = \begin{cases} 11.5 & \text{over land} \\ 5.4 & \text{over ocean} \end{cases} \tag{2.16}$$

The scaled effectivity (c_{eva}) is lower over land than over oceans reflecting the fact that for a given u_* more evaporation is simulated over oceans. This appears to be realistic considering that land has lower wind speeds near the surface for a given u_* due to the topography and vegetation. The value of $c_{eva} \cdot c_w$ closely match the observed values over oceans (Anderson and Smith, 1981; Merlivat, 1978).

The skin temperature difference approximated by $c_{eva-temp}$ is larger over land. It reflects that the GREB model does not simulate the daily cycle, and the larger daily cycle over land leads to an effectively larger difference between the simulated T_{surf} and the skin temperature. The offset of 1 K over oceans is also found by Feng et al. (2018).

The wind magnitudes (u_*) in the original GREB model were estimated on the basis of the monthly mean climatologies of the zonal and meridional wind components. This, however, is not an accurate estimate of the monthly mean wind magnitudes, as it neglects the turbulent term due to high frequent variability. In the new GREB model we estimate the monthly mean u_* climatology based on the original 6 hourly ERA-Interim time steps.

We can estimate how much each of these changes improved the evaporation model by including only one of these changes and fitting the parameters of these models individually, see Figures 2.4 b & e and Figure 2.8.

Fitting the evaporation efficiency c_{eva} and the turbulent wind factor improves evaporation over land, especially in the seasonal cycle (Figure 2.8d), and reduces the strength of evaporation over the ocean. The increase in evaporation over land is caused by the increase in the turbulent wind factor. c_{eva} would decrease the evaporation in the annual mean and the seasonal cycle. By including the new estimate of monthly mean wind speed u_* the pattern of evaporation is getting closer to observations, especially over the oceans (i.e. Figure 2.8f, North Atlantic), and by including the new estimate of skin temperature the seasonal cycle is improving slightly (Figure 2.4e).

The original GREB model was evaporating too much on the annual mean (see Figure 2.2e) especially over the equatorial Pacific and Atlantic. The new hydrological cycle model parameterisation largely decreases evaporation over these regions and the flux corrections are reduced over the globe in the annual mean (Figures 2.6e & f). The correlation of the annual mean experiences the largest changes from changing the reference climatology (Figure 2.4b).

In the seasonal cycle, each included variable improves the simulation of evaporation
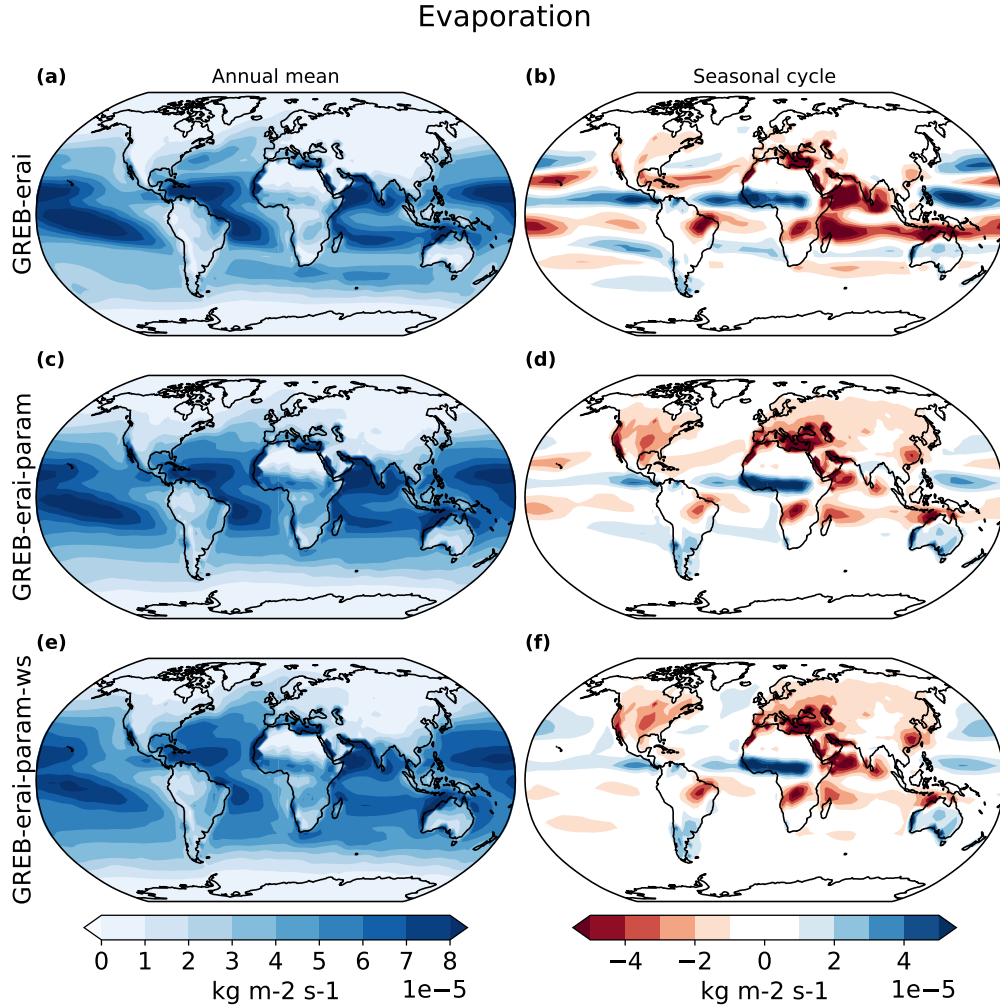
Figure 2.8: *Annual mean evaporation for three development steps of the GREB evaporation parametrisation (a, c, e) and their corresponding seasonal cycles (b, d, f) in kg/m2/s. The first step was changing the boundary climatology (a) and (b). Then subsequently more variables have been added to the evaporation parametrisation: fitting the evaporation parameters separately for ocean and land (c, d) and fitting parameters and prescribing the wind speed (e, f).*

in the GREB model (Figure 2.4e). The seasonal cycle of flux corrections caused by evaporation in the original GREB model is large over land and large over oceans. There are positive flux corrections around the equator and negative flux corrections over the oceans north of the equator (Figure 2.7e). The improved evaporation seasonal cycle mainly removes this distinct pattern over the oceans and reduces flux corrections over most land areas. (Figures 2.7e & f). Overall, the new evaporation model is slightly better than in the original GREB model, but it still has substantial limitation in simulating the seasonal cycle correctly (Figures 2.2h & 2.3h).

2.4.3 Transport

The original GREB model transport of moisture was very weak and had little agreement with observations (Figures. 2.2f and 2.2f). Atmospheric transport of moisture in GREB (Eq. (2.10)) is controlled by diffusion and advection with mean winds. This model considered a divergence free two-dimensional flow. However, moisture convergence, as it occurs, for example in the ITCZ, is important for the transport of moisture in these regions. The mean convergence by advection including the moisture convergence term is:

$$\overline{\vec{\nabla}(\vec{u} \cdot q_{air})} = \overline{\vec{u} \cdot \vec{\nabla} q_{air}} + \overline{q_{air} \cdot \vec{\nabla} \vec{u}} \tag{2.17}$$

The second term on the right-hand side was not considered in the original GREB model, but is now considered in the new model. The moisture convergence term can be approximated by knowing the mean vertical air flow assuming continuity and hydrostatic balance:

$$\overline{\vec{\nabla}(\vec{u} \cdot q_{air})} = q_{air} \cdot f \cdot \frac{dt_{crcl}}{z_{vapour} \cdot \rho_{air} \cdot g} \cdot (-\omega_{mean}) \tag{2.18}$$

with the known parameters scaling height of water vapour, z_{vapour}, density of air, ρ_{air}, gravitational acceleration, g, and the circulation time step, dt_{crcl}. The scaling factor, f, should theoretically be 1.0, but the mean large-scale horizontal winds and vertical velocities may not perfectly match because of the coarse horizontal resolution. Other factors that influence f could be, the single layer approximation, the GREB scaling height of water vapour that is larger than literature values or calculating the reference circulation as residual. A fit of Eq. (2.18) to observations finds that f = 2.5.

This new model has now a fairly realistic transport in the annual mean and the seasonal cycle (Figures 2.2i and 2.3i), with clear moisture transport out of regions with diverging flow (e.g. in the subtropics off the coast of Peru) and into converging zones (e.g. ITCZ). The new parameterisation of convergence also reduces the flux corrections in the annual mean and the seasonal cycle (Figures. 2.6g & h and 2.7g & h).

2.4.4 Boundary Conditions and Input Data

The original GREB model used the NCEP reanalysis as boundary conditions and as references for estimating the parameterisation of the model. New generations of reanalysis

products have improved, because of the use of better models, better input data and better assimilation products (Dee et al., 2011). This is shown by Chen (2016) who investigated the variability and trends of the vertically integrated water vapour and found that ECMWF's ERA-Interim reanalysis has a higher accuracy than NCEP and a better agreement with observations over oceans and in the tropics. NCEP underestimates water vapour in troposphere (Kishore et al., 2011). We therefore changed the reference climatology of specific humidity in the GREB model from NCEP to ERA-Interim. To get a consistent model, we also take surface temperature, horizontal winds, the climatology of ω and standard deviation of ω from ERA-Interim. The effect of changing the mean climatology from the years 1950-2008 to 1979-2015 is small compared to the differences between NCEP and ERA-Interim. The parameters of our new GREB hydrological cycle model are then fitted against the new reference climatologies.

We estimate the effect that the change in reference climatologies will have on the new GREB hydrological cycle model by fitting the parameters of the new model as described above to both the NCEP and ERA-interim reanalysis. The resulting hydrological cycle models are evaluated against observations (GPCP and ERA-Interim) in Taylor diagrams for the annual mean. Changing the reference climatology does not lead to major improvements in the representation of the hydrological cycle in the GREB model, but it increases the correlation of precipitation, evaporation and circulation and reduces the RMSE (Figure A1 in the Appendix). The main improvement is in the tropics and might be related to the underestimated value of specific humidity in the tropics found by Chen (2016) and Kishore et al. (2011).

2.5 Model Verification

We now test the new hydrological model in a series of three different sensitivity experiments. The discussion focuses on evaluating the new model. The three examples test the hydrological cycle model response to changes in the boundary conditions. These changes are beyond those used to fit the model parameterisation and can therefore be a test of the model's skill. We will leave more in-depth analysis of some of these experiments to future studies.

2.5.1 Seasonal Cycle

The response of the hydrological cycle to seasonal changes is a good test for evaluating the skill of the hydrological cycle model. The GREB model applies monthly flux correction terms to maintain a mean atmospheric humidity as observed. Thus, by construction the specific humidity in each calendar month in the GREB model is identical to the observations; see Figure 2.9a.
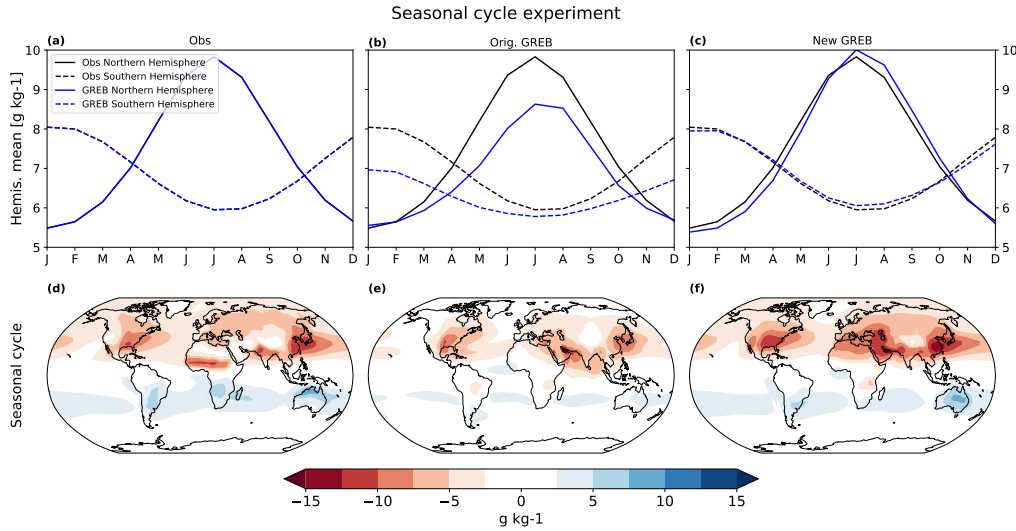
Figure 2.9: *Annual cycle of specific humidity with seasonal varying flux corrections (a, d) and annual mean flux corrections for original GREB (b, e) and improved GREB (c, f) in g/kg. The top row shows the northern (solid) and southern (dashed) hemispheric mean for observations (black) and GREB (blue). The bottom shows the respective seasonal cycle (DJF minus JJA). For the seasonally varying flux corrections (a) GREB (blue) matches observations (black).*

To illustrate that the seasonal cycle is not a feature of the seasonally varying flux corrections, we changed the flux corrections to an annual mean value for the original GREB model (middle column in Figure 2.9) and for the new GREB model (right column in Figure 2.9). This annual mean flux correction value is added on every time step to the tendency equation of specific humidity (Eq. (2.4)).

With the new parameterisations for precipitation, evaporation and circulation the new GREB model resolves the seasonal cycle better than the original GREB model (Figure 2.9). The seasonal cycle of the original GREB model was too weak in the Northern Hemisphere when compared to observations, and throughout the year the GREB model was too dry (Figure 2.9b). For the Southern Hemisphere, the original GREB model was too wet. The new GREB model captures the high humidity in northern hemispheric summer and the low values in winter (Figure 2.9c). This makes the seasonal

cycle stronger in the new GREB model and it is closer to the reference climatology. In summary, the new GREB hydrological cycle model simulates the seasonal evolution of the atmospheric humidity very well and significantly better than the original GREB model.

2.5.2 El Nino Southern Oscillation

Strong El Nino and La Nina events lead to significant changes in the tropical precipitation and associated hydrological cycle changes. Since these natural modes of climate variability are well documented, they present a good test case for the GREB model.

We therefore conducted a set of sensitivity experiments with the GREB model forced by the mean conditions for strong El Nino and La Nina events. The GREB model was forced with mean composites of surface temperature, horizontal winds and ω from observations for four El Nino (1982/83, 1887/88,19 91/92, 1997/98) and La Nina (1988/89, 1999/00, 2007/08, 2010/11) events. The anomalies are calculated around El Nino/La Nina from May before the peak in December to April in the following year and against the climatological mean. In the GREB model simulation, they are added on top of the reference climatology. The observed anomalies in the hydrological cycle during these El Nino events are shown in Figures 2.10a-c. The skill of simulating La Nina events are qualitatively the same. We clearly note strong regional changes in the precipitation in the tropical Pacific that match changes in moisture transport (Figure 2.10c), illustrating that El Nino-Southern Oscillation (ENSO) events mark strong regional changes in the hydrological cycle related to changes in the circulation.

The new GREB response in precipitation shows a strong similarity with the observed changes (Figure 2.10g). There is a shift of rainfall from the Maritime Continent towards the NINO3.4 region (5°N to 5°S & 170°W to 120°W) over the Pacific. However, the overall amplitude in the precipitation response is in general weaker than observed. In contrast, the original GREB model has nearly no precipitation response to the ENSO forcings. This is consistent with the weak response in the circulation in the original GREB model (Figure 2.10f). The correlation between the GREB simulated El Nino response increases from 0.0 for the original GREB model to 0.9 with the new GREB model.

The observed evaporation response to ENSO events in the tropical Pacific somewhat counteracts the precipitation response, as we observe mostly decreased evaporation over regions with enhanced precipitation and increased evaporation over regions with reduced
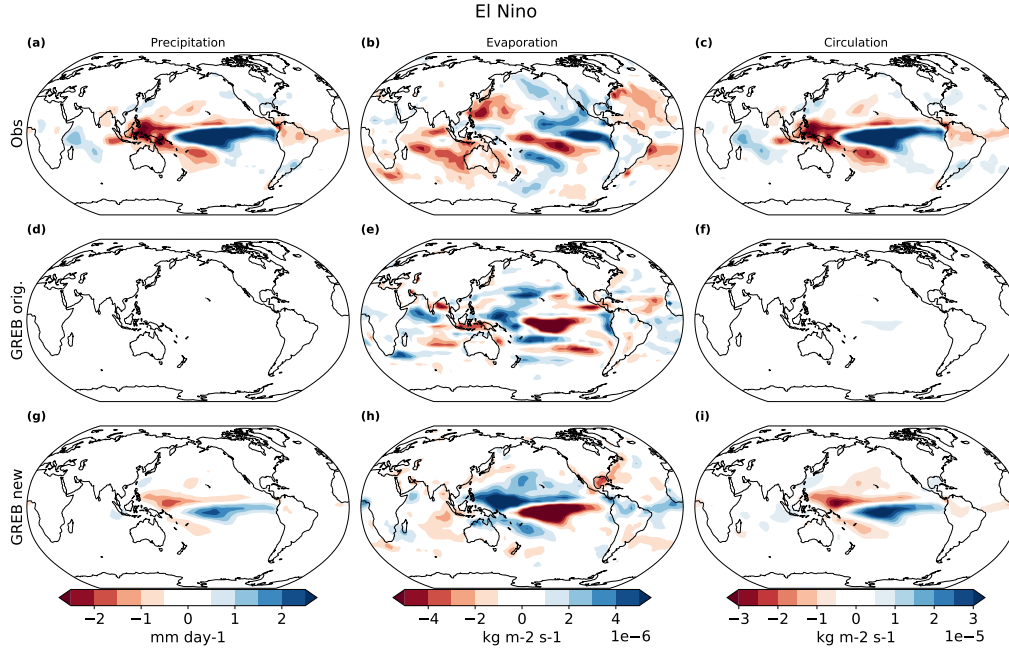
Figure 2.10: *The El Niño response of the hydrological cycle in: observations for precipitation (a) in mm/day, evaporation (b) and circulation (c) in kg/m2/s (upper), original GREB model for precipitation (d), evaporation (e) and circulation (f) (middle) and the improved GREB model for precipitation (g), evaporation (h) and circulation (i) (lower). GREB uses prescribed anomalies from an El Niño composite mean of surface temperature, horizontal winds and vertical winds (omega).*

precipitation (Figures 2.10a and b). These evaporation changes are mostly caused by changes in winds, with decreased evaporation over regions were the winds have weakened (e.g. NINO3.4 region). The new GREB model somewhat captures this pattern, but shows a stronger evaporation response, which partly explains the weaker precipitation response. However, both the original and the new GREB model evaporation have only a weak spatial correlation (0.3) with the observed evaporation changes overall.

The observed strong changes in the circulation of atmospheric humidity (Figure 2.10c) is mostly due to changes in the convergence of moisture (e.g. ω). Since convergence of moisture was not considered in the original GREB model, the simulated changes in the circulation are very weak in the original GREB model (Figure 2.10f). The new GREB model does consider convergence of moisture and simulates the changes in the circulation of atmospheric humidity very similar to the observed (Figure 2.10i). The new circulation parameterisation in the new GREB model improves the correlation between the observed and the simulated circulation tendency from 0.3 (original GREB) to 0.95.

In summary, the new GREB model does simulate the precipitation and circulation response to ENSO conditions fairly well, whereas the original GREB model has very little

skill, illustrating the significant improvement of the new GREB model over the original GREB model. However, the evaporation response in both models is not as well simulated as the precipitation and circulation response.

2.5.3   Global Warming

The response of the hydrological cycle to global warming is one of the potential applications of the GREB model and a comparison of the GREB model with the CMIP model simulations response to global warming provides a good test. The CMIP5 ensemble mean response of precipitation shows a distinct increase of rainfall in the equatorial Pacific, decreases of mean rainfall in some subtropical regions (i.e. east Pacific) and increases in some areas of the midlatitudes; see Figure 2.11a. This pattern is normally referred to as wet-get-wetter paradigm (Held and Soden, 2006). Although this approach has been questioned by more recent studies (Chadwick et al., 2013) it still gives a good first order approach to the changes in the global hydrological cycle, although changes over land might be muted or even reversed (He and Soden, 2016).
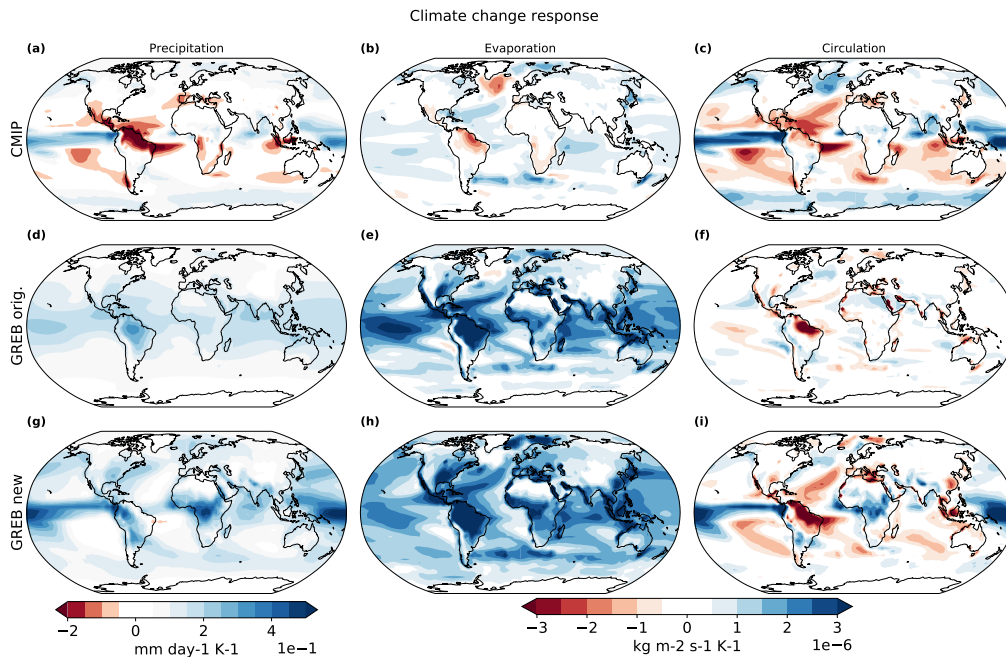
Figure 2.11: *Response of the hydrological cycle to an RCP8.5 forcing in the: CMIP5 ensemble mean for precipitation (a) in mm/day, evaporation (b) and circulation (c) in kg/m2/s (upper), original GREB model for precipitation (d), evaporation (e) and circulation (f) (middle) and the improved GREB model for precipitation (g), evaporation (h) and circulation (i) (lower). GREB uses prescribed anomalies from CMIP5 ensemble mean of surface temperature, horizontal winds and vertical winds (omega). All responses are shown per degree of warming.*

To evaluate the GREB hydrological cycle model independent of the other GREB model components, such as the surface temperature tendencies, we force the original and new GREB models with RCP8.5 equivalent CO_2 concentrations and all other input variables for the hydrological cycle model taken from CMIP model simulations. That is, we add surface temperature, horizontal winds and vertical velocity RCP8.5 CMIP5 ensemble mean anomalies from the models described in Table 2.1 on top of the GREB control reference climatologies. In the control run, the reference boundary conditions of surface temperature, horizontal winds and ω are taken.

The precipitation response in the original GREB model is positive in all locations and it closely follows the pattern of specific humidity in the control simulation (see Eq. (2.1) and Figure 2.11d). This is mainly due to an increase in the saturation water vapour pressure of about 7% per degree of warming (Clausius-Clapeyron). The original GREB precipitation response pattern is not correlated to the CMIP5 ensemble mean response pattern (Figure 2.12a), suggesting that local differences in the precipitation response are very different from those in the CMIP simulations.
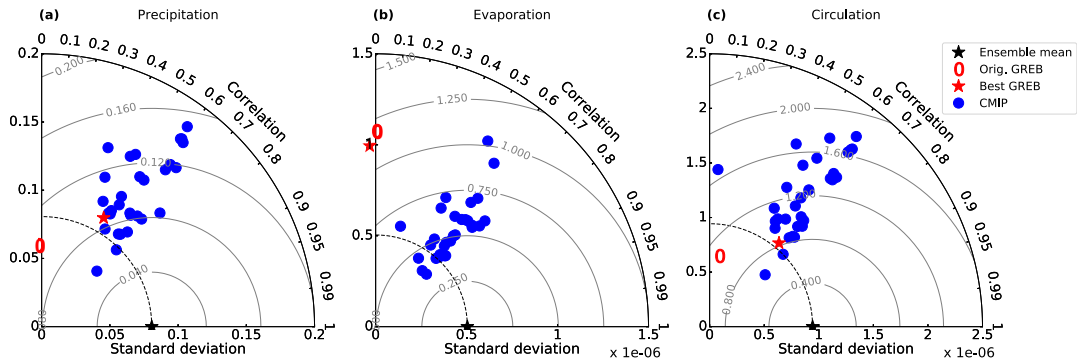
Figure 2.12: *RCP8.5 response of CMIP5 models (blue), original GREB (0) and improved GREB (*) per degree of global warming against the CMIP5 ensemble mean (black star). Precipitation is shown on the left, evaporation in the middle and circulation on the right column. GREB uses prescribed anomalies from the CMIP5 ensemble mean of surface temperature, horizontal winds and vertical winds (omega). The pattern correlation of the original GREB model precipitation response with the ensemble mean is zero. The original and improved GREB model have zero correlation with the ensemble mean evaporation and the standard deviation is one for both.*

The improved GREB model response pattern is similar to the CMIP models with enhanced and reduced response roughly at similar locations. This is strongly related to the moisture transport changes. The precipitation pattern correlation improves from 0 to

0.5 and the water vapour circulation pattern correlation from 0.05 to 0.65 (Figures 2.12a and c). However, the overall global mean precipitation response in the new GREB model is shifted upwards, which is not measured by the correlation coefficient, compared to the CMIP5 ensemble mean, which is related to the much stronger response in evaporation (compare Figures 2.11b and h). Evaporation is still a problem in the GREB model with no improved correlation in the new hydrological cycle model. In CMIP5 models, we see a muted response of evaporation mainly due to changes in surface relative humidity and surface stability (Richter and Xie, 2008).

2.6   Chapter Summary and Discussion

In this study, we introduced the newly developed hydrological cycle model for the GREB model. It consists of three parts: precipitation, evaporation and transport. The development of these models started from the existing zero-order hydrological cycle model of the GREB model and used physical reasoning and observations for fitting parameters.

The simulation of precipitation and transport of moisture in the new hydrological cycle model is now comparable in skill to CMIP models in terms of annual mean and the seasonal cycle of rainfall. The simulation of precipitation in the GREB model is closer to the observed precipitation pattern than any CMIP5 model in both the annual mean and the seasonal cycle. This is directly related to the fact that the GREB mode has a prescribed atmospheric circulation, which is the main driver of the global precipitation pattern. It is important to point out that while the atmospheric circulation is prescribed in the GREB model specific humidity is free to respond, which leads to some differences between the GREB model and the CMIP5 model water vapour circulation (see Fig. 2.11 and Eq. 2.18).

The evaporation has only improved slightly but does simulate the annual mean values fairly well. However, it is still different from the observed seasonal cycle and the skill is much lower than that of the CMIP model. This suggests that the evaporation model is still a limiting factor in the GREB model.

We applied the new hydrological cycle model to a number of sensitivity studies, which illustrated that the new hydrological cycle model is much improved over the original GREB model. The annual cycle simulation without any correction terms is very realistic

with the new model, and the precipitation response to ENSO events is now very similar to the observed, due to the much-improved transport of moisture. Finally, the response to global warming now shows a precipitation response pattern that is comparable to that of the CMIP models. Again, a limiting factor in this sensitivity experiment was the evaporation response of the GREB model in comparison to that of CMIP models. Additionally, changes in ω_{std} have not been considered in this chapter, but do play an important role in the precipitation response to climate change. This will be discussed more in the next chapter.

All three parts of the GREB hydrological cycle (precipitation, evaporation, moisture transport) interact through specific humidity (2.4). This interaction allows the GREB hydrological cycle to be globally balanced (i.e. $\Delta q_{precip} = \Delta q_{eva}$) without artificially forcing precipitation to match evaporation. This is important for the following chapters.

An interesting aspect of the GREB model is that it has the atmospheric circulation (vertical and horizontal winds), humidity and surface temperatures as boundary conditions. This allows the GREB model to be used as a diagnostic tool to understand how different boundary conditions affect aspects of the climate system, such as the hydrological cycle's response to global warming. The GREB has clear limitations in its response to global warming (i.e. no drying) and is limited through its simplicity and lack of a more dynamic response. The GREB model atmospheric circulation, mean horizontal winds, mean vertical velocity and vertical velocity variability are not dynamically responding to a warmer climate restricting the GREB model to take changes in these climate variables from more complex models (i.e. CMIP5). The course time resolution of the GREB model does not allow to consider vertical velocity on a daily time scale but rather as a standard deviation in order to consider weather events. While all this limits the GREB model there are advantages being able to exactly control the boundary conditions. The ability to prescribe the boundary conditions allows the GREB model to take any climate mean state and may help to study how biases in the hydrological cycle in CMIP models related to different boundary conditions from the atmosphere, such as biases in the vertical winds. A recent study by Yang et al. (2018) links circulation biases in CMIP models to biases in precipitation and moisture. Forcing GREB with the circulation of CMIP models could shed light on how discrepancies in circulation between CMIP models affect the hydrological cycle. The new GREB hydrological cycle model is therefore a good tool

in helping to conceptually understand the hydrological cycle and its response to global warming or other external forcings. It will further help in understanding CMIP model biases in the simulation of the hydrological cycle.

Chapter 3

Conceptual Deconstruction of the Simulated Precipitation Response to Climate Change

3.1 Preface

State-of-the-art climate change projections of the CMIP5 simulations suggest a fairly complex pattern of global precipitation changes, with regions of reduced and enhanced precipitation. Conceptual understanding of these projected precipitation changes is difficult if only based on coupled general circulation model (CGCM) simulations, due to the complexity of these models. In this study we describe a simple deconstruction of the ensemble mean CMIP5 projections based on sensitivity simulations with the globally resolved energy balance (GREB) model. In a series of sensitivity experiments we force the GREB model with four different CMIP5 ensemble mean changes in: surface temperature, evaporation and the vertical atmospheric velocities mean and its standard deviation. The resulting response in the precipitation of the GREB model is very close to the CMIP5 ensemble mean response, suggesting that the precipitation changes can be well represented by a linear combination of these four forcings. The results further provide good insights into the drivers of precipitation change. The GREB model suggests

that not one forcing alone can be seen as the main driver, but only the combination of all four changes results in the complex response pattern. However, the dominant forcings are the changes in the large-scale circulation, rather than the pure thermodynamic warming effect. Here, it is interesting to note that changes in high-frequency atmospheric variability of vertical air motion (weather), that are partly independent of the changes in the mean circulation, have a control on the pattern of the time-mean global precipitation changes. The approach presented here provides a powerful basis on which the hydrological cycles of CGCM simulations can be analysed.

3.2 Introduction

In his attempts to explain ice ages Arrhenius (1896) was the first to link variations in CO2 concentration to the greenhouse effect using basic physical considerations. Decades after him others followed using basic energy balance models to estimate the effect increasing levels of greenhouse gases have on the climate (Budyko, 1972; North et al., 1981; Sellers, 1969). Since the first numerical weather forecast by L.W. Richardson in the 1920s was produced by hand, the computational revolution helped develop simple energy balance models into fully complex coupled general circulation models (CGCMs) (Manabe and Stouffer, 1980; Meehl et al., 2007; Meehl and Stocker, 2007). Since then the main aim of model development has been to improve the physical representation of the processes in the climate system by either including more processes that have not been considered before, or by increasing the resolution of models. These CGCMs simulate processes in the ocean, on land and in the atmosphere and are therefore focusing on the most realistic and best representation of the climate system as a whole.

In recent decades increasing computer power has allowed these highly complex CGCMs to progressively increase their resolution and there is a strong interest in the research community to push the resolution of climate models to new boundaries (Haarsma et al., 2016; Marotzke et al., 2017). It has been shown that increasing the model resolution addresses a lot of common problems seen in CGCMs (Haarsma et al., 2016), such as aspects of the large-scale circulation (Masson et al., 2012; Shaffrey et al., 2009), the global water cycle (Demory et al., 2014), movements of the Atlantic inter-tropical convergence zone (ITCZ) (Doi et al., 2012) and the diurnal precipitation cycle (Birch et al.,

2014; Sato et al., 2009). While expanding the scope of climate models by adding more processes and increasing the resolution, several existing problems, such as substantial precipitation biases, remain unsolved. In addition, constantly increasing the resolution and complexity of climate models does not help to gain a more conceptual understanding of climate change, as multiple processes interact with each other (Dommenget and Flöter, 2011).

Projections of how rainfall is changing are primarily based on CGCMs simulations of the Coupled Model Intercomparison Project version 5 (CMIP5) or earlier. These simulations project an increase in global mean precipitation of roughly 2% per degree of warming (Held and Soden, 2006). The 2% change in precipitation comes in contrast to an increase in atmospheric water vapour of about 7% per degree of warming closely following the Clausius-Clapeyron equation. This muted response is explained by a general slowdown of the atmospheric circulation (Chadwick et al., 2013; Held and Soden, 2006) and changes in radiative cooling (Allen and Ingram, 2002; Pendergrass and Hartmann, 2014). That is, as water vapour increases, the atmosphere cannot emit radiation at a large enough rate to support precipitation matching the rate of increase in water vapour (Stephens and Ellis, 2008). Many studies have suggested that changes in radiative cooling dictate the global precipitation response and in turn control the global evaporation response, which on long time scales have to match. However, Webb et al. (2018) showed that increases in surface evaporation can have a substantial impact on radiative cooling itself. Richter and Xie (2008) looked at this muted response of precipitation from the perspective of evaporation and found that the evaporation response is mainly limited through increases in surface relative humidity and surface stability. This highlights the fact that precipitation and evaporation are closely linked and makes it a complex cycle to study.

Although precipitation is increasing by 2% per degree of warming globally, this does not mean it is increasing at the same rate everywhere. Precipitation is generally projected to increase in the ITCZ, with a large-scale precipitation decline in the subtropics and an increase in precipitation in mid- to high- latitude storm tracks (Allen and Ingram, 2002; Chou and Neelin, 2004; He and Soden, 2016; Held and Soden, 2006; Neelin et al., 2006). This pattern change is often referred to as the 'wet-get-wetter' (Held and Soden, 2006). The wet-get-wetter hypothesis is mainly built on the idea that a warmer atmosphere

holds and therefore transports more moisture out of dry regions into wet regions if the circulation remains unchanged (Chadwick et al., 2013). The thermodynamic response would also lead to a high correlation between the mean, historical precipitation and the change of precipitation with climate change. However, Chadwick et al. (2013) have shown that on regional scales the precipitation response is poorly correlated with pre-industrial precipitation, leaving the conclusion that the dynamics are changing. There has been an observed weakening of the Walker circulation (Vecchi et al., 2006), a weakening of the Hadley cells (Lu et al., 2007; Vecchi and Soden, 2007) and a poleward shift of storm tracks (Bengtsson et al., 2006; Mbengue and Schneider, 2017; Yin, 2005) while a shift in tropical convergence zones (Chadwick et al., 2013) has been shown in GCM projections.

In this chapter we present a conceptual deconstruction of the CMIP5 ensemble mean precipitation changes, to better understand the climate change forcings that drive these changes. The forcings that control precipitation changes can be illustrated by a simplified sketch of the atmospheric water cycle (Fig. 3.1). Here an atmospheric volume contains a water reservoir (humidity) that is controlled by the in and out flow of water due to horizontal transport, evaporation and precipitation. Given this mass balance, precipitation changes result from changes in the humidity, horizontal transport, evaporation or in the processes that control precipitation.

We will use the Globally Resolved Energy balance (GREB) model from Dommenget and Flöter (2011) with the hydrological cycle model from chapter 2 to investigate how the CMIP5 ensemble mean projected changes in the surface temperatures, atmospheric circulation and evaporation lead to the projected changes in precipitation. We will illustrate the feasibility of this approach and discuss how the individual elements of the changing climate contribute to the projected changes in precipitation. The following section will introduce the data, models and methods used. It will in particular discuss the GREB model and how we make use of it as an analytical tool. In section 3.4 the main results of this study will be presented. Finally, we give a discussion and summary of the results.

Atmospheric water cycle
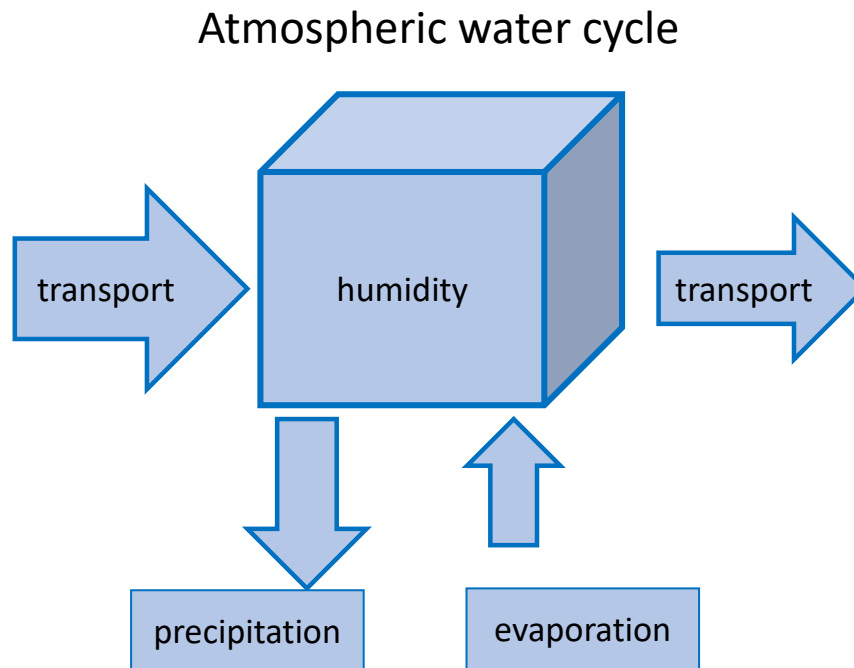
Figure 3.1: *GREB simplified hydrological cycle. Precipitation and evaporation do not have to be balanced locally (here shown as two different sized arrows).*

3.3 Data and Methods

This section provides an overview on the CMIP5 model data used. It further gives a short introduction to the GREB model, how it differs from other climate models (e.g. CGCMs) and discusses the hydrological cycle model in the GREB model, which is a key element for this study. We then explain the main analysis approach of this study: sensitivity studies with the GREB model forced by changes in the boundary conditions according to the CMIP5 RCP8.5.

3.3.1 CMIP data

The models of Coupled Model Intercomparison Project phase 5 (CMIP5) (Taylor et al., 2012) used in this study are summarized in Tab. 3.1. We used all available models of the historical and RCP8.5 scenario that provided the variables and time frequency needed for the analysis presented in this study. All datasets are re-gridded to a horizontal resolution of $3.75^o \times 3.75^o$ to match the GREB model horizontal resolution and monthly

climatologies are calculated. For the climatology of ω_{mean} and ω_{std} a daily output frequency is used and an unweighted vertical mean over all levels is applied to smooth the data. The multi-model ensemble mean over all models in Tab. 3.1 is calculated. Models with more than one realization are considered by the average of all realisations (i.e. a model with one realisation and a model with many realisations are weighted equally in the multi model ensemble mean).

Table 3.1: *List of CMIP5 models used for the conceptual decomposition of the climate change precipitation response.*

Models	
ACCESS1-0	ACCESS1-3
BNU-ESM	CMCC-CM
CSIRO-Mk3-6-0	FGOALS-g2
GFDL-ESM2G	GFDL-ESM2M
IPSL-CM5A-LR	MIROC-ESM-CHEM
MIROC5	MPI-ESM-LR
MPI-ESM-MR	MRI-CGCM3

3.3.2 GREB model

The GREB model and its new hydrological cycle have been described in chapter 1.2 and chapter 2. The GREB model simulated precipitation and its seasonal cycle for control conditions are shown in Fig. 3.2 a and b.

3.3.3 GREB sensitivity experiments

The main analysis part of this study is based on a series of sensitivity experiments with the GREB model. For these experiments we use the ability of the GREB model to respond to changes in the boundary conditions and to control the mean Tsurf. For the study of the precipitation response to changes in environmental factors (eq. (2.11)) the key controlling factors are the boundary conditions of ω_{mean}, ω_{std}, and the model variables q and rq.

If the precipitation is free to respond, then q and rq are largely controlled by the evaporation (Δq_{eva}; eq. (2.12)) and the atmospheric temperatures. The latter is strongly linked to Tsurf. Thus, to study the precipitation response to changes in environmental factors, the GREB model can be driven by changes in ω_{mean}, ω_{std}, Δq_{eva} and Tsurf.
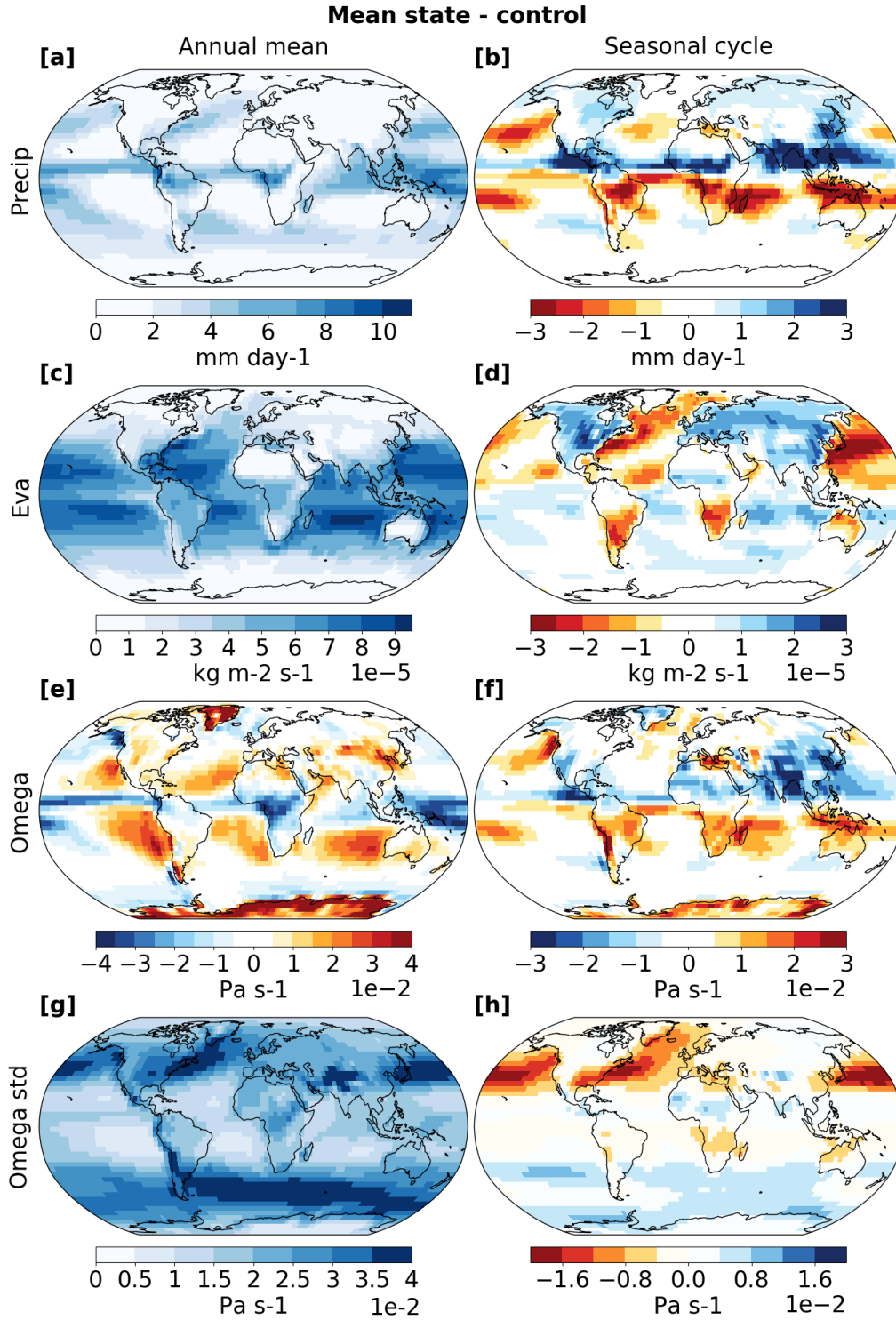
Figure 3.2: *GREB control annual mean and seasonal cycle (JJA-DJF) precipitation (a, b), mean evaporation (c, d), mean vertical wind (e, f) and daily variability of vertical wind (g, h). The annual mean is shown on the left (a, c, e, g) and the seasonal cycle is on the right (b, d, f, h).*

The model will respond to these changes in boundary conditions by simulated changes in the atmospheric temperature, humidity and subsequently the relative humidity. These changes will then lead to changes in precipitation following from eq. (2.11). The annual

mean values and the seasonal cycle of the key drivers, ω_{mean}, ω_{std} and Δq_{eva} are shown in Fig. 3.2 and the control precipitation is shown in Figs. 3.2 a and b.

We will use the simplicity of the GREB model to separate thermodynamic and dynamic processes, which in nature and CGCMs are tightly coupled. That is, for example, changing surface temperature not only influences evaporation and atmospheric moisture but also change the circulation patterns of the atmosphere. This makes it hard to investigate the relative importance of thermodynamic and dynamic processes with climate change.

For the control simulations the GREB model is run with observed boundary conditions, as described above, and q and Tsurf are free to evolve. For the sensitivity experiments we add the anomaly values of ω_{mean}, ω_{std}, Δq_{eva} and Tsurf from the CMIP5 RCP8.5 ensemble mean to each of the control forcings for one or all boundary conditions while the remaining boundary conditions are kept at control values. Thus, in these sensitivity experiments Δq_{eva} and Tsurf are not free to evolve but are prescribed by the CMIP5 RCP8.5 ensemble mean values. Atmospheric temperatures, humidity and precipitation are free to respond. The difference between control and sensitivity simulations are defined as the response to the CMIP5 RCP8.5 ensemble mean forcings.

3.4 Precipitation Response to Climate Change Deconstruction

In this section we discuss the large-scale response of precipitation to changes in Tsurf, Δq_{eva}, ω_{mean} and ω_{std} in the ensemble mean CMIP5 RCP8.5 based on the GREB sensitivity experiments (see section above). We start the discussion with illustrating the concept and then focus on how each of the four forcings contribute to the change in precipitation.

Fig. 3.3 shows annual mean and seasonal cycle of the four different forcings for the ensemble mean CMIP5 RCP8.5 changes. Tsurf shows the well-known pattern of stronger warming over land, high latitudes and during winter time. Evaporation is mostly increasing over oceans and has some locations with significant decrease. The seasonal signature of the evaporation changes is fairly complex, but are somewhat marked by reduced increase in evaporation during summer time.
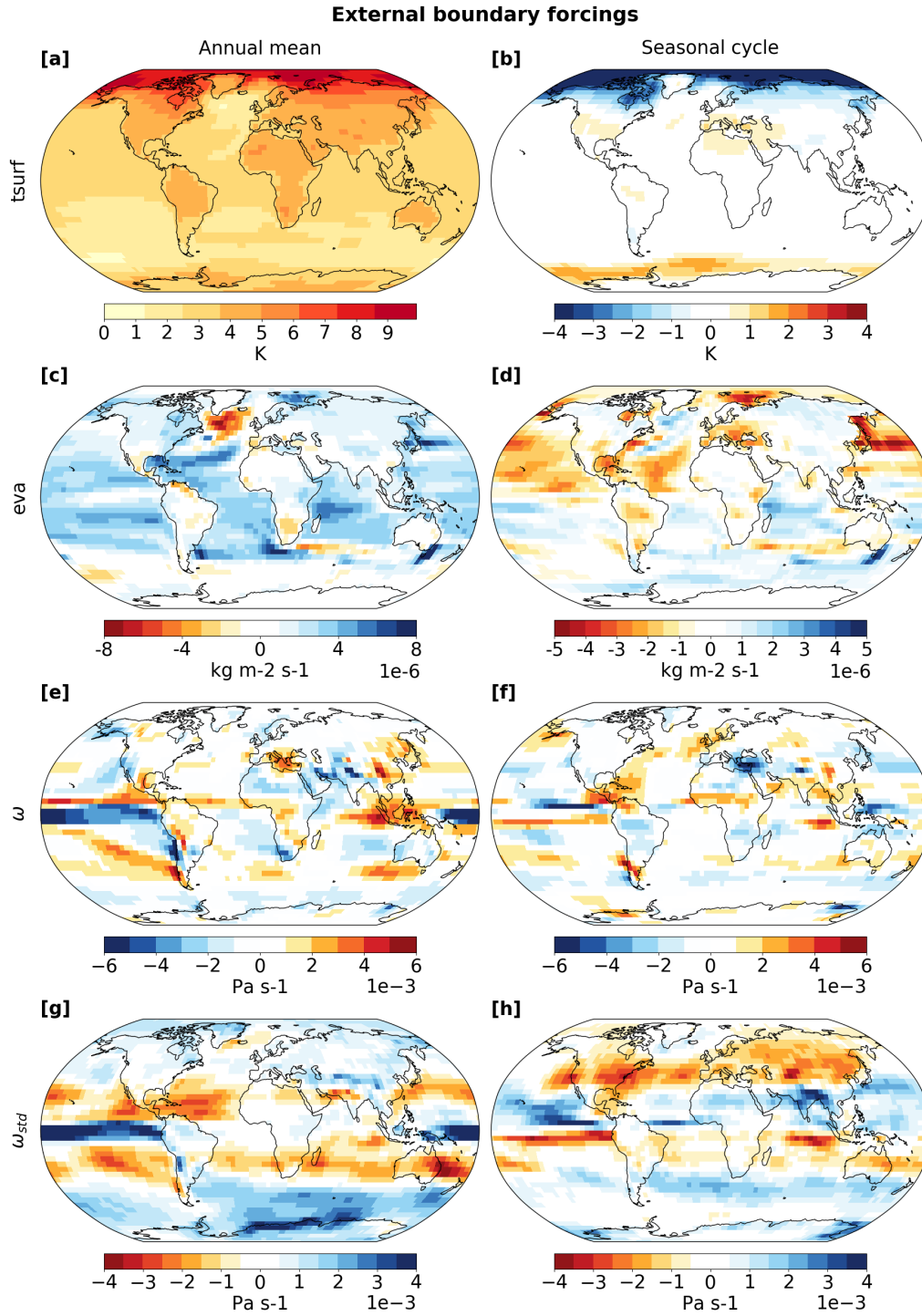
Figure 3.3: *CMIP5 RCP8.5 ensemble mean external boundary forcings for the GREB model of surface temperature (a, b), evaporation (c, d), mean vertical winds (e, f) and the daily variability of vertical winds (g, h). The annual mean is shown on the left (a, c, e, g) and the seasonal cycle (JJA-DJF) is on the right (b, d, f, h).*

Changes in ω_{mean} are marked by strong increase in upward motion over the central and eastern equatorial Pacific together with a fairly complex seasonal cycle change. For the tropical and subtropical regions outside the tropical Pacific regions the changes in

ω_{mean} are mostly a weakening of the mean state (e.g. increase in ω_{mean} where ω_{mean} is negative and decrease in ω_{mean} where ω_{mean} is positive). However, overall the changes in ω_{mean} do not project strongly on the control mean state (see Tab. 3.2).

ω_{std} strongly increases in the equatorial Pacific, mostly decreases in the subtropics and increases in the Southern Ocean. The seasonal cycle changes are similar in both hemispheres with increased variability in the subtropics and decreased variability in the mid-latitudes in summer relative to winter. It is important to note here, that the regional difference in change of ω_{std} does not match the changes in ω_{mean} (see weak correlation in Tab. 3.3).

The GREB model response of the precipitation to these four forcings is shown in Fig. 3.4 for the annual mean and the seasonal cycle. It compares very well with the ensemble mean CMIP5 response (Fig. 3.4a and e) and better than in in the previous chapter Fig. 2.11 because the climate change response of ω_{std} is included. The pattern correlation and amplitude of the annual mean and seasonal cycle of the GREB model is closer to the ensemble mean CMIP5 response than most CMIP5 models, indicating that the GREB model is representing the precipitation response in the CMIP5 ensemble well (Fig. 3.5). It is important to remember that the GREB model boundary conditions are forced by the CMIP5 ensemble mean. It further suggests that the ensemble mean CMIP5 precipitation response can be well understood in the context of the GREB model (eq. (2.11)) forced by the changes in the four environmental variables (Tsurf, Δq_{eva}, ω_{mean} and ω_{std}). In the next steps we will force the GREB model with only one environmental variable at a time, while keeping the others at control values. This will illustrate how each of the four forcings contribute to the precipitation changes. We will finish this section with a discussion of the relative role of each of the four forcings.

Table 3.2: *Correlation coefficient between precipitation and vertical velocity omega (mean and daily variability) for control and the climate change response.*

	Precip (control)	Omega (control)	Omega variability (control)
Change omega	0.24	-0.16	0.08
Change omega variability	-0.05	-0.16	0.29

Table 3.3: *Correlation between the external boundary forcings and the precipitation response of the sensitivity experiments.*

	Change evaporation	Change omega	Change omega variability	Change precip (Tsurf)	Change precip (evaporation)	Change precip (ω)	Change precip (ω variability)
Change precip (full)	0.19	-0.4	0.6	0.41	0.39	0.74	0.56
Change evaporation		0	-0.21	-0.06	0.82	0.04	-0.17
Change omega			-0.26	0.1	0.09	-0.58	-0.3
Change omega variability				0.25	-0.11	0.44	0.67
Change precip (Tsurf)					0.25	-0.15	-0.09
Change precip (evaporation)						0	-0.13
Change precip (ω)							0.48

Precipitation response

[a]   Annual mean   [b]   Seasonal cycle
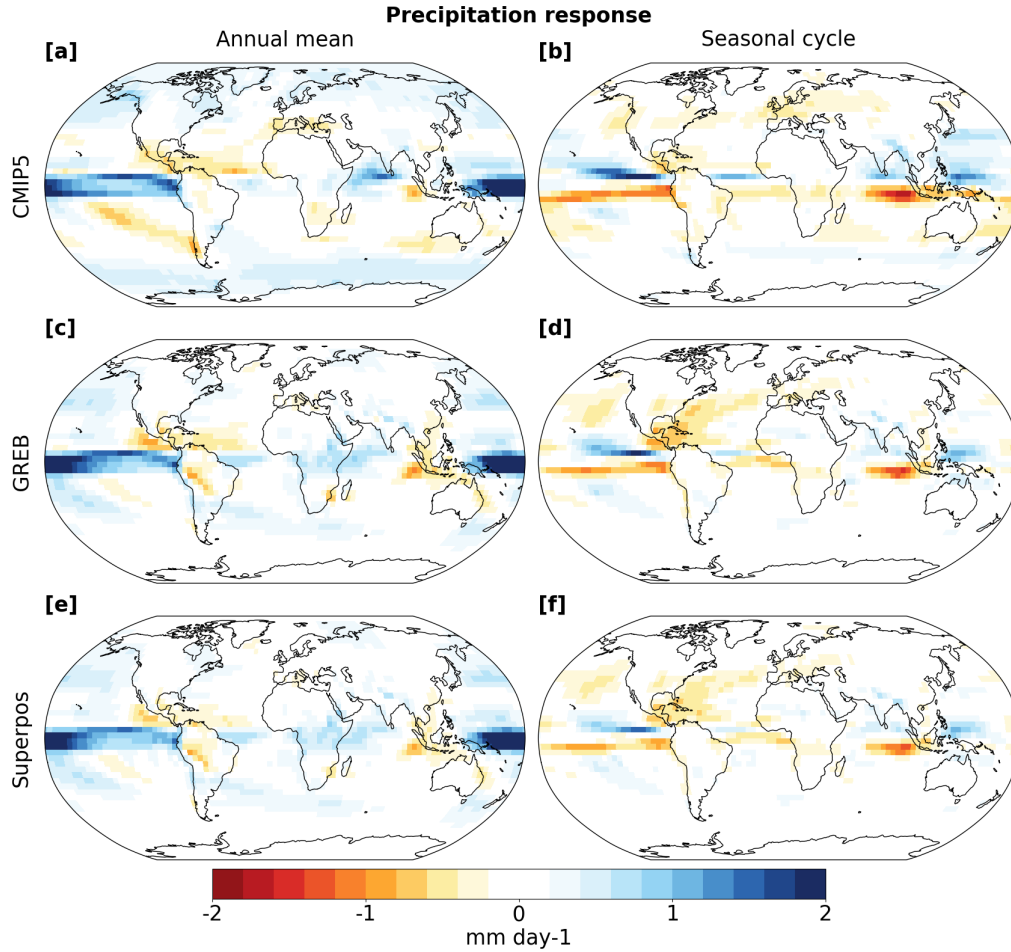
Figure 3.4: *Precipitation response to an RCP8.5 forcing in the CMIP5 ensemble mean (a, b), in the GREB model with all (surface temperature, evaporation, mean- and daily variability of vertical winds) forcings turned on (c, d) and the linear superposition of the single forcings (e, f). The annual mean is shown on the left (a, c, e) and the seasonal cycle (JJA-DJF) on the right (b, d, f).*

3.4.1   Surface temperature changes

We start with the Tsurf forcing, as it is the most robust forcing of climate change (Fig. 3.3a and b). Given that evaporation is kept at control values, the global mean precipitation cannot change, as it is in direct balance with evaporation at the global scale. However, it can have regional changes. In the GREB model the increase in Tsurf leads to an enhanced annual mean precipitation in the ITCZ and mid- to high latitudes and decreases precipitation in the subtropical dry zones in the annual mean (Fig. 3.6a). The annual mean response pattern compares well to the annual mean control precipitation in GREB (Fig. 3.2a) and has a correlation of 0.62 (Tab. 3.4). It thus fits moderately
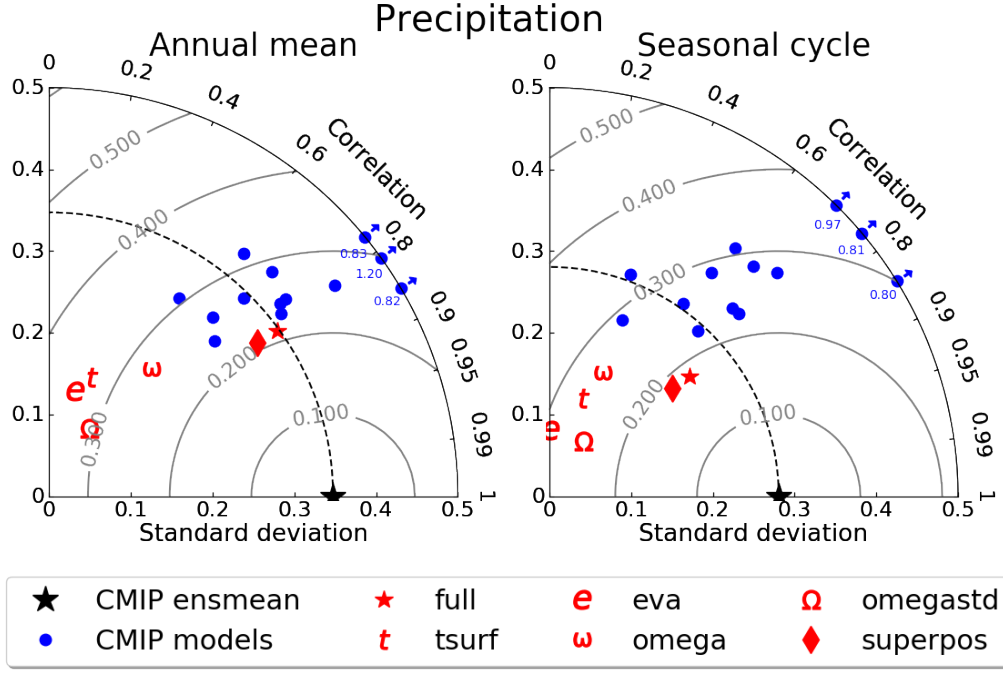
Figure 3.5: *Taylor diagram of the RCP8.5 precipitation response of CMIP5 models (blue), the GREB model with all (surface temperature, evaporation, mean- and daily variability of vertical winds) forcings turned on (⋆) and the linear superposition of the single forcings (♦) against the CMIP5 ensemble mean (★). The GREB model with single forcings of surface temperature (t), evaporation (e), mean vertical winds (ω) and daily variability of vertical winds (Ω) are also shown. The annual mean is shown on the left and the seasonal cycle (JJA-DJF) on the right. Some CMIP5 models are off the scale and indicated with a blue arrow and a number showing their standard deviation. The prescribed evaporation response is uncorrelated to the precipitation response but is the only process controlling the global mean change.*

well with the concept of the wet-get-wetter.

The increased Tsurf leads to an increase in atmospheric temperature (not shown), which initially, while the atmospheric humidity has not responded yet, leads to a strongly decreased relative humidity in the atmosphere. This in turn initially reduces the precipitation (see eq. (2.11)), which is controlled by relative humidity. Given the unchanged evaporation, the atmospheric humidity will start to increase until a new equilibrium between precipitation and evaporation is reached. This new equilibrium is at higher atmospheric humidity (Fig. 3.7d, but lower relative humidity (Fig. 3.7e). The latter changes reflect the now more effective precipitation terms in eq. (2.11), as they are all proportional to the atmospheric humidity (q), see Figs. 3.8d, e, f.

The increase in atmospheric humidity, increases the atmospheric moisture transport (Fig. 3.7f), as the moisture transport is directly proportional to the atmospheric humidity (eq. (2.18). The pattern of the changes in moisture transport is identical to the overall
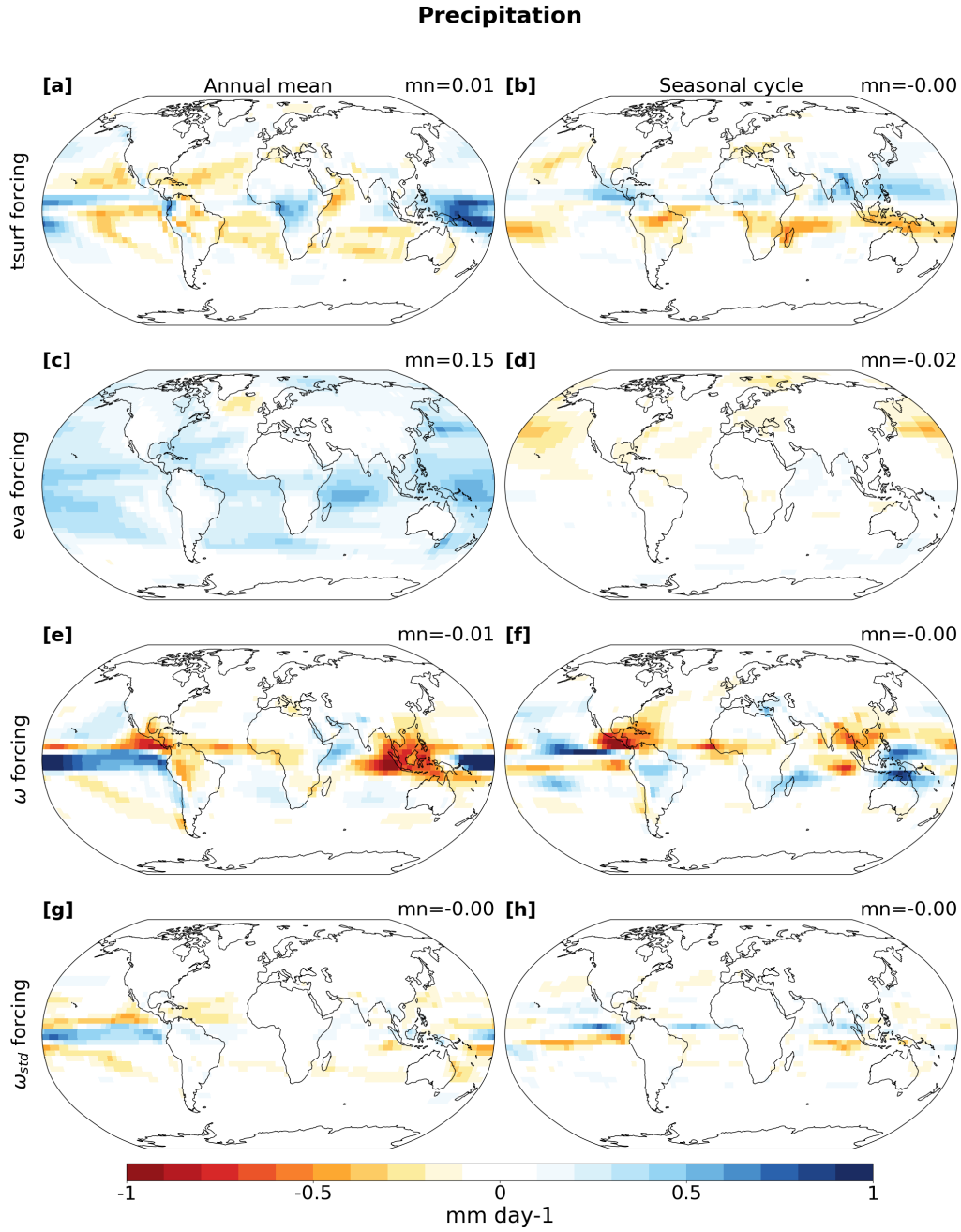
Precipitation

Figure 3.6: *Precipitation response decomposition for the single RCP8.5 forcings of surface temperature (a, b), evaporation (c, d), mean circulation ω (e, f) and the daily circulation variability ω_{std} (g, h). The annual mean is shown on the left (a, c, e, g) and the seasonal cycle (JJA-DJF) on the right (b, d, f, h). The top right of each plot shows the global mean value.*

changes in precipitation (compare Fig. 3.6a with 3.7f) with a correlation of 1.0 (Tab. 3.4). This is by construction, as evaporation is unchanged and any change in precipitation has then to come from changes in moisture transport. Thus, the precipitation changes due to Tsurf forcing lead to enhanced moisture transport that enhance precipitation in moisture convergence zones and reduces precipitation in regions with diverging moisture transport.

Table 3.4: *Correlation between control and climate change response for the four sensitivity experiments and the change in water vapour circulation.*

	Precip (control)	Omega (control)	Omega variability (control)	Change water vapour transport
Change precip (Tsurf)	0.62	-0.67	0.26	1
Change precip (evaporation)	0.61	-0.34	-0.29	-0.1
Change precip (omega)	-0.26	0.17	-0.09	1
Change precip (omega variab.)	-0.04	0.01	0.10	1

The same arguments hold for the changes in the seasonal cycle of precipitation. The response pattern shows an amplification of the control precipitation (compare Fig. 3.2b and Fig. 3.6b). Specific humidity increases more in winter than in summer (appendix Fig. B1a) and this amplification of the seasonal cycle of specific humidity leads to an enhanced seasonal transport (Fig. B1c). The enhanced seasonal transport of moisture supplies the enhanced seasonal precipitation (e.g. monsoon).

3.4.2 Evaporation changes

On the global scale, changes in precipitation must equate to changes in evaporation, to maintain the atmospheric moisture mass balance. Therefore, precipitation changes cannot in principle be separated from the prescribed evaporation changes in the GREB model. Here, it is interesting to note that the overall global pattern of precipitation (Fig. 3.4a) and evaporation changes (Fig. 3.3c) are fairly dissimilar (r=0.19, Tab. 3.3) despite the global constraint that the two have to be the same. This indicates, that the processes that control precipitation and evaporation on the local scale are fairly different. It is therefore useful to consider evaporation changes as a forcing for the precipitation on regional scales.

In the GREB model simulations the evaporation forcing, with all other forcings unchanged, leads to a global increase in annual mean precipitation with the largest increase in the tropics and sub-tropics (Fig. 3.6c). Only a few regions (e.g. Greenland) experience a decrease in annual mean precipitation. The response pattern is very similar to the forced evaporation pattern (r=0.82, see Tab. 3.3), when only evaporation is forced to change. Thus, the response in precipitation appears to be a direct local response
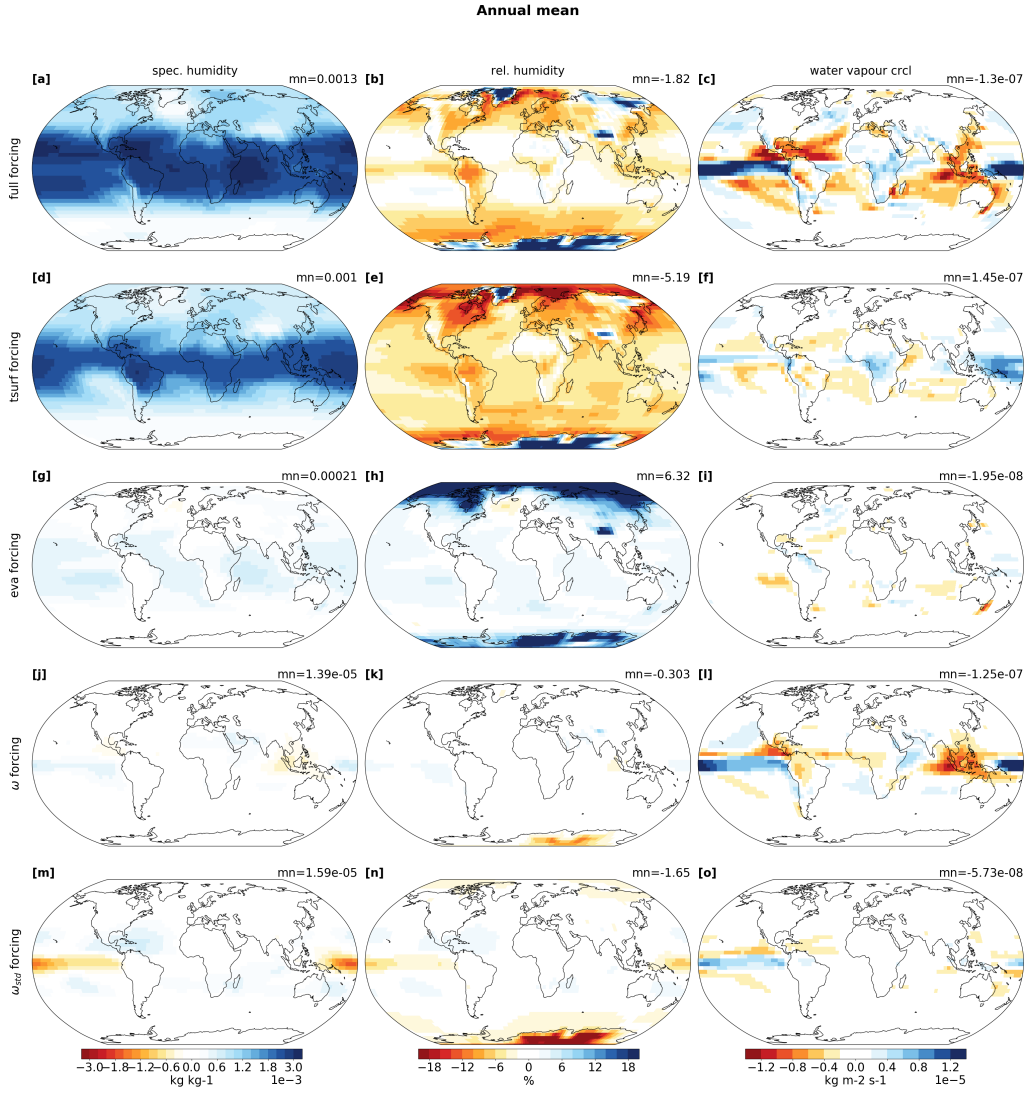
Figure 3.7: *Annual mean response of the specific humidity (a, d, g, j, m), relative humidity (d, e, h, k, n) and water vapour transport (c, f, i, l, o) for the fully forced GREB model (a-c), the single RCP8.5 forcings of surface temperature (d-f), evaporation (g-i), mean circulation ω (j-l) and the daily circulation variability ω_{std} (m-o). The top right of each plot shows the global mean value.*

to the evaporation forcing over oceans. Over land this direct relationship is weaker. Since atmospheric temperature is not changing, the atmosphere cannot take up more moisture (Figs. 3.7g and 3.7h), therefore any increase in evaporation has to immediately precipitate locally. This is further supported by the moisture terms of the precipitation parameterisation (eq. (2.11)) which is the main driver of the precipitation response (Fig. 3.8g), whereas the other two terms contribute little. As the water vapour in the atmosphere does not increase much, relative humidity is changing only marginally in the tropics and subtropics. The seasonal cycle changes of precipitation follow the same arguments.
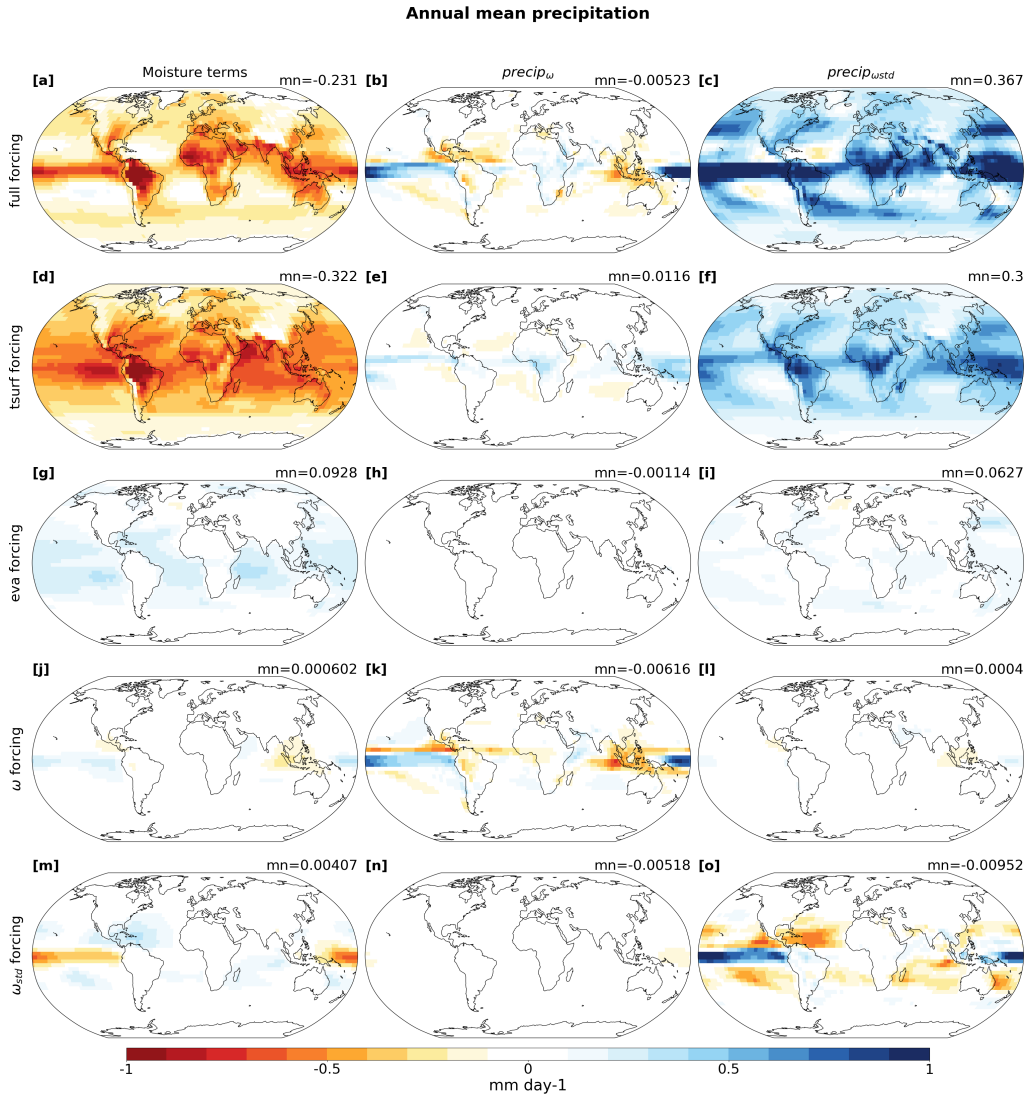
Figure 3.8: *Annual mean response of the specific humidity (a, d, g, j, m), relative humidity (d, e, h, k, n) and water vapour transport (c, f, i, l, o) for the fully forced GREB model (a-c), the single RCP8.5 forcings of surface temperature (d-f), evaporation (g-i), mean circulation ω (j-l) and the daily circulation variability ω_{std} (m-o). The top right of each plot shows the global mean value.*

While the global pattern of evaporation changes has very little relation to the global pattern of the fully forced precipitation changes (r=0.19, Tab. 3.3), the global mean evaporation changes do control the global mean precipitation changes (or vice versa). Here it is remarkable that the overall evaporation changes (Fig. 3.3c) are only about 2% per degree global warming in CMIP5 models. This is much less than the 7% per degree global warming expected from the simple thermodynamic Clausius–Clapeyron relation, assuming eq. (2.12) with no circulation changes and unchanged atmospheric relative humidity. Thus, the evaporation changes appear to be strongly affected by dynamical changes in the atmospheric circulation. See also discussion in Richter and Xie (2008).

3.4.3 Mean vertical velocity changes

Mean vertical velocity (ω_{mean}) in GREB has two main effects. It affects precipitation directly through the parametrisation (eq. (2.11)) and indirectly through the transport of moisture (eq. (2.18)) which in turn plays a role in the precipitation parametrisation through specific and relative humidity. The forced annual mean CMIP5 RCP8.5 change in the ω_{mean} boundary condition shows a strong increase in the tropical Pacific ascending motion and a general weakening of the subtropical descending motion (Fig. 3.3e). However, the Maritime Continent shows weaker ascent compared to control.

The precipitation response pattern in GREB (Figs. 3.6e and f) compares well to the pattern in the ω_{mean} change (Figs. 3.3e and f; r=-0.58 see Tab. 3.3), indicating that the precipitation changes are a direct response to the circulation changes. This is reflected in the precipitation terms (Figs. 3.8j, k, l), which only show changes in the $precip_{\omega mean}$ term and little changes in the other two terms. It is also illustrated by the small changes in humidity and relative humidity (Fig. 3.7j and k) and the clear changes in moisture transport (Fig. 3.7l). As in the previous sensitivity experiment the surface temperature is forced to stay at control values allowing the atmosphere not to take up much more moisture before reaching saturation and therefore keeping humidity nearly unchanged. Thus, the precipitation changes are the combined effect of changes in the $precip_{\omega mean}$ term of eq. (2.11) and the changes in moisture transport that both work in the same direction.

3.4.4 Vertical velocity variability

The ω_{std} boundary condition affects precipitation directly through eq. (2.11). The precipitation response in GREB to this sensitivity experiments roughly matches the external boundary forcing of ω_{std} (compare Figs. 3.3g and 3.6g) with a correlation coefficient of 0.67 (Tab. 3.3). There is an increase in annual mean precipitation in the tropical Pacific, generally decreasing precipitation in the subtropics and small to no changes in higher latitudes, especially in the southern hemisphere.

Although ω_{std} only acts through the precipitation parameterisation it has a strong effect on specific humidity (Fig. 3.7m) and water vapour circulation (Fig. 3.7o). A decrease of ω_{std} leads to a decrease in precipitation in these areas. Since evaporation

is at control values and precipitation decreased, moisture will accumulate and humidity increases. The opposite holds for the tropical Pacific where an increase in vertical velocity variability leads to more precipitation and depletes moisture. The general increase in specific humidity increases the moisture terms of the precipitation equation (eq. (2.11); Fig. 3.8m) and affects the moisture circulation (eq. (2.18)) which counteracts the accumulation of moisture and transports moisture from the subtropics into the tropical Pacific (Fig. 3.7o). This change in moisture transport then supplies the water vapour needed to keep up the changes in precipitation.

3.4.5 Superposition

All four sensitivity experiments described above (Tsurf, evaporation, ω_{mean} and ω_{std}) are added together in a linear superposition to evaluate if they sum up to the fully forced GREB model precipitation response in the annual mean and the seasonal cycle (Figs. 3.4e and 3.4f). The superposition is close to the fully forced GREB model precipitation response and to the CMIP5 response in both the annual mean and seasonal cycle patterns (Fig. 3.5), suggesting that we can think of the precipitation response as a linear combined effect of the four individual forcings. This is somewhat surprising, considering the non-linear nature of precipitation processes. It is further remarkable that none of the four individual forcings dominate the total precipitation response (Fig. 3.5). The total precipitation is indeed a clear combination of all four forcings. The annual and seasonal cycle precipitation response is most strongly related to the changes in ω_{mean}, indicating that atmospheric circulation changes are the main drivers of the precipitation changes. The thermodynamic warming effect (Tsurf) has a somewhat weaker contribution to the total precipitation changes, suggesting that the thermodynamic, wet-get-wetter, processes are less important than dynamical changes.

Changes in the evaporation patterns are less correlated with the patterns of precipitation changes (Fig. 3.5), but they do control the global mean precipitation changes (which are not evaluated by Fig. 3.5), as the global moisture mass balance is a direct balance between total precipitation and evaporation. Thus, the processes of evaporation changes are essential for understanding the precipitation changes.

An alternative and simplified presentation of the combined precipitation and evaporation changes is the zonal mean precipitation minus evaporation (P-E) changes, which

gives a good presentation of the large-scale changes (Fig. 3.9). The main changes in the CMIP5 ensemble are best described by the wet-get-wetter idea: increase in p-e near the wet equator, decrease in the dry subtropics and increase in the wet higher latitudes. This main signature is captured by both the GREB model with all forcings and by the superposition of the GREB model forced with individual forcings. However, the GREB model does overestimate the equatorial response and does underestimate the higher latitudes response. When we look at how each of the individual forcings contribute to this zonal p-e pattern, it is interesting to note that all four elements contribute to it. Most similar in terms of the overall structure, though, is the ω_{std} contribution, indicating that changes in the atmospheric variability contribute to this p-e pattern. However, GREB does have some limitations when compared to the CMIP5 ensemble mean response. GREB is too wet in the ITCZ and the decrease of precipitation in the subtropics is too weak (Fig. 3.9). In the mid- to high-latitudes in both hemispheres GREB does not capture the drying that can be seen in CMIP5.
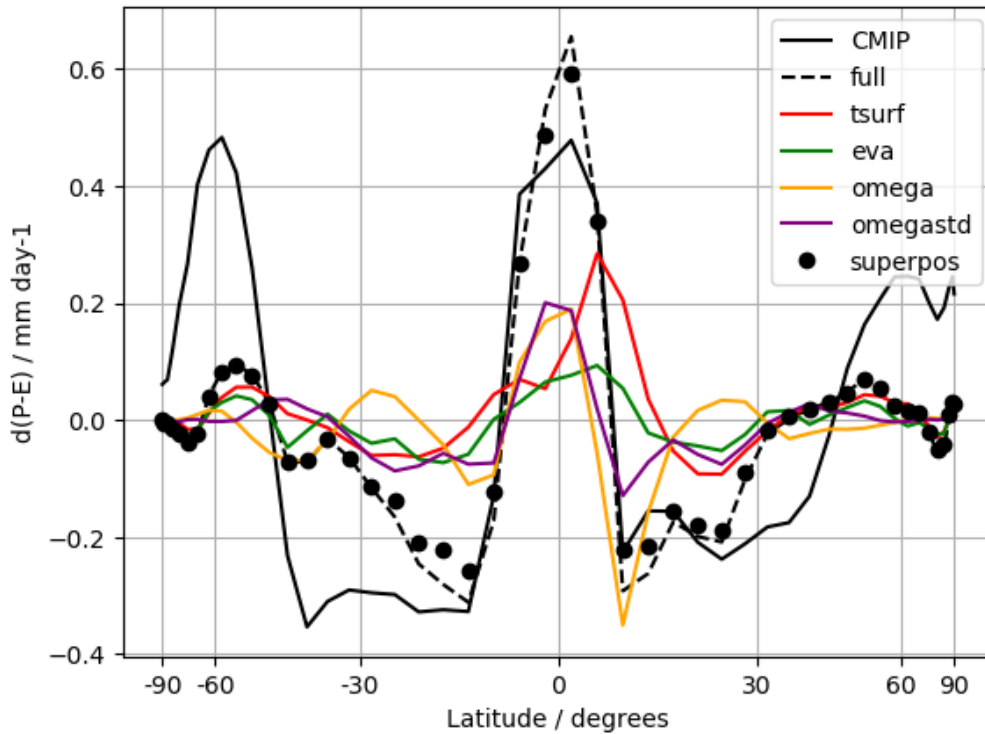
Figure 3.9: *Annual and zonal mean precipitation minus evaporation response for the CMIP5 RCP8.5 ensemble mean (black solid), the GREB model with all (surface temperature, evaporation, mean- and daily variability of vertical winds) forcings turned on (black dashed), the single forcing of surface temperature (red), evaporation (green), mean circulation (yellow) and circulation variability (purple) and the linear superposition of the single forcings (black circles). The x-axis is weighted by the cosine of latitude.*

3.5　Chapter Summary and Discussion

In this chapter we used the simple climate model GREB to decompose the CMIP5 simulations response of precipitation to climate change. The simplicity of the GREB model allows us to force single aspects of the climate system to change according to the CMIP5 ensemble mean response while other aspects remain at control values. We presented the precipitation changes as the result of four different forcings: surface temperature, evaporation, mean circulation and circulation variability changes. The four different forcings of precipitation changes add almost linearly in the GREB model, while still giving a good representation of the changes in the CMIP simulations. This suggests that the CMIP precipitation changes can, to a large part, be considered as linear superposition of these four forcings. The effect of each of the four forcings is illustrated in the sketch of Fig. 3.10. The main findings of each of the four forcings can be summarised as follows:

Surface temperature: The increase in surface temperature, with the directly associated increase in atmospheric temperature, results in an increase in atmospheric humidity (Fig. 3.10a). This intensifies the atmospheric transport of humidity, which increases precipitation in convergence zones and decreases precipitation in divergence regions. This is the wet-get-wetter principle. In this direct effect of atmospheric warming, the surface warming pattern has little to no effect on the pattern of precipitation changes, as the latter is primarily a reflection of the mean atmospheric circulation state. However, in reality the surface warming pattern does have an important control on the atmospheric circulation changes, which do affect precipitation changes more strongly than the direct warming effect. Further the atmospheric circulation changes induced by the warming pattern do also affect the evaporation changes (Richter and Xie, 2008).

Evaporation: In the absence of any other changes, an increase in evaporation leads to a direct local increase in precipitation (Fig. 3.10b). However, the more important control of evaporation is on the global scale, as global precipitation is directly balanced by global evaporation changes. Here is it interesting to note that global evaporation is only increasing by about 2% per degree global warming, exactly balancing the global precipitation changes by construction. This is in contrast to the $+7\%$ per degree global warming that would be expected from the evaporation bulk formula eq. (2.12), if there are no circulation and no relative humidity changes. This is also what the GREB model
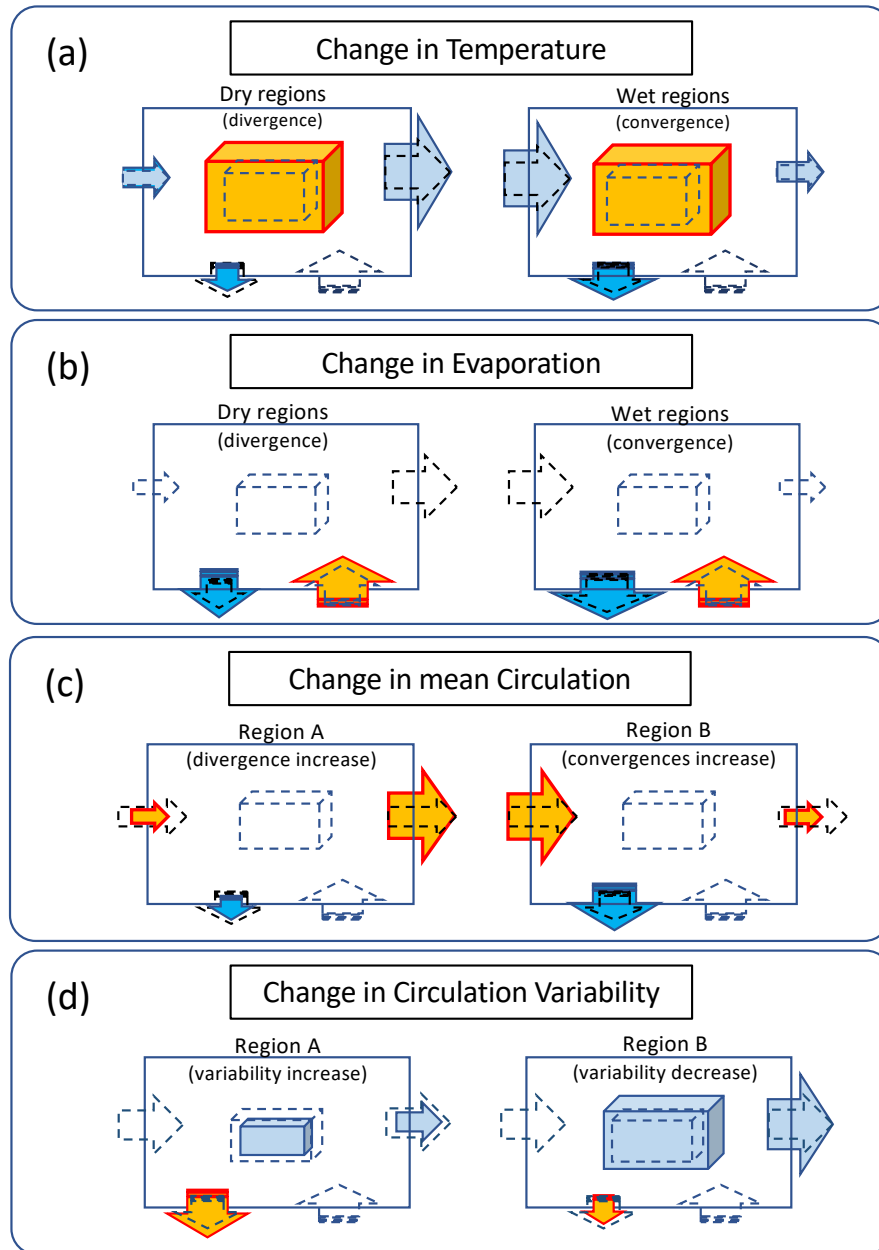
Figure 3.10: *Schematic illustration of how changes in the four boundary conditions affect precipitation. Dashed cubes and arrows mark the control state values. Orange cubes and arrows mark changes directly forced by change in the boundary conditions. Blue cubes and arrows are resulting changes due to the response of the climate system to the forcings (orange).Panel (d) only illustrates the forced changes in precipitation (orange), but not the resulting changes (blue), as they depend on the mean circulation.*

would simulate in response to CO2 or surface warming forcing if no circulation changes are imposed (not shown; see also Stassen et al., 2019). While precipitation and evaporation are balanced on a global scale, it is unclear which of the two processes is forcing the

muted 2% increase per degree global warming. The differences in the evaporation and precipitation patterns in both the mean state and the changes suggest that the processes controlling them are different. The strong impact of circulation and relative humidity changes on the evaporation (Richter and Xie, 2008) therefore suggest that studying the processes that control evaporation changes could be essential for understanding precipitation pattern changes. Future studies, using the GREB model or otherwise, need to focus on the conceptual understanding of the processes that control future evaporation changes.

Mean circulation: Changes in the mean circulation affect the precipitation in two ways: they change the atmospheric transport of the humidity (Fig. 3.10c) and they change the precipitation directly by the parameterisation eq. (2.11). Both combine to increase (decrease) precipitation in regions with increased convergence (divergence). The change in mean circulation is the single most important direct effect of the four forcings. This is consistent with previous studies using GCM data, which have emphasised the importance of dynamic rather than thermodynamic drivers of precipitation change at regional scales (Chadwick et al., 2013; Kent et al., 2015; Muller and O'Gorman, 2011; Seager et al., 2010). Circulation changes also affect precipitation changes indirectly by affecting the evaporation changes, which further increases the importance of atmospheric circulation changes.

Circulation variability: In the GREB model the effect of weather variability on precipitation is parameterised in eq. (2.11) by ω_{std}. An increase (decrease) in ω_{std} directly increases (decreases) precipitation. In the absence of any other changes (e.g. no evaporation changes) it does decrease (increase) the atmospheric humidity and subsequently decrease (increase) the atmospheric moisture transport (Fig. 3.10d). While the overall direct impact of ω_{std} changes are the smallest of the four forcings, they are still relevant. In the context of time-mean precipitation changes this effect has not been discussed much in the literature, although Vecchi and Soden (2007) discussed a reduction in the daily omega variability in the context of the weakening of the tropical circulation. Pendergrass and Gerber (2016) also found a decrease of standard deviation of the daily vertical velocity distribution. Weller et al. (2019) found that the ω_{std} response might be related to a decrease in low-level convergence lines. Further, the study of Richter and Xie (2008) suggests that in reality the ω_{std} will also affect the evaporation. In particular,

the reduction of ω_{std} in the subtropical ocean regions (Fig. 3.3g) has a high potential of affecting evaporation, as it is the region where evaporation is strongest (Fig. 3.2c). This suggest that studying changes in high-frequency (weather) variability may be important to understand large-scale precipitation and evaporation changes.

A combined effect of the warming (Tsurf) and changes in the weather variability (ω_{std}) is that the relative importance of the different precipitation terms in eq. (2.11) are changing (see Fig. 3.8a-c). This suggests that the importance of the steady, thermodynamic, precipitation is decreasing (Fig. 3.8a), while the importance of precipitation associated with weather variability is increasing (Fig. 3.8c). Thus, the nature of precipitation is changing globally (e.g. extreme precipitation increases by 7%/K Ban et al., 2015; Muller and O'Gorman, 2011) while mean precipitation is radiatively constrained (i.e. Allen and Ingram, 2002). The focus of this chapter was the conceptual understanding of projected precipitation changes. However, this chapter also introduced a new approach of analysing precipitation changes by using the GREB model as a diagnostic tool. This approach is indeed capable of analysing the projected precipitation change of the CMIP model with a focus on understanding the processes forcing these changes. This approach can also be used to understand problems in the CMIP model simulations to simulate the mean climate or to understand the diversity in the future CMIP projections of the hydrological cycle changes.

Chapter 4

Precipitation Biases in CMIP5 models

4.1 Preface

The simple deconstruction approach developed in chapter 3 provides a powerful basis on which the hydrological cycle of CGCM simulations can be analysed and was applied to get a more quantitative understanding of precipitation biases in CMIP5 models. To achieve this, the GREB precipitation equation is fitted to observations and CMIP5 model data output using the least-squares method. The fitting parameters for the CMIP5 models are compared against the observed precipitation parameter set. The values of the fitting constants are used as an indication of how CMIP5 model precipitation reacts to changes in the boundary conditions. The results of the fitting indicate that CMIP5 models are overly sensitive to the vertical mean velocity, which is confirmed by other studies but show too little sensitivity to atmospheric variability of vertical air motion (weather). Although precipitation in CMIP5 models reacts too sensitive to the mean circulation the conceptual deconstruction highlights the importance of moisture transports to the total precipitation bias independent of the mean vertical velocity.

4.2   Introduction

Coupled general circulation models (CGCMs) used by the Intergovernmental Panel on Climate Change (IPCC) simulate processes in the ocean, on land and in the atmosphere. CGCMs focus on the most realistic and best representation of the climate system. The increasing computational power has allowed to consider more and more processes in the climate system to be included and the resolution of models to be increased. While it has been shown that increasing the model resolution addresses a lot of common problems seen in CGCMs (Haarsma et al., 2016), such as aspects of the large-scale circulation (Masson et al., 2012; Shaffrey et al., 2009), the global water cycle (Demory et al., 2014), movements of the Atlantic inter-tropical convergence zone (ITCZ) (Doi et al., 2012) and the diurnal precipitation cycle (Birch et al., 2014; Sato et al., 2009) several existing problems, such as substantial precipitation biases remain unsolved. On the global scale all CMIP5 models overestimate precipitation over land and there exists a large inter model spread in the tropics Liu et al. (2014), precipitation in the Atlantic ITCZ and eastern Pacific ITCZ is overestimated (Yin et al., 2013), there is generally too much precipitation south of the equator, particularly in boreal spring (Richter et al., 2014, 2016) and compared to the Global Precipitation Climatology Project (GPCP) and Tropical Rainfall Measuring Mission (TRMM) CGCMs rain too much (Stanfield et al., 2015).

Precipitation and atmospheric water vapour are closely related (Bretherton et al., 2004). This suggests that biases in precipitation are related to biases in water vapour and Li et al. (2014) found that water vapour is mostly underestimated over strong convective areas in the tropics. Yang et al. (2018) analysed four CMIP5 models and found that all overestimate precipitation over tropical oceans and Richter et al. (2016) found the same for a larger ensemble. Their results suggest that errors in the frequency of vertical velocity are a significant cause of biases in atmospheric moisture and precipitation. Additionally, the models were overly sensitive to a given vertical velocity regime compared to observations and strong upward motion was also overestimated in models.

The majority of these biases can be related to uncertainties in the model formulations (Bony et al., 2006; Meehl et al., 2007; Hawkins and Sutton, 2009). Physical parameters in climate models are generally tuned to minimise biases but, the 'true' values are mostly

unknown. This can be due to the lack of a measurable physical equivalent, or the inability to numerically test all possible parameter combinations (Severijns and Hazeleger, 2005; Randall et al., 2007; Mulholland et al., 2017).

While many studies use the perturbed physics ensemble approach to estimate the uncertainties that arise from uncertainties in model formulations (e.g. Murphy et al., 2004; Stainforth et al., 2005; Collins et al., 2006; Sanderson et al., 2008b,a) not many studies consider their effect on the climate mean state and how the mean state affects climate sensitivity (Dommenget, 2016).

Although some of the studies mentioned above highlight biases in the hydrological cycle and its processes (e.g. Yang et al., 2018) a much deeper understanding of the quantitative contribution of systematic model biases on the hydrological cycle is needed. Similarly to the approach of Dommenget (2016) the biases in the hydrological cycle mean state can be separated into biases in the model formulations and biases in the mean state. Building on the precipitation equation developed in chapter 2 biases in precipitation will be separated into biases in the fitting constants (e.g. c_ω) and biases in the boundary conditions (e.g. ω_{mean}). In particular the contribution of surface temperature, evaporation, mean circulation and circulation variability biases will be quantified. Thus, different from previous work we will investigate the biases in precipitation in conjunction with biases in mean state in four climate variables to provide a wholesome picture of biases in precipitation. The importance of biases in vertical velocity are highlighted and are then further subdivided into their quantitative contribution to a direct bias on precipitation and biases in the moisture transport.

The following section will introduce the data, models and methods used. It will in particular discuss the Globally Resolved Energy Balance (GREB) precipitation equation and how we make use of the GREB model and the precipitation equation itself as an analysis tool. In section 4.4 the main results of this study will be presented. Finally, we give a chapter discussion and a summary of the results.

4.3   Data and Methods

This section provides an overview on the CMIP5 model data used. It further gives a short introduction to the precipitation equation, which is the main focus for this chapter.

4.3.1 Data

The models of Coupled Model Intercomparison Project phase 5 (CMIP5) (Taylor et al., 2012) used in this study are summarized in Tab. 4.1. We used all available models of the historical and RCP8.5 scenario that provided the variables and time frequency needed for the analysis presented in this study. All datasets are re-gridded to a horizontal resolution of $3.75^o \times 3.75^o$ to match the GREB model horizontal resolution and monthly climatologies are calculated. For the climatology of ω_{mean} and ω_{std} a daily output frequency is used and an unweighted vertical mean over all levels is applied to smooth the data. The multi-model ensemble mean over all models in Tab. 4.1 is calculated. Models with more than one realization are considered by the average of all realizations (i.e. a model with one realisation and a model with many realisations are weighted equally in the multi model ensemble mean). The boundary conditions biases (deviation from the multi-model ensemble mean) of the precipitation equation, used to force the GREB model, are calculated against the ensemble mean and are shown in Fig. 4.1 for three models that are best mimicked by the GREB model. The precipitation biases against the ensemble mean for the same three models are shown in Fig. 4.2.

In this chapter less models were available than in the previous chapter. The main limiting factor, as previously, are models with a daily output frequency of vertical velocity, ω. Additionally, to fit the GREB model precipitation equation, surface specific humidity, q, is also required for the historical and RCP8.5 scenario further limiting the models available.

Table 4.1: *List of CMIP5 models used in the precipitation bias deconstruction.*

Models	
ACCESS1-0	ACCESS1-3
BNU-ESM	FGOALS-g2
GFDL-ESM2G	GFDL-ESM2M
IPSL-CM5A-LR	MIROC-ESM-CHEM
MIROC5	MRI-CGCM3

4.3.2 GREB model

The GREB model has been described in chapter 1.2 and 2.
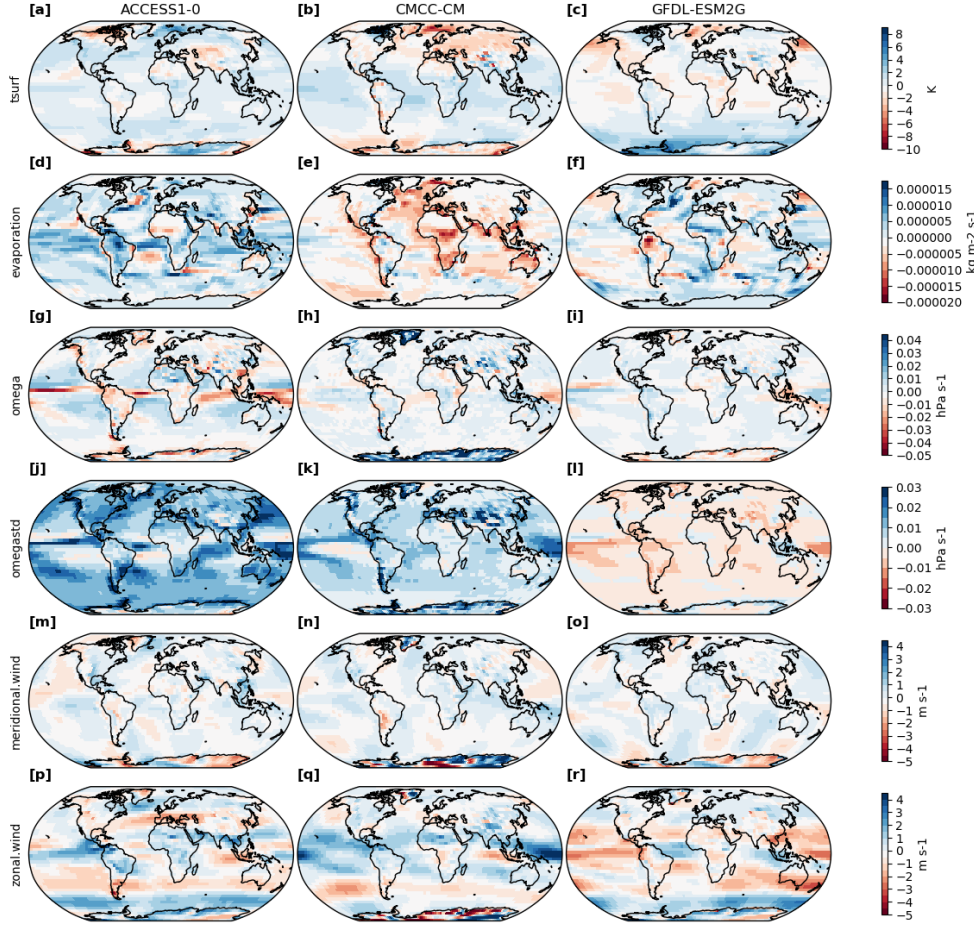
Figure 4.1: *Biases against the ensemble mean of surface temperature (a,b,c), evaporation (d,e,f), mean vertical velocity (g,h,i), vertical velocity variability (j,k,l), meridional wind (m,n,o) and zonal wind (p,q,r) for the ACCESS1-0 (left), CMCC-CM (middle), and GFDL-ESM2G (right) model. The sum of anomalies of all models in Tab. 4.1 is zero.*

4.4 Quantitative analysis of precipitation biases

Assuming the GREB model precipitation equation (eq. 2.11) were a perfect estimation for precipitation if given the 'correct' set of fitting constant and the 'correct' boundary conditions: specific humidity, q, relative humidity, rq, mean vertical velocity, ω_{mean} and vertical velocity variability, ω_{std}, precipitation biases in this equation can have two sources of origin. Either the fitting constants are 'incorrect' or there are biases in the boundary conditions. It is therefore a reasonable approach to test both hypotheses.

In the previous two chapters the model precipitation parameters, c_q, c_{rq}, c_ω and $c_{\omega std}$ were fitted to minimise the root mean square error between observations (i.e. GPCP) and the GREB simulated precipitation. The external boundary conditions of

Precipitation
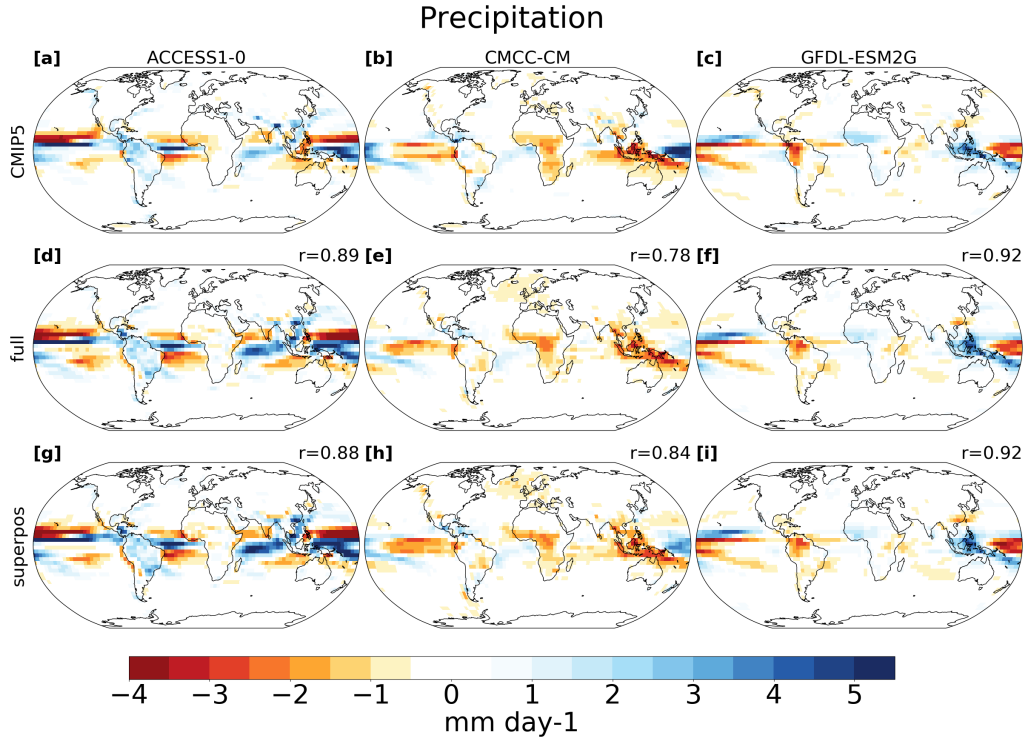
Figure 4.2: *Anomalies against the ensemble mean of surface temperature (a,b,c), evaporation (d,e,f), mean vertical velocity (g,h,i), vertical velocity variability (j,k,l), meridional wind (m,n,o) and zonal wind (p,q,r) for the ACCESS1-0 (left), CMCC-CM (middle), and GFDL-ESM2G (right) model. The sum of anomalies of all models in Tab. 4.1 is zero.*

mean vertical velocity, ω_{mean}, and vertical velocity variability, ω_{std}, were taken from the ERA-Interim reanalysis. The performance of the GREB model with this 'observed' precipitation equation is discussed in detail in the model development chapter, chapter 2.

However, the precipitation that the GREB model is fitted to (i.e. GPCP) and the boundary conditions used as precursors (e.g. ω_{mean} taken from ERA-Interim) can easily be replaced by model output taken from CMIP5 models (e.g. precipitation and ω_{mean} taken from CMIP5). This fitting process can be done independently for each CMIP5 model and for each scenario (i.e. historical and RCP8.5) as long as all variables needed for the fitting are available. Considering the precipitation equation (eq. 2.11) the following variables are required for the historical and RCP8.5 simulation: precipitation, specific humidity, surface temperature, vertical velocity. Apart from ω, which is required at a daily output frequency, a monthly output frequency is sufficient. For the fitting routine a multivariate regression has been used.

This leaves two possibilities how biases in CMIP5 precipitation can be analysed in GREB. The method described above of fitting the precipitation parametrisation against

the output of CMIP5 models and using the conceptual deconstruction method described in chapter 3 to drive the GREB model by forced changes in ω_{mean}, ω_{std}, Δq_{eva} and surface temperature. Both methods will be discussed in this order in the next two sections.

4.4.1   CMIP5 Precipitation Parameters

Fitting the GREB precipitation equation to the CMIP5 models listed in Tab. 4.1 returns 11 sets of new precipitation parameters (10 CMIP5 models plus the ensemble mean of the 10 models). The optimised parameters for each of the CMIP5 models are summarised in Tab. 4.2.

Table 4.2: *Precipitation parameters for observed precipitation, 10 different CMIP5 models, the ensemble mean of the 10 CMIP5 models and the average of the fitted parameters. The spread of the model parameters is shown as standard deviation.*

Variable	$c_{q_{ctrl}}$	$c_{q_{rcp}}$	$c_{rq_{ctrl}}$	$c_{rq_{rcp}}$	$c_{\omega_{ctrl}}$	$c_{\omega_{rcp}}$	$c_{\omega std_{ctrl}}$	$c_{\omega std_{rcp}}$
Observed	-1.88		2.25		-17.69		59.07	
ensmean	-0.65	-0.72	1.67	1.56	-41.97	-38.83	33.26	27.86
ACCESS1-0	-0.58	-0.65	1.74	1.66	-30.38	-30.02	21.63	20.03
ACCESS1-3	-0.13	-0.18	1.05	1.01	-29.26	-28.64	24.56	22.14
BNU-ESM	-1.23	-0.98	2.29	1.87	-39.57	-38.40	35.66	30.97
FGOALS-g2	-1.02	-1.00	2.24	2.13	-32.81	-30.73	28.01	26.59
GFDL-ESM2G	-0.75	-0.78	1.84	1.75	-40.43	-39.56	27.62	27.43
GFDL-ESM2M	-0.75	-0.77	1.84	1.87	-40.93	-40.18	27.54	27.79
IPSL-CM5A-LR	-1.40	-0.81	2.50	1.36	-39.47	-35.23	33.89	25.36
MIROC-ESM-CHEM	-0.72	-0.7	1.55	1.41	-37.95	-37.70	26.81	23.81
MIROC5	-0.94	-1.12	2.09	2.39	-36.16	-35.80	31.00	31.61
MRI-CGCM3	-1.06	-0.96	1.99	1.79	-37.67	-37.60	29.96	27.19
average	-0.86	-0.86	1.91	1.72	-36.46	-35.39	28.67	26.3
std	0.34	0.25	0.39	0.37	4.00	3.95	3.95	3.44

The value of the precipitation parameters can be used as an indication on how important they are in producing rainfall. That is for instance in observations the fitting parameter for circulation variability, $c_{\omega std}$, is by far the largest value making ω_{std} the most important of the fitting variables. This means the 'observed' precipitation model is most sensitive to the circulation variability and its changes. Therefore, the value of the individual precipitation parameters will now be used to explain how sensitive the model is to the four atmospheric variables for each CMIP5 model.

Comparing the observed precipitation parameter set to the one fitted to each CMIP5 model listed in Tab. 4.1 several interesting differences can be found. Starting with the parameters fitted to the control simulation (indexed with 'ctrl' in Tab. 4.2) when compared to the observed precipitation parameter set it is found that consistently all CMIP5 models used in this chapter underestimate the moisture parameters c_q and c_{rq} compared to the observed parameters. This means that for a given specific humidity less precipitation falls in the CMIP5 fitted parametrisation than for the observed parametrisation. This general underestimation gets very extreme for the ACCESS1-3 model which has nearly no sensitivity to specific humidity, c_q parameter, and is also the least sensitive model to relative humidity, c_{rq} parameter.

Both moisture related terms are used in combination rather than looking at them individually. This is done firstly because specific humidity and relative humidity are closely related to each other but also because the specific humidity parameter, $c_{q_{ctrl}}$, is negative for the observations and all models, which might be caused by having two moisture terms ($precip_q$ and $precip_{rq}$) in the GREB precipitation equation. A negative specific humidity precipitation term does physically not make sense when considered by itself as more specific humidity would lead to less rainfall. However, when considered in combination with the relative humidity parameter, $c_{rq_{ctrl}}$, they become physically more meaningful. Considering only the moisture terms of the precipitation equation (eq. 2.11) and rearranging the equation for $\Delta q_{precip} = 0$ leads to:

$$rq_{\Delta q_{precip}=0} = \frac{q}{q_s} = -\frac{c_q}{c_{rq}} \cdot 100 \tag{4.1}$$

For the observed parameter combination ($c_q = -1.88$ and $c_{rq} = 2.25$) the moisture terms are balanced at a relative humidity of 84% and are neither producing nor suppressing rainfall in the GREB precipitation equation. Yet, even small increases in relative

humidity would lead to a strong response in precipitation in the moisture terms. It is important to note here that each individual precipitation term, apart from the circulation variability term, in the GREB precipitation equation can become negative and thus produce negative rainfall. However, the sum of all precipitation terms is hardly ever negative for non-arid regions (Fig. 4.3 top) and if negative negligible when compared to the global annual mean precipitation value (Fig. 4.3 bottom). To avoid any negative rainfall there is an additional fail safe implemented to force the sum of all precipitation terms to be positive at all time.
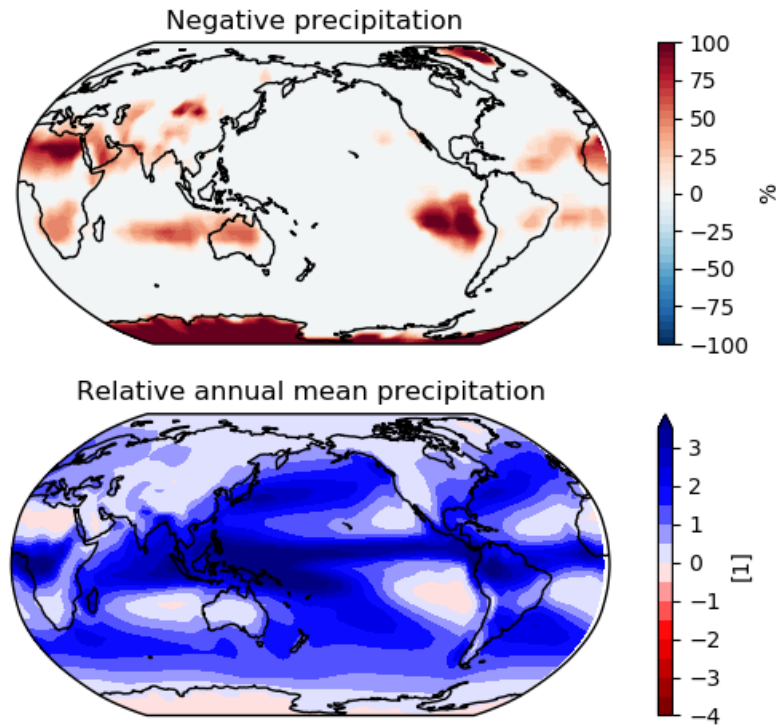
Figure 4.3: *Top: Annual mean of the relative occurrence of negative precipitation in % without fail safe. Bottom: Annual mean precipitation divided by global annual mean precipitation (unit-less).*

That the combined moisture terms generate precipitation at a relative humidity larger than 84% has also been used by other simple climate models (e.g. Weaver et al., 2001). Yet, this is not the equilibrium relative humidity found in the humidity terms when the GREB model equation is fitted against CMIP5 models. According to eq. 4.1 and using the CMIP5 fitted parameters all models produce rain at a relative humidity much lower than 84% (Tab. 4.4). This does not mean that the CMIP5 models start precipitating at this lower relative humidity (e.g. ACCESS1-3 does not precipitate at a relative humidity of 12%). It does however, indicate that the models in general show too little sensitivity

to moisture changes.

The four forcing terms are likely interrelated (e.g. relative humidity and ω_{mean}) thus when the dominant term is regressed out there is little left for the other terms to explain. This is explored further by excluding the two terms with the highest regression coefficients, c_ω and $c_{\omega std}$, from the precipitation equation and re-fitting the precipitation equation to observations and CMIP5 models. Then the importance of the relative humidity moisture term increases while the value of the specific humidity term changes only marginally for the observations (see Tab. 4.3). The CMIP5 models are closer to the observed values when only humidity terms are used for fitting. However, most CMIP5 models still underestimate the sensitivity compared to observations. Indicting a different sensitivity of precipitation in CMIP5 models compared to observations.

The role of the moisture terms and the sensitivity to different vales of c_q and c_{rq} is explored in more detail in Fig. 4.4. Increasing c_{rq} leads to an increase in the zero precipitation line (black solid line) and this change is larger for a larger c_q value. On the other hand, increasing the c_q parameter leads to a decreased zero precipitation line and the role of c_q is larger for smaller c_{rq} parameters.

As CMIP5 models show too little sensitivity to the moisture terms this is to some degree compensated by the remaining precipitation terms. Tab. 4.2 highlights an increased sensitivity to the mean circulation parameter, c_ω. All models have nearly double the sensitivity to mean circulation than the observed precipitation model. Thus, for a given vertical velocity ω_{mean} the CMIP5 fitted precipitation equation leads to too much precipitation and highlights an overestimated sensitivity of CMIP5 models to the mean circulation. The overestimated sensitivity of CMIP5 models to the mean circulation has also been found by (Yang et al., 2018). It is interesting to note that the average of the CMIP5 model parameters $c_{\omega ctrl}$, $c_{\omega rcp}$, $c_{\omega std ctrl}$, $c_{\omega std rcp}$ are not within the range of the observed value for at least 4 standard deviations, highlighting significant differences between the CMIP5 and observed precipitation parameters.

Interestingly this high sensitivity of CMIP5 models to the atmospheric mean circulation represented through ω_{mean} does not apply to the circulation variability term, $c_{\omega std}$. In observations the circulation variability term was the most important part of the precipitation equation. But, compared to the observed sensitivity all CMIP5 models persistently underestimate the $c_{\omega std}$ parameter by a factor of nearly two.
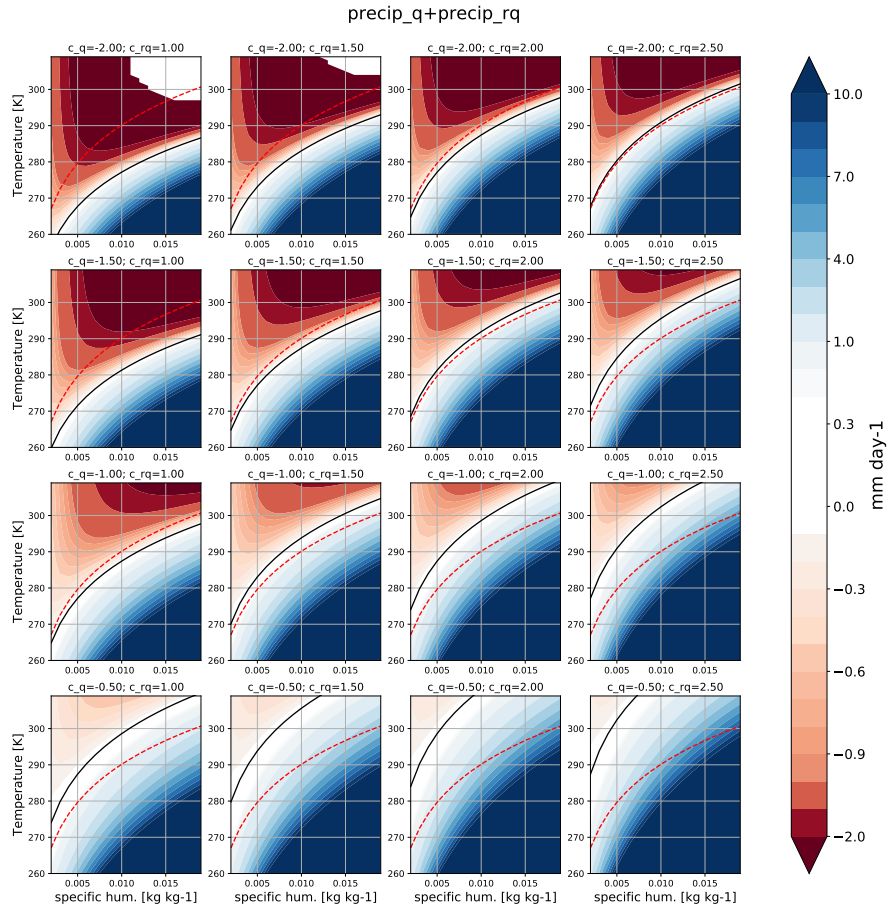
Figure 4.4: *Sensitivity of the moisture terms to parameter variation of c_q (up-down) and c_{rq} (left-right). The black solid line highlights the zero precipitation line for each c_q, c_{rq} set and the red dashed line indicates where the relative humidity is 84%.*

To evaluate how sensitive the GREB precipitation equation is to a warmer climate the parametrisation has also been fitted against the RCP8.5 CMIP5 model output. That is the boundary conditions (e.g. specific humidity) and the precipitation have been taken from the RCP8.5 CMIP5 archive for the models listed in Tab. 4.1. It is found that the parameters change only marginally between the control simulation and the RCP8.5 simulation for each model (Tab. 4.2). Most notably there is a general decrease in sensitivity to the mean circulation (green columns) with the RCP8.5 forcing and similar for the sensitivity to the circulation variability (blue columns). However, those changes are small in comparison to the inter model differences and to the differences between all CMIP5 models and the observed parameters. This discrepancy is most obvious for the circulation parameters. The observed precipitation parameter set is not even within the

model fitted precipitation parameter spread for both $c_{\omega mean}$ and $c_{\omega std}$.

4.4.2 Boundary condition anomalies

Precipitation biases in CMIP5 can not only be understood as a result of biases in the precipitation parameters but biases in other climate variables that influence precipitation (e.g. vertical velocity) also contribute to biases in precipitation. However, gaining an understanding of the quantitative contribution of parametrisation biases and boundary condition biases is far from trivial. This has several reasons. Firstly, biases in the parametrisation influence the climate mean state and it is therefore hard to distinguish the two; secondly, precipitation and vertical velocity are closely related, and it is therefore hard to determine which one causes biases of the other. Nonetheless, separating the precipitation parameter biases and the boundary condition biases can help to give a first order estimate each causes.

The main analysis of this section is using a similar decomposition approach as in the previous chapter and is based on a series of sensitivity experiments with the GREB model. For these experiments we use the ability of the GREB model to respond to changes in the boundary conditions and to control the mean surface temperature. For the study of the precipitation bias in CMIP5 the same key controlling factors as previously are studied, which are the boundary conditions of ω_{mean}, ω_{std}, and the model variables q and rq.

As previously, to study the precipitation biases, the GREB model can be driven by changes in ω_{mean}, ω_{std}, Δq_{eva} and surface temperature. The model will respond to these changes in boundary conditions by simulated changes in the atmospheric temperature, humidity and subsequently the relative humidity. These changes will then lead to changes in precipitation following from eq. 2.11.

For the control simulations the GREB model is run with observed boundary conditions, as described above, and q and surface temperature are free to evolve. For the sensitivity experiments we add the bias anomaly of ω_{mean}, ω_{std}, Δq_{eva} and surface temperature of each CMIP5 model to the control forcings for one or all boundary conditions while the remaining boundary conditions are kept at control values. Thus, in these sensitivity experiments Δq_{eva} and Tsurf are not free to evolve but are prescribed through the boundary conditions. Atmospheric temperatures, humidity and precipitation are free to respond. The difference between control and sensitivity simulations are defined as

the response. The biases for each CMIP5 model, used as boundary condition in GREB, are calculated against the CMIP5 ensemble mean and therefore the sum of all CMIP5 model biases is zero.

As it was discussed in the previous section there are differences between the precipitation parameters when fitted to CMIP5 models and it is most likely that these differences contribute to the biases found in the boundary conditions (e.g. ω_{mean}). For example, differences in the model precipitation parametrisations lead to a misrepresented precipitation which in turn forces the atmospheric moisture to be biased. Biases in atmospheric water vapour lead to biases in the amount of evaporation. Biases in the atmospheric water vapour might also lead to biases in triggering convection and thus vertical velocity. However, in this section we treat the biases independently.

The large-scale response of GREB precipitation to forced boundary condition biases in surface temperature, Δq_{eva}, ω_{mean} and ω_{std} taken from CMIP5 control output is evaluated against the CMIP5 precipitation biases. Considering that there are five deconstruction simulations for all 10 CMIP5 models the findings are summarised in a single figure using the spatial correlation of the annual mean bias and the root mean square (rms). That is, for each GREB deconstruction the spatial correlation coefficient against the CMIP5 precipitation bias is calculated. The spatial rms is calculated for the GREB sensitivity experiment and divided by the rms of the CMIP5 precipitation bias. The rms is used as a measure of spatial variability and value of 1 would indicate that rms in CMIP5 and GREB deconstruction are identical. Combined with the correlation coefficient this metric provides a good summary of the spatial correlation and variability between the GREB deconstruction and the CMIP5 annual mean bias in precipitation.

Superposition: All five sensitivity experiments described above (CMIP5 parameter, surface temperature, evaporation, ω_{mean} and ω_{std}) are added together in a linear superposition to evaluate if they sum up to the fully forced GREB model precipitation response in the annual mean (Fig. 4.5 black diamonds). The superposition is close to the fully forced GREB model precipitation response (Fig. 4.5 black diamonds) and to the CMIP5 response represented as how close the single markers get to the top right (correlation and relative rms equal to 1). However, the total precipitation response is clearly dominated by ω_{mean} followed by ω_{std} in these sensitivity experiments while the parameter, surface temperature and evaporation forcing contribute little.

Figure 4.5: *Correlation of the GREB deconstruction experiment bias to CMIP5 bias and the relative rms (rms_{GREB}/rms_{CMIP}) for each sensitivity experiment: the fully forced GREB model (black star), precipitation parameter (yellow), surface temperature (red), evaporation (green), ω_{mean} (blue), ω_{std} (cyan) and the superimposed (black diamond) of all deconstruction experiments. The closer each point is to the intersection of the grey lines (r=1 and relative rms=1) the better is the agreement between GREB sensitivity experiment and the CMIP5 bias.*

CMIP5 parameters: The biases of the precipitation parameters discussed in the previous section are mostly uncorrelated to the total CMIP5 precipitation bias (Fig. 4.5, yellow dots) and have a small spatial amplitude in relation to the CMIP5 biases.

Surface temperature bias: The surface temperature bias has no direct relation to the precipitation bias in GREB. The correlation between the precipitation bias for the surface temperature forcing is nearly zero for all CMIP5 models (Fig. 4.5 red dots) and the relative spatial variation is negligible.

Evaporation bias: The evaporation forced precipitation bias has a spatial correlation and relative rms of around 0.25 (Fig. 4.5 green dots). However, with evaporation being the only source of water vapour in the atmosphere globally, biases in evaporation have to match biases in precipitation in the global mean. But they do not influence the pattern of biases in CMIP5 models.

Omega mean bias: When the GREB model is forced with the mean state anomaly of vertical velocity the precipitation anomaly has the most similarity with the CMIP5

bias (Fig. 4.5 blue dots). The correlation of this deconstruction is around 0.75 and above for most models and the highest of all deconstruction experiments. The ω_{mean} decomposition is nearly as good as the fully forced GREB model anomaly. Therefore, ω_{mean} is the largest contributor to biases in the GREB experiments (Fig. 4.5). It is important to be noted here that ω_{mean} controls two key elements of the hydrological cycle in GREB: it affects the precipitation equation itself, and it controls the transport of moisture in the atmosphere. Thus, a bias in ω_{mean} leads to a bias in precipitation and moisture transport, which could see the total contribution of ω_{mean} overestimated in the GREB model.

Omega variability bias: The precipitation anomalies caused by the mean state bias in omega variability are the second largest contributor to the overall bias simulated by GREB (Fig. 4.5 cyan dots) in terms of the spatial pattern. In spatial variability of precipitation biases ω_{std} contributes less than ω_{mean}.

4.5 Water vapour circulation

ω_{mean} has a strong impact on the precipitation equation itself in the observations and even more important role in CMIP5 models with the sensitivity of CMIP5 models to the mean circulation being doubled compared to observation (measured using the fitting constant, $c_{\omega_{mean}}$ in Tab. 4.2). Additionally, ω_{mean} is a controlling factor of the water vapour circulation in the GREB model. That makes it impossible at this stage to differentiate between biases caused through the moisture transport and biases caused directly through the precipitation parametrisation. To investigate this in more detail a new water vapour circulation will be developed in the GREB model that can be controlled independently from the mean vertical velocity.

4.5.1 Water vapour circulation in GREB

In the newly developed GREB model described in chapter 2 the moisture convergence term was approximated by knowing the mean vertical air flow assuming continuity and hydrostatic balance:

$$\overrightarrow{\vec{\nabla}(\vec{u} \cdot q_{air})} = q_{air} \cdot f \cdot \frac{dt_{crcl}}{z_{vapour} \cdot \rho_{air} \cdot g} \cdot (-\omega_{mean}) \qquad (4.2)$$

with the known parameters scaling height of water vapour, z_{vapour}, density of air, ρ_{air}, gravitational acceleration, g, and the circulation time step, dt_{crcl}. The scaling factor, f, should theoretically be 1.0 but is found to be 2.5. For more details can be found in chapter 2.4.3.

For the new water vapour circulation, we want to use a parametrisation that is independent of ω_{mean}. For this method the horizontal winds are used instead of mean vertical velocity to calculate convergence/divergence. To calculate convergence/divergence from horizontal winds the finite volume method is applied. We therefore make use of the divergence theorem,

$$\int_V (\nabla \cdot \vec{F})dV = \oint_S (\vec{F} \cdot \vec{n})dS \tag{4.3}$$

to express the convergence/divergence of a volume through the fluxes over its boundaries. The fluxes across the boundaries are calculated for each grid cell using the mean winds of the neighbouring grid points. For numerical stability the fluxes across the boundaries are further restricted by a flux-limiter to ensure numerical stability.

To validate the finite volume method the annual mean for both moisture transport parametrisations is calculated and compared (Fig. 4.6).

Both methods yield similar results (Fig. 4.6). The finite volume method is weaker in the inter tropical convergence zone (ITCZ) over the Pacific and has more divergence surrounding the ITCZ (Fig. 4.6c). Over land the difference between both methods are smaller. However, South America is an exception with much more moisture convergence using the finite volume method. The similarity of the results is to be expected. Assuming an incompressible atmosphere, which for longer time scales is a reasonable assumption, horizontal convergence/divergence are balanced by vertical air motion. Thus, moisture transport calculated using either method should not result in any differences. The differences found in Fig. 4.6c might be caused by regridding the data to the GREB model resolution or by using the vertical mean of ω. Different to the ω_{mean} controlled moisture transport there was no need for a scaling factor, f.

The annual mean maps show similar features overall and the finite volume method can confidently be applied to control moisture transport independently from the mean vertical velocity.

Moisture transport
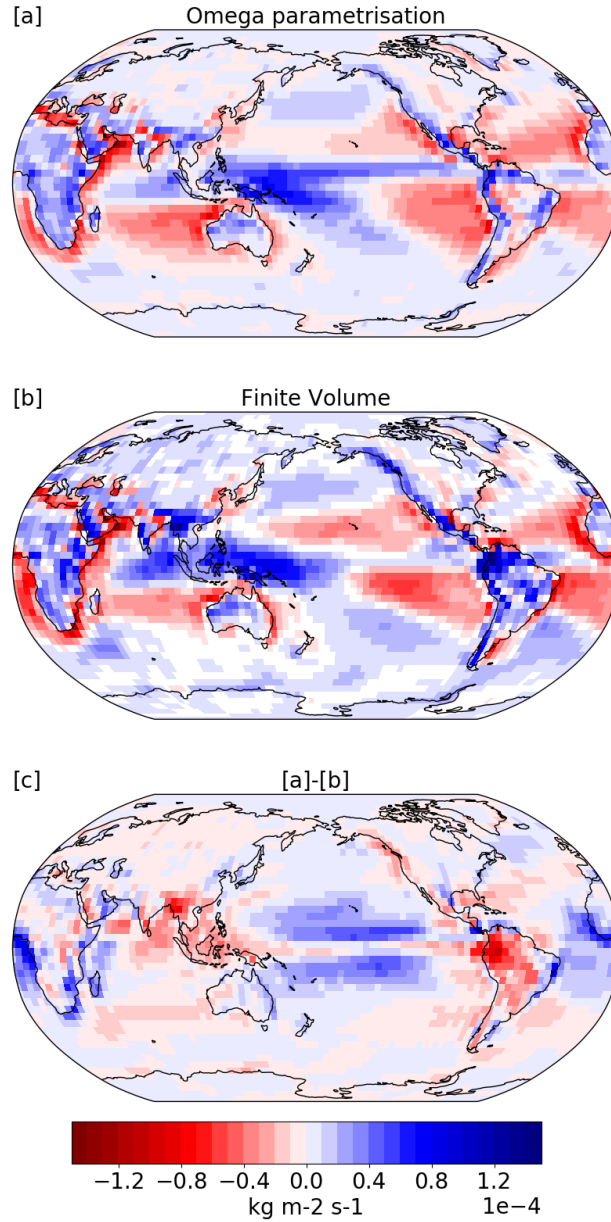
Figure 4.6: *Annual mean moisture transport in GREB using ω_{mean} [a] and finite volume method [b] to calculate convergence/divergence of water vapour and the difference between the two methods [c].*

4.5.2 Water vapour circulation bias

In the previous section the importance of the mean circulation for the total anomaly was highlighted. This is somewhat expected considering that ω_{mean} controls the two major parts of precipitation in GREB. ω_{mean} directly influences the precipitation equation (eq. 2.11) and therefore any bias in ω_{mean} is instantly translated into a bias in GREB precipitation. It also controls the water vapour transport in GREB through the water vapour

circulation parametrisation. Because evaporation is forced to stay at control values in the mean circulation deconstruction (Fig. 4.5 blue dots) any changes in precipitation have to draw moisture through the circulation changes.

In this section a closer look is taken into the importance of the water vapour circulation as contributor to the precipitation anomalies. To do this the water vapour circulation term in GREB was modified to be independent from ω_{mean} and to be calculated using the horizontal winds instead. However, convergence/divergence calculated from horizontal winds instead of ω_{mean} are not independent of each other, assuming an incompressible fluid but, it gives a chance in the GREB model to look at the role of water vapour transport and 'pure' precipitation biases to be separated.

Fig. 4.7 shows the deconstruction of the precipitation biases as in the section before but, this time the convergence and divergence of moisture transport in the atmosphere is calculated using horizontal winds rather than ω_{mean}.

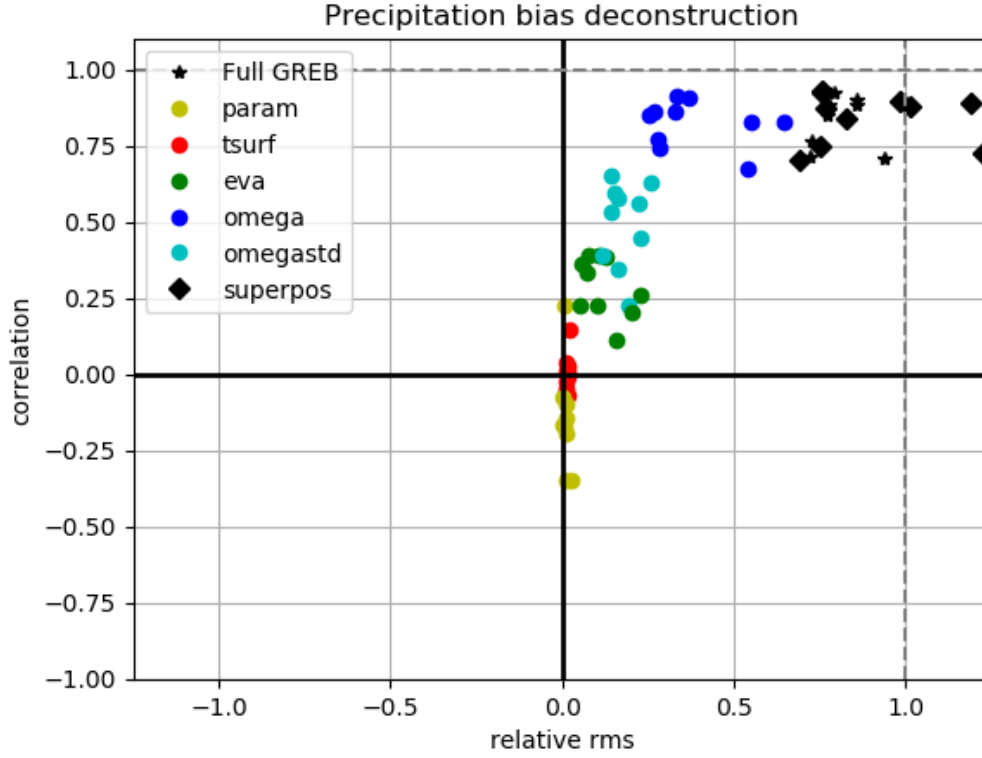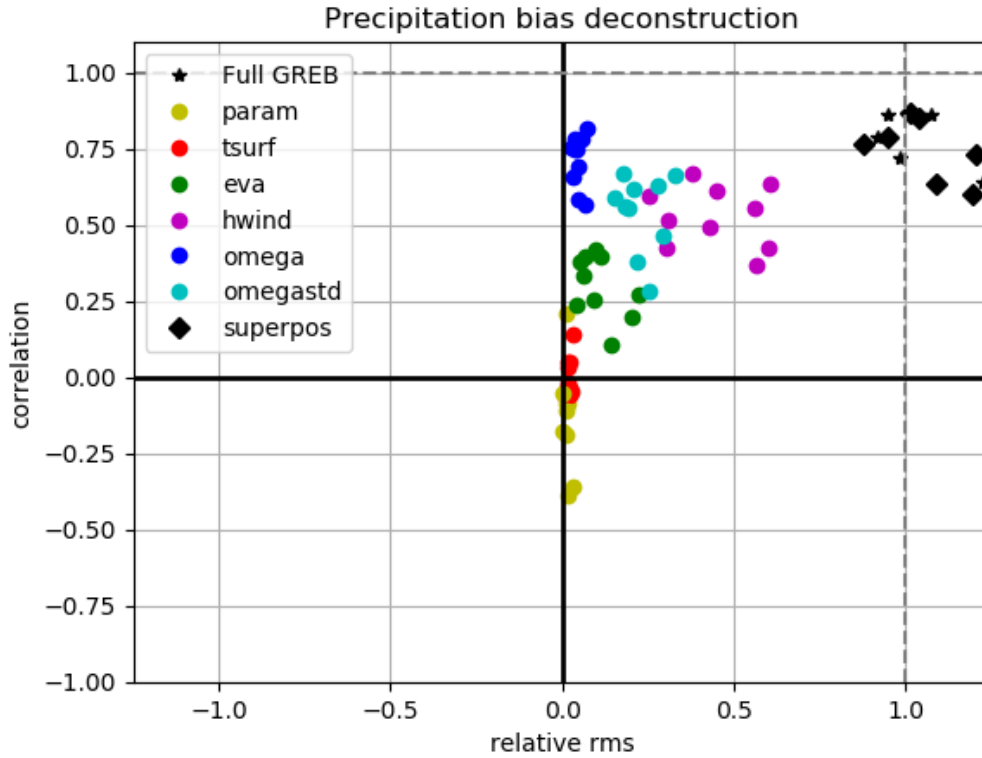**Figure 4.7:** *Same as Fig. 4.5 but with moisture transport independent from ω_{mean}. Correlation of the GREB deconstruction experiment bias to CMIP5 bias and the relative rms (rms_{GREB}/rms_{CMIP}) for each sensitivity experiment: the fully forced GREB model (black star), precipitation parameter (yellow), surface temperature (red), evaporation (green), ω_{mean} (blue), ω_{std} (cyan) and the superimposed (black diamond) of all deconstruction experiments. The closer each point is to the intersection of the grey lines (r=1 and relative rms=1) the better is the agreement between GREB sensitivity experiment and the CMIP5 bias.*

Overall there is a small decrease in the correlation coefficient between the CMIP5 anomaly and the GREB modelled anomaly compared to Fig. 4.5. Yet, even with moisture transport calculated by horizontal winds the GREB model does well in mimicking the anomalies seen in CMIP5 for the fully forced GREB model and the superimposed response. The smallest correlation coefficient found is 0.61.

For most of the conceptual deconstruction experiments the results remain unchanged to the previous section. That is, the parameters uncertainties, surface temperature and evaporation biases contribute little to the overall bias in terms of correlation and relative rms. The variability of vertical velocity is important, but the results have not changed with respect to the previous section. However, there is a drastic change in the importance of the mean vertical velocity (Fig. 4.7, blue dots).

When ω_{mean} controls the precipitation equation and the moisture transport it is the dominating factor in the total precipitation biases. When the atmospheric water vapour transport is controlled by the horizontal winds, ω_{mean} on average still has the highest correlation with the precipitation biases but, contributes little to the amplitude. The horizontal winds, which now control the convergence/divergence of water vapour, have a comparable contribution to the total precipitation bias and have the largest relative rms of all experiments.

It is important to point out that in this sensitivity experiment not a single external forcing can be ruled as dominating factor. Overall when using the horizontal winds to calculate atmospheric moisture transport the contribution of the dynamic contributors ω_{mean}, ω_{std} and horizontal winds is more evenly distributed.

4.6   Chapter Summary and Discussion

In this chapter we used the simple climate model GREB to decompose the CMIP5 simulations inter model spread of precipitation. Assuming the precipitation equation used in GREB is 'perfect' if given the correct set of fitting constant and 'correct' boundary conditions, biases in CMIP5 models were split to two different sources: uncertainties in the precipitation parametrisation (i.e. the fitting parameters in the GREB precipitation equation) and biases in the mean state of other climate variables (e.g. the mean circulation). Starting with the uncertainties in the precipitation parameters the GREB model

precipitation parametrisation was fitted against 10 different CMIP5 models. Thus, gaining 10 new sets of precipitation parameters. The value of the fitting parameters was used as indication on how sensitive each model is to different drivers of precipitation.

It was found that the CMIP5 models consistently overestimated the sensitivity of precipitation to the mean vertical velocity, ω_{mean}, by a factor of 2. These findings are confirmed by other studies (i.e. Yang et al., 2018). Interestingly the sensitivity of CMIP5 model precipitation to the circulation variability, ω_{std} was underestimated in all models. To our knowledge this study is the first to highlight this but, this might be related to CMIP5 models raining too lightly too often (e.g. Dai, 2006; Stephens et al., 2010).

In the second half of this study the role of biases in climate variables and their influence in precipitation was investigated. We presented the precipitation changes as the result of four different forcings of surface temperature, evaporation, mean circulation and circulation variability biases. The four forcing biases were calculated against the CMIP5 ensemble mean and therefore the sum of all biases is zero. Additionally, the parameter uncertainties discussed above have also been considered. The simplicity of the GREB model allows us to force single aspects of the climate system to take any bias in the mean state (e.g. mean circulation) while other aspects remain at control values using the conceptual deconstruction used developed in chapter 3.

Initially the biases in mean vertical velocity were the dominating factor controlling the total precipitation bias. It was then considered that mean vertical velocity contributes to the overall precipitation bias in two ways, by influencing the precipitation parametrisation directly and through the moisture transports. To further dissect the individual contribution of the precipitation equation itself and the moisture transport a new water vapour circulation parametrisation was introduced. The new water vapour circulation parametrisation relies on the horizontal winds to calculate moisture convergence/divergence instead of the mean vertical velocity.

The new moisture transport equation is using the finite volume method to calculate convergence/divergence of water vapour and the results compare well to the mean vertical velocity parametrisation. But, because the finite volume method uses horizontal winds rather than mean vertical velocity it is now possible to separate the biases caused by moisture transport and the direct biases in the precipitation equation caused by mean vertical velocity. Using the new moisture transport parametrisation showed that it is

indeed the water vapour transport that contributes substantially to the total precipitation bias. The three dynamically driven biases, mean vertical velocity, vertical velocity variability and water vapour transport have an important contribution to the total bias.

The five different forcings of precipitation anomalies add almost linearly in the GREB model, while still giving a good representation of the inter model spread in the CMIP simulations against the ensemble mean. This suggests that the CMIP precipitation changes can, to a large part, be considered as linear superposition of these five forcings although most of the biases are driven by dynamics (i.e. mean vertical velocity, vertical velocity variability and moisture transport).

It is important to point out that vertical velocity ω, is a diagnostic variable in re-analysis products and therefore not directly restrained through observations. This means that the ω_{mean} and ω_{std} from ERA-Interim used as references here is merely the output of another CGCM. Which raises the questions why ERA-Interim has such a different sensitivity to ω_{mean} than CMIP5 models.

In more complex models (i.e. CMIP5 models) this conceptual decomposition of biases is not possible. All of those five biases highlighted in this section are most likely highly dependent on each other (e.g. in the tropics biases in surface temperature most likely causes biases in vertical velocity) . Especially, biases in mean circulation, ω_{mean}, control biases in precipitation, but also precipitation influences the mean circulation. Latent heating released during condensation warms the atmosphere and leads to dynamical changes in the mean circulation. Whereas biases in the mean circulation also affect evaporation which is influenced by the mean winds. Therefore, none of these biases can be separated easily.

However, there are several shortcomings in this chapter:

- The GREB precipitation parameters (e.g. c_ω) do not directly relate to the precipitation parametrisation used in CMIP5 models. The GREB precipitation parameters can be more understood as how CMIP5 model precipitation reacts to changes in the boundary conditions (e.g. surface temperature changes). Therefore, in order to relate the GREB precipitation parameters better to the actual CMIP precipitation parametrisation future work should focus on better understanding the CMIP precipitation parametrisations.

- It is not straight forward to compare the GREB precipitation parameters. The

parameters have different units (e.g. c_q is unit less while $c_\omega = [\frac{s}{hPa}]$) and the climatological fields they are multiplied with (e.g. $c_{rq} \cdot rq$) have different magnitudes and a different strong seasonal cycle. For example the annual mean of relative humidity is in the order of $O(10^0)$ while the annual mean of specific humidity, ω_{mean} and ω_{std} are in the order of $O(10^{-2})$. This could, at least to some extend, explain why the moisture and circulation parameters have different orders of magnitude and this has not been considered in this chapter. To overcome this, the fitting constants could be multiplied with their representative climatological value (e.g. multiply c_q with the annual mean specific humidity).

- It was found that the GREB precipitation parameter biases contribute little to the overall bias. However, it was not investigated if the parameter biases compensate each other. Considering that the CMIP5 fitted parameters were too sensitive to the mean circulation but showed little sensitivity to the moisture term, compensating biases between the mean circulation and moisture terms seems to be a reasonable assumption. This could be tested using the observed GREB precipitation model and replacing only a single fitting constant (e.g. c_ω) with the CMIP5 value.

- Although arid regions often experience negative precipitation in the GREB model the annual mean negative rainfall amount is negligible compared to the amount of global mean precipitation. Nonetheless, this deserves some attention when further developing the GREB model.

Despite the shortcomings, this study has shown that the GREB model in general is able to reproduce precipitation biases in CMIP5 models skilfully and that the deconstruction approach used is indeed capable of analysing the precipitation biases of the CMIP5 models. The discussion highlighted some shortcomings of this chapter but showed possible pathways on how to extend this research to gain more insights into precipitation biases and how the GREB model can be applied as an analysis tool. The value of this decomposition approach and the importance of considering the precipitation biases is further highlighted in the next chapter, especially in section 5.5.

Table 4.3: *As Tab. 4.2 but for the moisture terms only: Precipitation parameters for observed precipitation, 10 different CMIP5 models, the ensemble mean of the 10 CMIP5 models and the average of the fitted parameters for the moisture terms only. The spread of the model parameters is shown as standard deviation.*

Variable	$c_{q_{ctrl}}$	$c_{q_{rcp}}$	$c_{rq_{ctrl}}$	$c_{rq_{rcp}}$
Observed	-1.78		3.48	
ensmean	-1.15	-0.64	2.79	1.97
ACCESS1-0	-1.62	-0.94	3.73	2.55
ACCESS1-3	-1.36	-0.98	3.27	2.54
BNU-ESM	-1.49	-1.06	3.17	2.41
FGOALS-g2	-1.02	-0.80	2.81	2.13
GFDL-ESM2G	-1.18	-0.65	2.97	2.24
GFDL-ESM2M	-0.94	-0.64	2.64	2.02
IPSL-CM5A-LR	-1.13	-0.58	2.69	1.81
MIROC-ESM-CHEM	-0.53	-0.35	1.78	1.35
MIROC5	-1.26	-0.68	3.15	2.13
MRI-CGCM3	-1.96	-1.45	3.66	2.89
average	-1.26	-0.81	2.98	2.19
std	0.36	0.29	0.53	0.41

Table 4.4: *Equilibrium relative humidity of the moisture precipitation terms. Any higher relative humidity will lead to precipitation.*

Variable	relative humidity balance in %
Observed	84
ensmean	39
ACCESS1-0	34
ACCESS1-3	12
BNU-ESM	54
FGOALS-g2	46
GFDL-ESM2G	41
GFDL-ESM2M	41
IPSL-CM5A-LR	56
MIROC-ESM-CHEM	46
MIROC5	45
MRI-CGCM3	53

Chapter 5

Southern Hemisphere Precipitation Trend Reversal

5.1 Preface

The decrease of precipitation in the subtropics is a prominent feature in climate change projections. However, geological records of warmer-than-present climate states show a wetter and not drier mean climate in the Southern Hemisphere subtropics. The initial drying in the Southern Hemisphere subtropics in the twenty-first century shows a positive precipitation trend in the twenty-third century in some CMIP5 models and the ensemble mean. The simple GREB model deconstruction of chapter 3 is used to investigate the sources of the precipitation trend reversal in the Southern Hemisphere. The precipitation trend reversal is decomposed into four separate forcings (surface temperature, evaporation, mean vertical velocity and vertical velocity variability). The results indicate that of the four forcings only evaporation contributes positively to the Southern Hemisphere precipitation trend. The GREB model is unable to reproduce the trend reversal seen in the CMIP5 ensemble mean and it was tested what role the precipitation parameters play. Nonetheless, the results provide good insights into the drivers of precipitation change beyond results of chapter 3 and highlight the importance of the precipitation parameters.

5.2   Introduction

Climate change projection based on the Couple Model Intercomparison Project phase 5 (CMIP5) project an increase in global mean precipitation of roughly 2% per degree of warming (Held and Soden, 2006). The 2% change in precipitation comes in contrast to an increase in atmospheric water vapour of about 7% per degree of warming closely following the Clausius-Clapeyron equation. This muted response has been extensively discussed in chapter 3.4 and is explained by a general slowdown of the atmospheric circulation (Chadwick et al., 2013; Held and Soden, 2006) and changes in radiative cooling (Allen and Ingram, 2002; Pendergrass and Hartmann, 2014).

Although precipitation is increasing by 2% per degree of warming globally, this does not mean it is increasing at the same rate everywhere. Precipitation is generally projected to increase in the ITCZ, with a large-scale precipitation decline in the subtropics and an increase in precipitation in mid- to high- latitude storm tracks (Allen and Ingram, 2002; Chou and Neelin, 2004; He and Soden, 2016; Held and Soden, 2006; Neelin et al., 2006). This pattern change is often referred to as the 'wet-get-wetter' (Held and Soden, 2006). The wet-get-wetter hypothesis is mainly built on the idea that a warmer atmosphere holds and therefore transports more moisture out of dry regions into wet regions if the circulation remains unchanged (Chadwick et al., 2013). However, in chapter 3.4 we highlight the importance of dynamical changes. The simulations that show the decrease of precipitation of the subtropics are based on rapidly increasing emission scenarios (RCP8.5), before the temperature trend stabilises and can therefore be seen as a transient rather than an equilibrium response. The rapid, transient adjustment, is insufficient to explain the time evolution of the hydrological cycle and Zappa et al. (2020) showed that the drying will not continue after greenhouse gas concentrations are stabilised.

Contrary to this drying trend in the fast, transient precipitation response, geological records show a wetting of the subtropics in warmer-than-present climate state (Haywood et al., 2013; Sniderman et al., 2016, 2019). Sniderman et al. (2019) link the meridional temperature gradient, which influences the strength of the Hadley circulation, and thus the strength and position of the descent in the subtropics, to the initial drying. The meridional temperature gradient trend reverses soon after the CO2 concen-

tration stabilises and this is generally associated with a reversal of winter precipitation in the southern hemisphere subtropics.

This chapter is based on the analysis done by Sniderman et al. (2019) and is an extension of chapter 3. It looks at much longer simulations of the RCP8.5 emission scenario. The conceptual deconstruction ability of the GREB model, highlighted in the previous chapters, is used to better evaluate which forcings drive the precipitation trend reversal. This last chapter nicely combines the findings of all previous chapters, using the new GREB hydrological cycle model described in chapter 2, applying the deconstruction method of chapter 3, and indicating the importance of the precipitation parameters of chapter 4. In the next section the data and models of CMIP5 used are described and in section 5.4 the findings of the conceptual deconstruction are discussed. The last section concludes and summarises this chapter.

5.3   Data and Methods

The models of Coupled Model Intercomparison Project phase 5 (CMIP5) (Taylor et al., 2012) used in this study are summarized in Tab. 5.1. We used all available models of the historical and RCP8.5 scenario that provided the variables, the time frequency needed for the analysis and the length of simulation record until the year 2999. All datasets are re-gridded to a horizontal resolution of $3.75^o \times 3.75^o$ to match the GREB model horizontal resolution and monthly climatologies are calculated for each century. For the climatology of ω_{mean} a monthly output frequency is used and a weighted vertical mean over all levels is applied to smooth the data. For the climatology of ω_{std} a daily output frequency is needed in order to calculate the daily standard deviation. Only three models provided daily output of ω (highlighted in green in Tab. 5.1). For those three models a weighted vertical mean is applied to smooth the data and the daily standard deviation is calculated. For the multi-model ensemble mean all models in Tab. 5.1 are used.

5.4   Trend Reversal in CMIP5 Models

In this section the precipitation trend reversal is investigated in CMIP5. The trend for precipitation (Fig. 5.1) itself and the four external boundary forcings of, surface temperature (Fig. 5.2), evaporation (Fig. 5.3), mean vertical velocity (Fig. 5.4) and

Table 5.1: *List of CMIP5 models used for the southern hemisphere precipitation reversal. Green text indicates models with daily output frequency of ω available.*

Models	
BCC-CSM1-1	CCSM4
CNRM-CM5	CSIRO-Mk3.6.0
GISS-E2-H	GISS-E2-R
HadGEM2-ES	IPSL-CM5A-LR
MPI-ESM-LR	

vertical velocity variability (Fig. 5.5) are calculated for the ensemble mean and the time series of the southern hemisphere subtropics (35^oS - 25^oS) for each variable is calculated. The circulation variability response to the control simulation is shown in Fig. 5.6. The feasibility and importance of those four external boundary condition forcings has been discussed extensively in chapter 3 and will therefore be considered in this chapter again.

In the first of the three centuries the precipitation trend is negative for most of the southern hemisphere subtropics, while the tropical Pacific and the mid- to high latitudes see a positive precipitation trend. This pattern does not change much into the second century from the year 2100 to 2199 although some regions in the southern hemisphere subtropics already experience a reversal in the trend (e.g. Fiji and Indian Ocean). The time series of the ensemble mean is plateauing between 2100 and 2199. Between the years 2200 and 2299 the reversal of the precipitation trend becomes more obvious with the time series having a clear positive trend, eventually reaching even higher precipitation values than at the beginning of the time series. The precipitation reversal is only seen in 5 of 8 ensemble members in the climate change projections.

The temperature trend in the years 2006-2099 and 2100-2199 are again similar to each other. The trend is strongest in the northern hemisphere and generally more pronounced over land than over ocean and is weakest in the Southern Ocean. From 2200 to 2299 the temperature stabilises in the time series and the trend decreases (Fig. 5.2). All models agree well on this trend.

Evaporation has a positive trend nearly everywhere for all three centuries. There are only a few regions that have a negative trend (e.g. Greenland) and most negative trends turn positive between 2200 and 2299.

Mean vertical velocity, ω_{mean}, shows a trend in the first century that looks similar to the precipitation trend. This is expected because the circulation changes play an
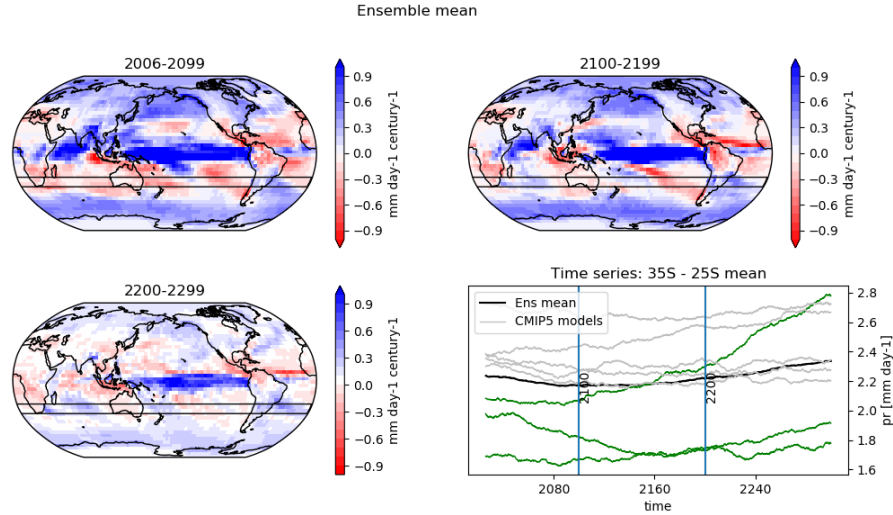
Figure 5.1: Precipitation trends. *Precipitation trends (mm day-1 century-1) are shown for the twenty-first (top-left), twenty-second (top-right), twenty-third (bottom-left) century and the time series of Southern Hemisphere subtropical 20 year rolling mean precipitation. The thick black line indicates the ensemble mean, while the grey lines represent single models. The three green lines are the models that have daily output of ω available.*
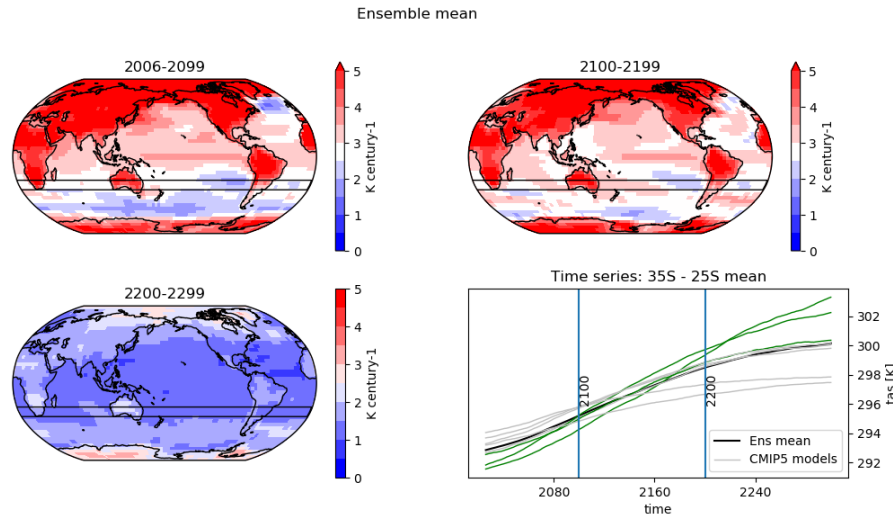
Figure 5.2: Surface temperature trends. *Surface temperature trends (K century-1) are shown for the twenty-first (top-left), twenty-second (top-right), twenty-third (bottom-left) century and the time series of Southern Hemisphere subtropical 20 year rolling mean precipitation. The thick black line indicates the ensemble mean, while the grey lines represent single models. The three green lines are the models that have daily output of ω available.*

important role in the precipitation response as highlighted in chapter 3. From 2100 to 2199 the pattern stays the same, but the trend gets slightly weaker. In the century from 2200 to 2299 the trend in ω_{mean} weakens substantially and it seems that the circulation changes are nearing a new equilibrium (i.e. trends are plateauing). In the time series it can be seen that only one model has daily output available for every day from 2006 to
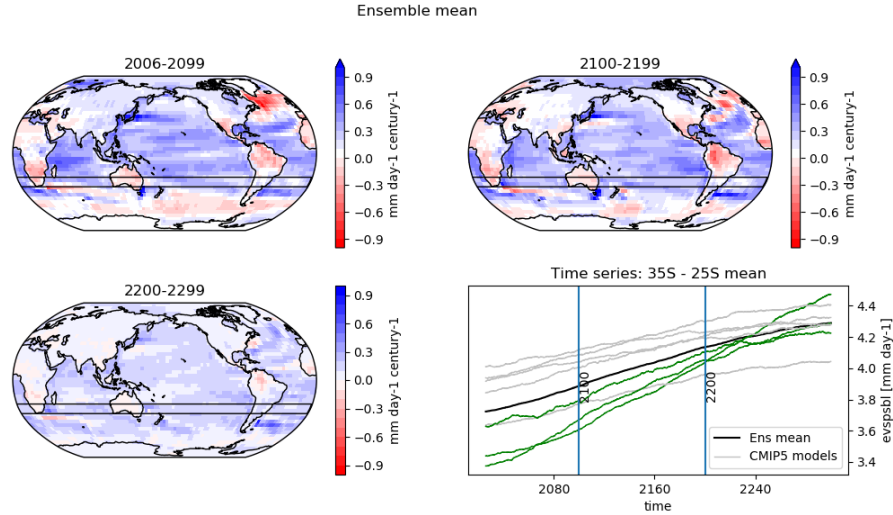
Figure 5.3: Evaporation trends. *Evaporation trends (mm day-1 century-1) are shown for the twenty-first (top-left), twenty-second (top-right), twenty-third (bottom-left) century and the time series of Southern Hemisphere subtropical 20 year rolling mean precipitation. The thick black line indicates the ensemble mean, while the grey lines represent single models. The three green lines are the models that have daily output of ω available.*

2299 while the other two only simulated the end of each century.
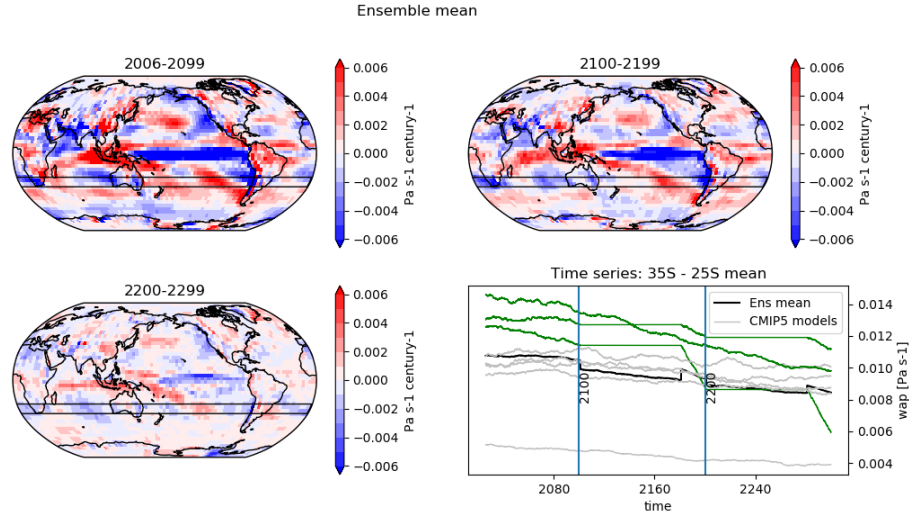
Figure 5.4: Mean circulation trends. *ω_{mean} trends (hPa s-1 century-1) are shown for the twenty-first (top-left), twenty-second (top-right), twenty-third (bottom-left) century and the time series of Southern Hemisphere subtropical 20 year rolling mean precipitation. The thick black line indicates the ensemble mean, while the grey lines represent single models. The three green lines are the models that have daily output of ω available.*

The whole century is used to calculate daily standard deviation of ω. This means each century only has one climatology available and it is not possible to calculate a trend for centuries independently. However, the century mean shows a clear decrease of $omega_{std}$ from 2006 to 2299 (Fig. 5.5). The pattern of the ω_{std} response stays

93

similar throughout the centuries but increases in magnitude. The last century shows a strong decrease in variability in the subtropics in both hemispheres and an increase in variability in the tropical Pacific. The importance of high frequency weather changes was highlighted in chapter 3.
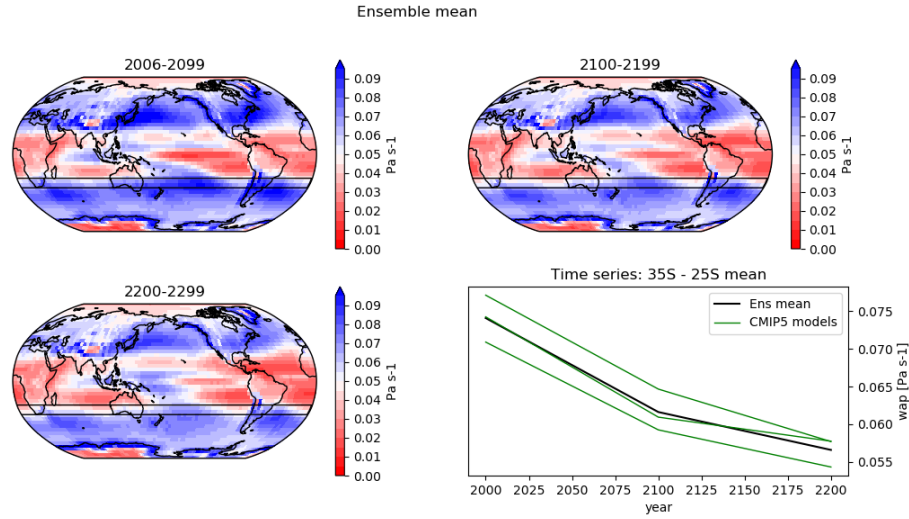
Figure 5.5: Circulation variability trends. ω_{std} *trends (hPa s-1 century-1) are shown for the twenty-first (top-left), twenty-second (top-right), twenty-third (bottom-left) century and the time series of Southern Hemisphere subtropical 20 year rolling mean precipitation. The thick black line indicates the ensemble mean, while the grey lines represent single models. The three green lines are the models that have daily output of ω available.*
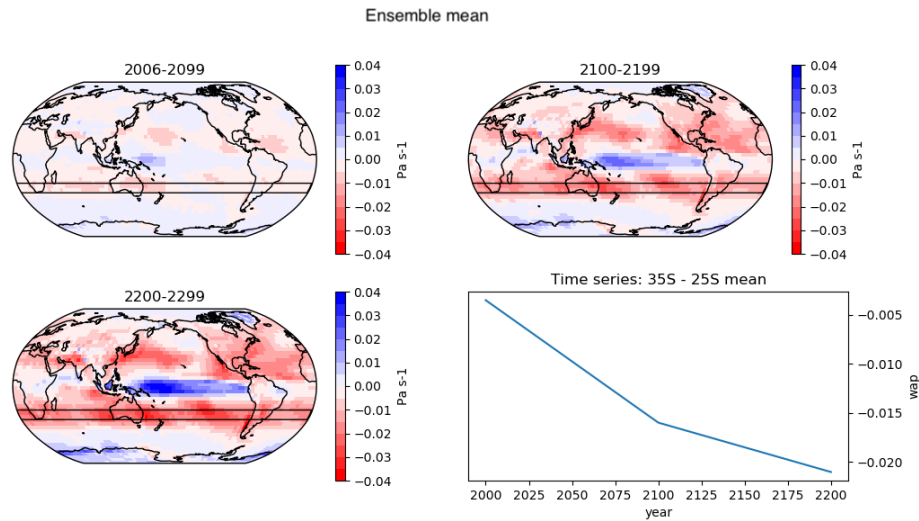
Figure 5.6: Circulation variability response trends. ω_{std} *response trends (hPa s-1 century-1) are shown for the twenty-first (top-left), twenty-second (top-right), twenty-third (bottom-left) century and the time series of Southern Hemisphere subtropical 20 year rolling mean precipitation. The thick blue line indicates the ensemble mean.*

5.5   Trend Reversal Deconstruction in GREB

This chapter is an extension of the analysis in chapter 3 and looks at much longer model simulations. It is using the same decomposition approach and is based on a series of sensitivity experiments with the GREB model.

If the precipitation is free to respond, then q and rq are largely controlled by the evaporation (Δq_{eva}) and the atmospheric temperatures. The latter is strongly linked to the surface temperature. Thus, to study the precipitation response to changes in environmental factors, the GREB model can be driven by changes in ω_{mean}, ω_{std}, Δq_{eva} and surface temperature. Each of those changes is forced through boundary conditions taken from the CMIP5 RCP8.5 ensemble mean while atmospheric temperatures, humidity and precipitation are free to respond.

Fig. 5.7 shows for each century the conceptual deconstruction of the precipitation response to the four different forcings (surface temperature, evaporation, mean vertical velocity and vertical velocity variability) compared to the control simulation. The fully forced GREB model compares reasonably well with the global CMIP5 simulated precipitation response. Yet, the GREB model fails to reproduce the reversal trend of precipitation seen in CMIP5. Generally, the areas of precipitation decrease are overestimated (i.e. southern hemisphere sub-tropical Pacific and Australia) compared to CMIP5.

Surface temperature changes: We start with the precipitation response of the surface temperature forced sensitivity experiment (Fig. 5.7i-l). Increasing the temperature enhances the existing moisture transport in the atmosphere and thus, results in an enhanced control precipitation. Changing the surface temperature, does not affect the global precipitation and only changes the precipitation pattern. This has been discussed extensively in chapter 3. The trend in precipitation response in GREB shows no sign of plateauing even though the temperature trend itself is levelling out (Fig. 5.2).

Evaporation changes: As evaporation is increasing globally with a warmer climate (Fig. 5.3) this also leads to more global precipitation in this sensitivity experiment (Fig. 5.7m-p) . Southern hemisphere subtropical rainfall increases by 0.5 mm/day in 2299. This is in line with the increase of evaporation of the ensemble mean (Fig. 5.3). As discussed in chapter 3 this added moisture is recycled mostly instantly as the atmosphere

is not warming and is close to saturation.

Mean circulation changes: The mean circulation sensitivity experiment response (Fig. 5.7q-t) has a similar pattern in all three centuries. However, in the twenty-first century the southern hemisphere subtropical precipitation response is zero while the other two show an increase in subtropical rainfall with nearly 2 mm/day more precipitation in the twenty-third century. ω_{mean} controls the precipitation equation directly and also alters the moisture transport. Therefore, the change in precipitation compares well to the forced change of the ω_{mean} boundary condition. The evaporation changes and the mean circulation changes are the only two of the four deconstruction sensitivity experiments that show an increase in precipitation.

Circulation variability changes: The circulation variability precipitation response has a clear pattern and generally shows a strong decrease in subtropical precipitation (Fig. 5.7u-x). This has been discussed in chapter 3. In the twenty-second and twenty-third century circulation variability is decreasing even more. With a reduction of 0.75 mm/day it becomes the dominating factor of precipitation reduction in the subtropics.

Figure 5.7: *Precipitation response decomposition in mm/day for the fully forced and the single RCP8.5 forcings of surface temperature, evaporation, mean circulation and the daily circulation variability. The right panel shows the mean values for the southern hemisphere subtropics for each century.*

Only the evaporation and mean circulation sensitivity experiment lead to an increase in precipitation. The other two experiments show a decrease in precipitation with the reduction in circulation variability being the most pronounced. The decrease in precipitation in the circulation variability deconstruction has the strongest response of all experiments being large enough to compensate both increases in precipitation (evaporation and mean circulation) and together with the reduction through the increased temperature causing the whole GREB model precipitation response to become negative.

Thus, the GREB model at this stage fails to reproduce the reversal of the precipitation trend found in CMIP5 models. In chapter 4 it was discussed that the set of precipitation parameters in CMIP5 models is different to the 'observed' set of precipitation parameters used to deconstruct the precipitation response shown in Fig. 5.7. Therefore, it is only reasonable to test if this reversal in the precipitation trend of the southern hemisphere subtropics can only be accurately simulated in GREB if we use the CMIP5 set of precipitation parameters.

Changing the set of parameters gives each part of the precipitation equation a different weight. In CMIP5 models the mean circulation, ω, has a much higher weight than in the observed set of parameters (see Tab. 4.2). At the same time mean circulation variability, ω_{std} has less weight (Tab. 4.2) and therefore reductions in mean circulation variability might be less important in CMIP5 models. In short, with the CMIP5 precipitation parameter set the boundary condition that leads to an increase in precipitation (i.e. ω_{mean}) becomes more important while the boundary condition that lead to the strongest decrease in precipitation (i.e. ω_{std}) becomes less important. The deconstruction using the CMIP5 set of precipitation parameters is shown in Fig. 5.8. There are only minor changes for the surface temperature and evaporation deconstruction experiment. This is somewhat expected as neither influences the precipitation as directly as ω_{mean} and ω_{std} do. The response of precipitation to the surface temperature forcing is slightly stronger than before. This is due to the higher sensitivity of the GREB precipitation to circulation changes in the CMIP5 parameter set.

There is now more precipitation in the mean circulation deconstruction than in the 'observed' parameter set experiments highlighting the increased sensitivity of the GREB model precipitation equation to changes in the mean circulation. This is due to a larger c_ω parameter in the CMIP5 fitted set of precipitation parameters (Tab. 4.2). Therefore,
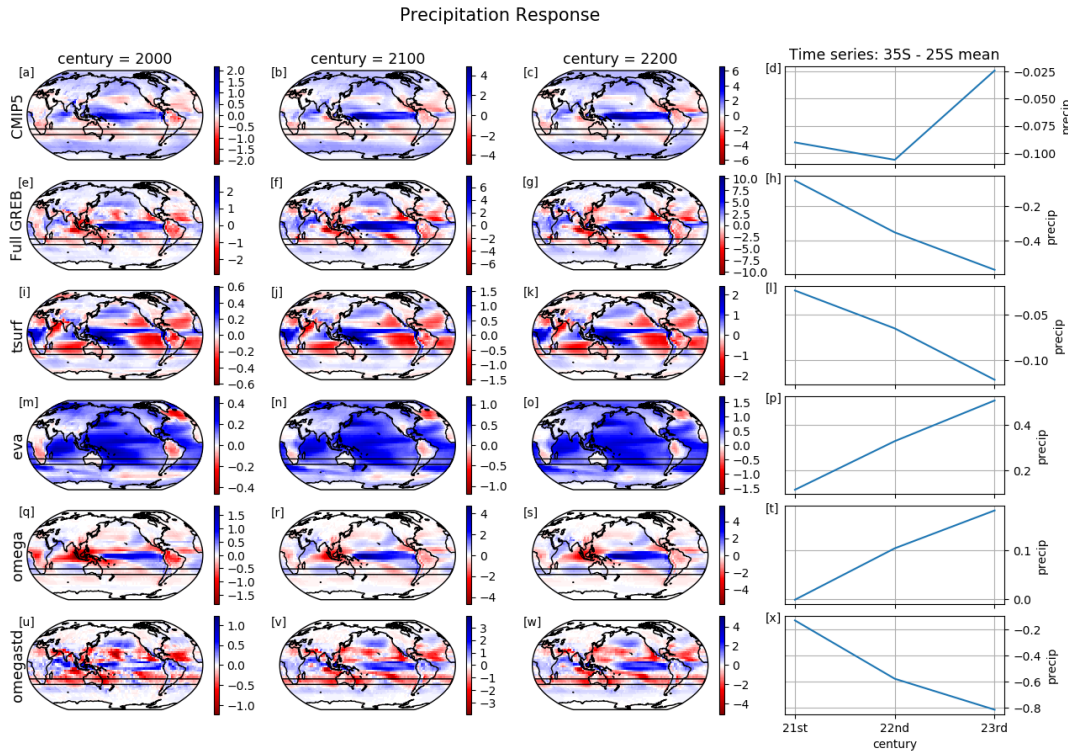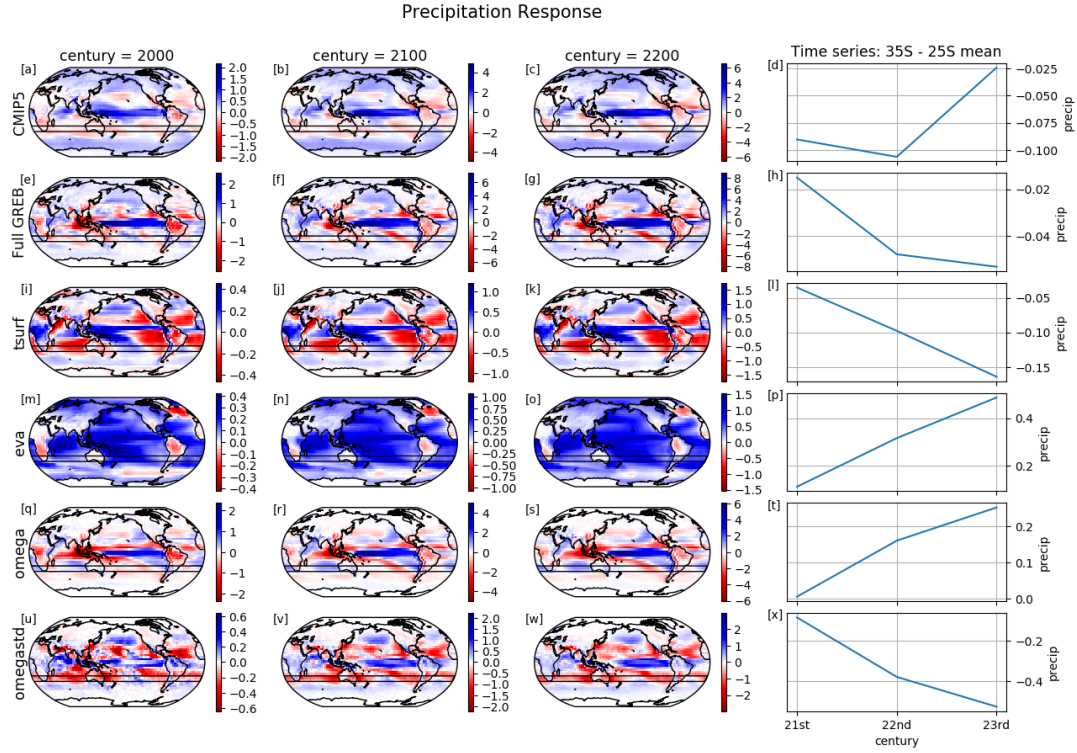
Figure 5.8: *As Fig. 5.7 but for CMIP5 fitted parameters. Precipitation response decomposition in mm/day for the fully forced and the single RCP8.5 forcings of surface temperature, evaporation, mean circulation and the daily circulation variability. The right panel shows the mean values for the southern hemisphere subtropics for each century. The CMIP5 fitted precipitation parameter set of the ensemble mean (Tab. 4.2) are used.*

any increase in ω leads to an even stronger increase in precipitation. For the same reasons the reductions of ω_{std} in the southern hemisphere subtropics are now less important than they were before.

The reduction of precipitation is now less than in the previous experiment (compare Figs. 5.7h and 5.8h) and seems to be plateauing but, the change of the precipitation parameters used in GREB is still not leading to a reversal in the precipitation deconstruction in the GREB model in the twenty-third century.

5.6   Summary and Discussion

This chapter can be seen as an extension of chapter 3 where the climate change response of the hydrological cycle in CMIP5 models was deconstructed. The ensemble mean of nine CMIP5 models with simulation model output spanning the three centuries from 2006 to the year 2299 were analysed to first confirm the findings of a reversal of the precipitation decrease as found by Sniderman et al. (2019). The model data for key

drivers of precipitation response identified in chapter 3, surface temperature, evaporation, circulation changes and circulation variability changes for century have been prepared and the ensemble mean calculated.

It is found that not all CMIP5 models show a reversal of the drying in the southern hemisphere subtropics and that the model spread is large, and the reversal is more pronounced in some models. The temperature is strongly increasing the first two centuries and slowly plateaus in the third century. Evaporation follows a similar trend. The mean circulation, here represented through the mean vertical velocity, is generally positive in the subtropics, indicating descending air masses has a steady negative trend in the twenty-first and twenty-second century and a slightly less but still negative trend in the twenty-third century. The circulation variability shows a distinct response pattern, with reduced variability in the southern hemisphere subtropics. The decrease in variability gets stronger from century to century. Unfortunately, only three models write the necessary ω output daily needed to calculate the circulation variability. Nonetheless, all three models agree strongly on the reduction of circulation variability.

The same deconstruction method as in chapter 3 was used and the GREB model was forced with four single aspects of the climate system (surface temperature, evaporation, mean circulation and circulation variability) taken from the CMIP5 ensemble mean response while keeping the other variables at control values.

The GREB model deconstruction was applied and it was found that two of the four sensitivity experiments lead to an increase in southern hemisphere subtropical precipitation. Evaporation increases precipitation by more than 4 mm/day in the southern hemisphere subtropics. The negative trend of mean vertical velocity adds another 2 mm/day increase of precipitation. The increase of precipitation through the evaporation is rather uniform throughout the subtropics while the precipitation response pattern of the ω sensitivity experiment shows some regional differences with decreases in precipitation in the eastern subtropical Pacific and increases east of Australia.

The other two sensitivity experiments, surface temperature and circulation variability forcing, cause a strong decline in subtropical precipitation with the latter being the most pronounced reduction. With a decline in subtropical circulation variability less precipitation falls in each century. The reduction of rainfall is evident throughout the southern hemisphere subtropics and there are mostly no regional differences. The second

sensitivity experiment that leads to less precipitation is the increase in surface temperature. The warmer atmosphere amplifies the existing precipitation patterns through an enhanced moisture transport. That is a warmer atmosphere can hold more water vapour and with mean circulation being held a control values transport more water vapour out of climatological dry regions into wet regions leading to an amplified precipitation response with no changes to the precipitation pattern. Interestingly although the surface temperature plateaus in the twenty-third century the precipitation response in GREB does not plateau but decreases steadily in all three centuries.

With the strong decrease in precipitation through circulation variability and none of the sensitivity experiments having an equal increase in precipitation the fully forced GREB model fails to reproduce the precipitation reversal seen in CMIP5. The fully forced GREB model strongly overestimates precipitation reductions in the southern hemisphere subtropics when compared to CMIP5 (i.e. precipitation reduction over Australia and Pacific). However, the GREB model is capable of reproducing the precipitation reversal in a single CMIP5 model (e.g. CSIRO-Mk3.6.0 see Fig. C1). Although the GREB model is overestimating the precipitation response compared to the CMIP5 model it generally follows the precipitation trend.

It was shown in chapter 4 that when the GREB precipitation model is fitted against CMIP5 models mean circulation changes are far more important while the circulation variability becomes less important. Considering that the mean circulation lead to an increase in precipitation (and more important for CMIP5 fitted) while the circulation variability had the largest reduction (and is less important for CMIP5 fitted) it is only reasonable to test the same deconstruction again with CMIP5 fitted parameters.

It was found that using the CMIP5 set of precipitation parameters does lead to less sensitivity to circulation variability changes and thus less precipitation reduction for the negative response of ω_{std}. Additionally, more precipitation is caused through the mean circulation than for the observed precipitation parameter set. With the CMIP5 parameter precipitation in the fully forced GREB model plateaus in the twenty third century instead of decreasing even further. However, those changes are not enough for the GREB model to reproduce the reversal in precipitation, but they are a step towards the right direction.

There could be several reasons why the GREB model is failing to reproduce the reversal of the precipitation trend in the southern hemisphere subtropics. Our analysis

was highly limited by the amount of model output available. In particular only three models had a daily output frequency of ω which is needed to create the ω_{std} boundary condition. Thus, only three models contributed to the ω_{std} boundary condition, while nine models contributed to the other three boundary conditions. Additionally, of the three models that have ω_{std} only two show a reversal, while one has not much precipitation response at all. In future work it might be interesting to limit this deconstruction to the three models writing all output necessary or even deconstruct the two models that show a reversal in the first place.

Nonetheless, the outcome of this study shows highly interesting results. This research nicely combined all three previous chapters and indicates that much more research needs to be done into the reversal of precipitation. Specifically, it needs to be considered that CGCMs are much more sensitive to mean circulation changes than observations justify. The role of the precipitation sensitivity of CMIP5 models to the mean circulation needs to be explored in more detail as the results of this chapter suggest that this could be a feature only seen in climate models and not necessarily in the real world.

Chapter 6

Conclusions

6.1 Thesis Summary

The hydrological cycle is one of the most important features of the Earth's climate system and influences the climate in many ways. Accordingly, in order to understand how the climate may change into the future, a thorough understanding of the hydrological cycle is required. One topic that deserves urgent and systematic attention is the response of the hydrological cycle (specifically precipitation) to climate change. Precipitation projections are one of the most important considerations under climate change as any change in rainfall may have a major impact on humanity. Despite its importance, there is little consensus on the observed or expected changes in spatial patterns of mean precipitation due to climate change. This is not surprising considering the high spatial and temporal variability of precipitation and given the relatively short observational record of reliable global precipitation observations of not much more than 40 years (e.g. GPCP starting in 1979).

Therefore global water cycle with all its sub processes (evaporation, rainfall, etc.) remains one of the least understood natural cycles. This leads to uncertainty in predicting changes in the hydrological cycle associated with climate change. To reduce these uncertainties, we must build the best models we can. Both a substantial increase in climate model resolution and, as this thesis argues, a more conceptual understanding of

the hydrological cycle is needed to identify where uncertainties lie.

To tackle these uncertainties this thesis aimed to address three key questions:

1. Can we simulate the large-scale features of the hydrological cycle on a monthly time scale (evaporation, advection and rainfall) in a simplified model (GREB) with a similar skill like CGCMs?

2. How do the climate boundary conditions (temperature, evaporation, mean circulation and circulation variability) for precipitation change with climate change and can we quantify their role in changing precipitation?

3. What processes cause large uncertainties in precipitation in CMIP5 simulations?

We will summarise our findings regarding each of those key questions in the sections below.

6.1.1 Hydrological Cycle Model Development

Starting from a rudimentary hydrological cycle introduced in chapter 1, in chapter 2 the hydrological cycle model as part of the Globally Resolved Energy Balance (GREB) model was developed. Three new models were introduced simulating: precipitation, evaporation and the horizontal transport of water vapour in the atmosphere.

The new precipitation model is based on the dynamically simulated specific humidity and relative humidity in GREB and the two prescribed boundary conditions of mean vertical velocity and daily vertical velocity variability. The evaporation bulk formula in GREB is slightly refined by considering differences in sensitivity to winds over ocean and land and by improving the estimate of wind magnitudes. A new parametrisation based on vertical winds was introduced to simulate the horizontal convergence and divergence of moisture transport and all new parametrisation were fitted against observations (GPCP) and reanalysis data sets (ERA-Interim). To validate the model three sensitivity experiments were performed: the simulation of the annual cycle, El Nino-Southern-Oscillation and climate change and it was found that the new hydrological cycle model performed with skill comparable to more complex CMIP5 models.

With the improved hydrological cycle the GREB model is now a useful tool. The GREB model can be applied to study the response of the climate system to external

forcings such as climate change but also to understand inter-model differences and can generally be applied to get a more conceptual understanding of the climate system.

6.1.2 Conceptual Deconstruction of the Simulated Precipitation Response to Climate Change

In the next chapter, chapter 3, the new GREB model was applied to gain a more conceptual understanding of the hydrological cycle under climate change. Current CMIP5 climate change projections suggest a fairly complex pattern of precipitation changes with strong regional differences. Due to the complex nature of CGCM simulations understanding what drives these changes is difficult. Although many studies exist highlighting the radiative constraint on global precipitation, these studies fail to explain the regional differences. Probably the most famous approach in explaining the regional differences is the wet-get-wetter idea relating an enhanced moisture transport in a warmer atmosphere to an amplified precipitation response. However, this approach is fails to consider circulation changes.

Given the mass balance of water, local changes in precipitation result from changes in humidity, horizontal transport of water vapour, evaporation or the processes the control precipitation. Thus, four important forcings for precipitation were isolated:

1. Changes in surface temperature which control the amount of water vapour the atmosphere can hold and therefore the amount of water vapour transported by the mean winds, and relative humidity which directly influences precipitation,

2. Changes in evaporation, which are the only of the four forcings to control global mean changes.

3. Mean circulation changes, which affect the precipitation directly through regional differences in ascending and descending air masses and indirectly through the transport of water vapour in the atmosphere.

4. Regional circulation variability changes, which influence the precipitation in GREB directly.

Using the simple climate model developed in chapter 2, the precipitation response was presented as the result of the four forcings highlighted above and it was found that the

CMIP5 precipitation response can be considered as a linear superposition of these four forcings. The precipitation response in GREB due to the surface temperature forcing showed an intensification of the control precipitation through an enhanced moisture transport. This follows the wet-get-wetter principle.

The evaporation forcing led to a direct local response in GREB precipitation. Evaporation is the only forcing that can control the global mean response and is only increasing by about 2% per degree of global warming exactly balancing the precipitation response. While globally evaporation and precipitation changes have to balance each other, it remains unclear which of the two controls the other. Therefore, any future studies should focus more on understanding evaporation changes.

It was found that the mean circulation changes affect precipitation in two ways, by changing the transport of water vapour in the atmosphere and through altering precipitation directly. The change in mean circulation was the single most important forcing of the four forcings discussed.

The circulation variability simulates the effect of weather variability in the GREB model. A general decrease of circulation variability in the subtropics was found that subsequently leads to a decrease in precipitation and accumulation of water vapour in the atmosphere thus modifying moisture transport. This enhanced moisture transport supplies the moisture needed to sustain precipitation changes, especially the increase of precipitation and circulation variability in the tropical Pacific. The response of circulation variability and its effect on mean precipitation has not been discussed much in the literature. However, areas of strongest evaporation (i.e. subtropics) match areas that experience a strong decline in weather variability. It is reasonable to assume that evaporation and weather variability are interlinked and that a decrease in weather variability affects evaporation. This connection between evaporation and and weather variability may be important to understand large-scale precipitation and evaporation changes.

6.1.3 Precipitation Biases in CMIP5 models

The aim of this chapter was to investigate what processes cause large scale uncertainties in CMIP5 precipitation. Initially biases in precipitation are split into two different origins: biases in the precipitation parametrisation itself and biases in the boundary conditions driving precipitation. Firstly, the uncertainties in the precipitation parameters themselves

it was found that CMIP5 models are too sensitive to mean vertical velocity and not sensitive enough to vertical velocity variability. The overestimated sensitivity to the mean vertical velocity has also been highlighted by other studies (i.e. Yang et al., 2018) but for the reduced sensitivity of circulation variability no references in the literature were found. However, the reduced sensitivity to weather variability could be related to the common bias in CMIP5 models to precipitate too lightly too often (e.g. Dai, 2006; Stephens et al., 2010)

Quantitatively the contribution of the parameter uncertainties was small when compared to biases in climate variables driving precipitation. Biases in mean vertical velocity were the dominant factor in the total precipitation bias, affecting the precipitation equation directly and the moisture transport in the GREB model. To separate the effects of ω_{mean} on the precipitation parametrisation and the moisture transport a new convergence/divergence parametrisation was introduced that relies on the horizontal winds.

Using the new convergence parametrisation, it was found that the moisture transport biases play an important role in the total precipitation bias in CMIP5 models. Some shortcomings of this chapter have been discussed but, it was shown how the GREB model can be used as a helpful tool to analyse biases in CMIP5 precipitation. Pathways have been highlighted, of how future work can build on these findings and were it can improve this research.

6.1.4   Southern Hemisphere Precipitation Reversal

This chapter is based on the southern hemisphere precipitation trend reversal shown by Sniderman et al. (2019). Geological records of previous warmer-than-present climates show a wetter rather than drier subtropics. This contradicts the wet-get-wetter hypothesis. Sniderman et al. (2019) showed that this drying trend seen in CMIP5 models might only be a transient rather than equilibrium response in climate models.

In this chapter the results of all three previous chapters were combined. That is the new hydrological cycle model developed in chapter 2 was used, the deconstruction method of chapter 3 was applied and the analysis of chapter 3 was extended for very long CMIP5 simulations. Additionally, the role of biases in the CMIP5 model parametrisations, discussed in chapter 4 were considered.

The southern hemisphere precipitation response for the twenty-first, twenty-second

and twenty-third century is deconstructed into the quantitative contribution of the precipitation boundary conditions of surface temperature, evaporation, mean circulation and circulation variability. The results indicate that only two of the four forcings, namely evaporation and mean circulation, contribute to an increase in southern hemisphere subtropical precipitation in all three centuries. However, the reduction, especially reduced precipitation through circulation variability, dominate the overall precipitation trend. This leads to the GREB model being unable to reproduce the precipitation reversal.

It was then tested what role the precipitation parameters play by replacing the observed precipitation parameter set with the CMIP5 fitted precipitation parameter set. This was a reasonable approach considering that in CMIP5 models the importance of mean circulation on precipitation is overestimated and the sensitivity to circulation variability underestimated. Thus, in CMIP5 models the increase of precipitation through mean circulation would be overstated while the reductions of precipitation by circulation variability underestimated. Replacing the set of observed parameters to the CMIP5 precipitation parameter set does push the GREB model closer to a precipitation reversal for above hypothesised reasons of different sensitivities in CMIP5 models to mean circulation and circulation variability. However, the change in parameters was not enough for a reversal in the precipitation trend.

Nonetheless the outcome of this chapter has been highly interesting. The results highlight the importance of considering climate model biases and sensitivities to boundary conditions of precipitation (e.g. mean circulation) and indicate that much more research needs to address the precipitation reversal in relation to model biases.

6.2   Future Work

This thesis developed a new hydrological cycle model for the Globally Resolved Energy (GREB) model. The new model was validated in a set of three sensitivity experiments and in the following chapters used to gain a more conceptual understanding of the precipitation response to climate change, for biases in CMIP5 models and the precipitation reversal a trend projected for the southern hemisphere subtropics. But ultimately this thesis developed a new powerful and quick tool to study the hydrological cycle and highlighted some applications of this new tool.

Although many interesting results were found in this research more questions remain. The importance of circulation variability on precipitation changes was highlighted, which in relation to precipitation change has mostly been neglected in the literature. However, what drives this clear pattern of circulation variability was not established in this thesis. Although Weller et al. (2019) found that this response might be related to a decrease in low-level convergence lines. It was hypothesised that the circulation variability might play a role beyond its controls on precipitation and might influence the evaporation response. This could have great impacts on the evaporation response considering that the regions of strong decline in variability match regions with strongest evaporation.

Another surprising result was the clear difference between the GREB precipitation equation when fitted to CMIP5 models rather than observations. The CMIP5 fitted equation showed a heightened sensitivity to the mean circulation and less sensitivity to circulation variability. The overestimated sensitivity to mean circulation has also been found by other studies (i.e. Yang et al., 2018), but the reduced sensitivity to circulation variability has not been discussed previously.

A caveat of the GREB model in this thesis is that important forcings for precipitation (i.e. ω_{mean} and ω_{std}) are prescribed as boundary conditions. This limits the GREB model to be a sophisticated diagnostic tool to analyse the climate rather than being a dynamic model. With forcing ω_{mean}, an important variable in precipitation and precipitation changes, a key part of the response is already given through the forcing. Therefore, the GREB model is unable to make suggestions where biases in ω_{mean} or ω_{std} originate from. Vertical velocity in reanalysis product is poorly constrained. Thus, comparing vertical velocity from reanalysis to CMIP5 models is in essence not much more than comparing the vertical velocity of different climate models to each other. This is most likely an even bigger issue for high-frequency variability of vertical velocity, ω_{std}.

Building on the findings of the previous chapters it was found that the GREB model is unable to reproduce the reversed precipitation trend in the southern hemisphere sub-tropics during the twenty-third century using the observed precipitation parameter set. Only when the CMIP5 parameter set with its increased mean circulation and reduced circulation variability is used the GREB model is somewhat able to show a reversal in the precipitation trend. This indicates that the positive response of rainfall in the southern hemisphere subtropics might only be a response in climate models. Therefore, much

more research should be done to investigate the role of biases in climate models.

Furthermore, the GREB model development is far from finished:

- The evaporation model in GREB is unable to reproduce evaporation changes under global warming in both, magnitude and pattern and needs further development;

- Precipitation in the mid- to high-latitudes in GREB needs further improvement. The GREB model generally does not precipitate enough in the extra-tropics in the control simulation and the response to climate change is too weak when compared to the CMIP5 multi model ensemble mean;

- The negative precipitation issue in GREB could be addressed further to limit negative precipitation in arid areas;

- A dynamic, tropical or global, circulation model as part of the GREB model that is capable of simulating circulation changes with climate change would allow to study the interaction between precipitation (and evaporation) and circulation in more detail. It would also allow the GREB model to react to changes (e.g. warmer surface temperature) more dynamically, rather than having changes in the boundary conditions (e.g. ω_{mean}) prescribed.

- Advancing the Monash Simple Climate Model (Dommenget et al., 2019) to include the new precipitation model and the climate change deconstruction.

Appendix A
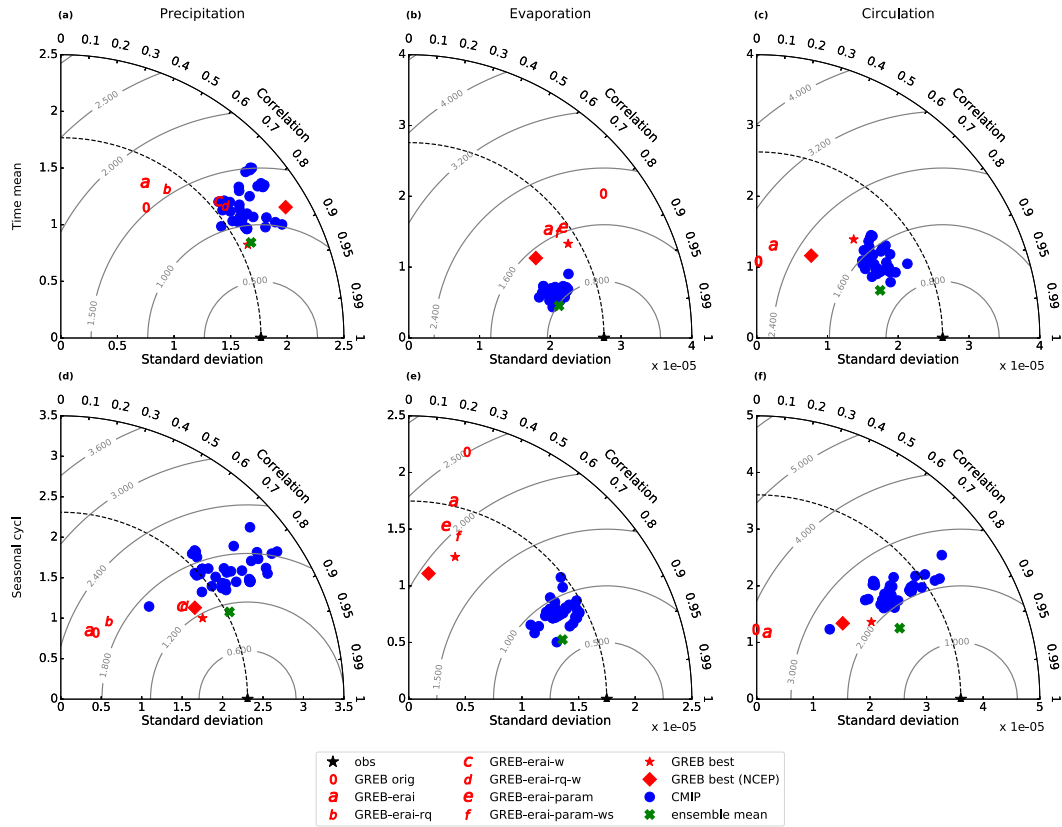
Figure A1: *Precipitation (left column), evaporation (middle column) and circulation (right column) in the annual mean (top row) and seasonal cycle (bottom row) in mm/day in a Taylor diagram against observations from GPCP and ERA-Interim. Red colours indicate different GREB parametrisations with 0 being the original and * the best parametrisation. Blue dots are pi-Control CMIP5 models and the green cross indicates the ensemble mean of all CMIP5 models. * is the best model for the ERA-Interim boundary conditions and diamond uses the NCEP boundary conditions. Blue dots are CMIP5 models and the green cross indicates the ensemble mean of all CMIP5 models.*

Appendix B
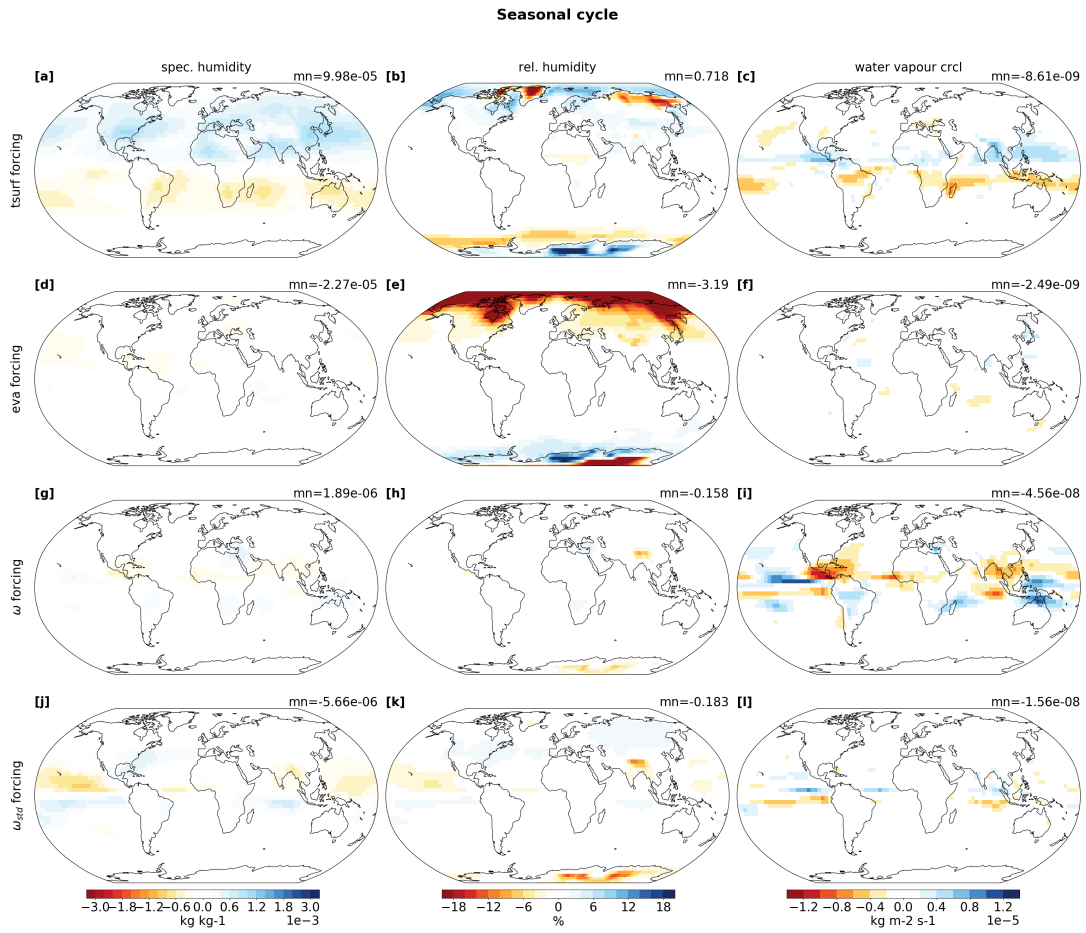
Figure B1: *Seasonal cycle (JJA-DJF) response of the specific humidity (a, d, g, j, m), relative humidity (d, e, h, k, n) and water vapour transport (c, f, i, l, o) for the fully forced GREB model (a-c), the single RCP8.5 forcings of surface temperature (d-f), evaporation (g-i), mean circulation ω_{mean} (j-l) and the daily circulation variability ω_{std} (m-o).The top right of each plot shows the global mean value.*

Appendix C
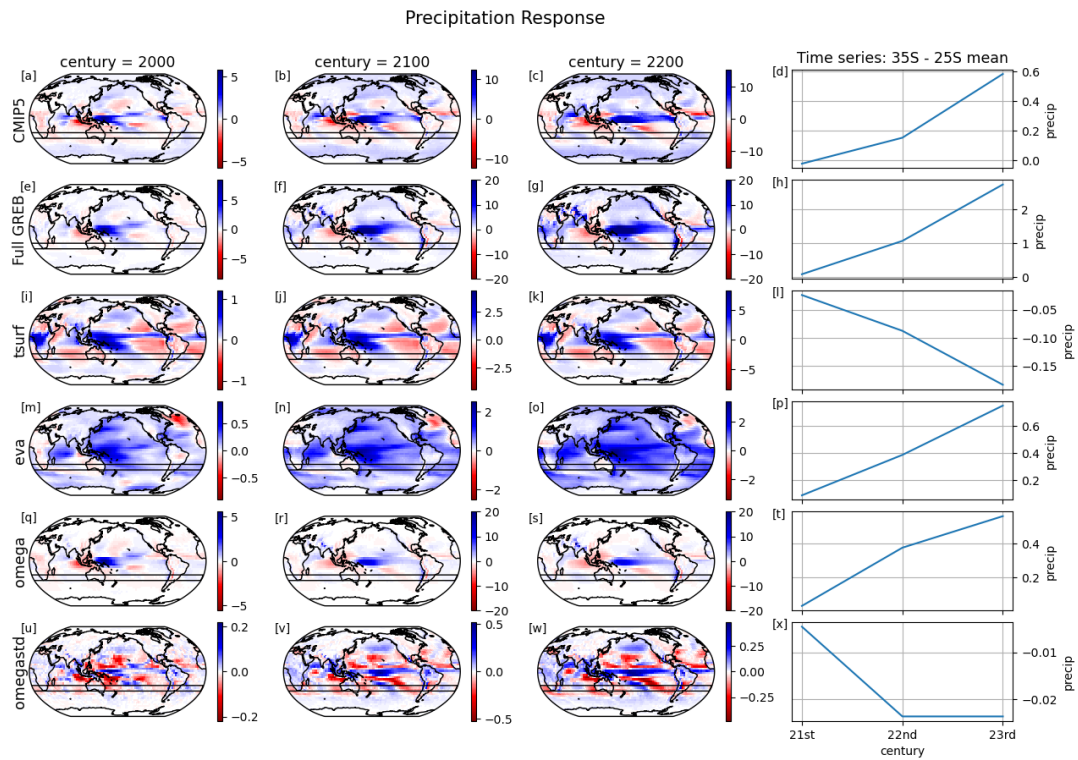
Figure C1: *Precipitation response decomposition in mm/day for the fully forced and the single RCP8.5 forcings of surface temperature, evaporation, mean circulation and the daily circulation variability for the CSIRO-Mk3.6.0 model. The right panel shows the mean values for the southern hemisphere subtropics for each century.*

Bibliography

Allen, M. R. and Ingram, W. J.: Constraints on future changes in climate and the hydrologic cycle, Nature, 419, 224–+, https://doi.org/10.1038/nature01092, URL <GotoISI>://WOS:000177931200052, 2002.

Anderson, R. J. and Smith, S. D.: Evaporation coefficient for the sea surface from eddy flux measurements, Journal of Geophysical Research, 86, 449–456, 1981.

Arrhenius, S.: On the influence of carbonic acid in the air upon the temperature of the ground, The London, Edinburgh, and Dublin Philosophical Magazine and Journal of Science, 41, 237–276, 1896.

Ban, N., Schmidli, J., and Schar, C.: Heavy precipitation in a changing climate: Does short-term summer precipitation increase faster?, Geophysical Research Letters, 42, 1165–1172, https://doi.org/10.1002/2014gl062588, URL <GotoISI>://WOS:000351851900026, 2015.

Bengtsson, L., Hodges, K. I., and Roeckner, E.: Storm tracks and climate change, Journal of Climate, 19, 3518–3543, https://doi.org/Doi10.1175/Jcli3815.1, URL <GotoISI>://WOS:000239943100003, 2006.

Birch, C. E., Marsham, J. H., Parker, D. J., and Taylor, C. M.: The scale dependence and structure of convergence fields preceding the initiation of deep convection, Geophysical Research Letters, 41, 4769–4776, https://doi.org/10.1002/2014gl060493, URL <GotoISI>://WOS:000340295300046, 2014.

Bony, S., Colman, R., Kattsov, V. M., Allan, R. P., Bretherton, C. S., L., D. J., Hall, A., Hallegate, S., M., H. M., Ingram, W., Randall, D. A., Soden, B. J., Tseliodis, G.,

and Webb, M. J.: How well do we understand and evaluate climate change feedback processes?, Journal of Climate, 19, 3445–3482, 2006.

Bosilovich, M. G., Robertson, F. R., and Chen, J.: Global energy and water budgets in MERRA, Journal of Climate, 24, 5721–5739, 2011.

Bretherton, C. S., Peters, M. E., and Back, L. E.: Relationships between water vapor path and precipitation over the tropical oceans, Journal of Climate, 17, 1517–1528, https://doi.org/Doi10.1175/1520-0442(2004)017⟨1517:Rbwvpa⟩2.0.Co;2, URL `<GotoISI>://WOS:000220609700007`, 2004.

Budyko, M. I.: Future Climate, Transactions-American Geophysical Union, 53, 868–&, https://doi.org/DOI10.1029/EO053i010p00868, URL `<GotoISI>://WOS:A1972N792400002`, 1972.

Byrne, M. P. and O'Gorman, P. A.: The Response of Precipitation Minus Evapotranspiration to Climate Warming: Why the "Wet-Get-Wetter, Dry-Get-Drier" Scaling Does Not Hold over Land, Journal of Climate, 28, 8078–8092, https://doi.org/10.1175/Jcli-D-15-0369.1, URL `<GotoISI>://WOS:000362661800011`, 2015.

Chadwick, R., Boutle, I., and Martin, G.: Spatial Patterns of Precipitation Change in CMIP5: Why the Rich Do Not Get Richer in the Tropics, Journal of Climate, 26, 3803–3822, https://doi.org/10.1175/jcli-d-12-00543.1, 2013.

Chadwick, R., Good, P., and Willett, K.: A Simple Moisture Advection Model of Specific Humidity Change over Land in Response to SST Warming, Journal of Climate, 29, 7613–7632, https://doi.org/10.1175/Jcli-D-16-0241.1, URL `<GotoISI>://WOS:000386205900004`, 2016.

Chahine, M. T.: The Hydrological Cycle and Its Influence on Climate, Nature, 359, 373–380, https://doi.org/DOI10.1038/359373a0, URL `<GotoISI>://WOS:A1992JQ62400044`, 1992.

Chen, B. Y.: Global water vapor variability and trend from the latest 36year (1979 to 2014) data of ECMWF and NCEP reanalyses, radiosonde, GPS, and microwave satellite, Journal of Geophysical Research-Atmospheres, 121,

11 442–11 462, https://doi.org/10.1002/2016jd024917, URL `<GotoISI>://WOS:000386976100039`, 2016.

Chou, C. and Neelin, J. D.: Mechanisms of global warming impacts on regional tropical precipitation, Journal of Climate, 17, 2688–2701, https://doi.org/Doi10.1175/1520-0442(2004)017⟨2688:Mogwio⟩2.0.Co;2, URL `<GotoISI>://WOS:000222703800014`, 2004.

Chou, C., Neelin, J. D., Chen, C. A., and Tu, J. Y.: Evaluating the "Rich-Get-Richer" Mechanism in Tropical Precipitation Change under Global Warming, Journal of Climate, 22, 1982–2005, https://doi.org/10.1175/2008jcli2471.1, URL `<GotoISI>://WOS:000266002800007`, 2009.

Collins, M., Booth, B. B., Harris, G. R., Murphy, J. M., Sexton, D. M., and Webb, M. J.: Towards quantifying uncertainty in transient climate change, Climate Dynamics, 27, 127–147, 2006.

Collins, M., Knutti, R., Arblaster, J., Dufresne, J.-L., Fichefet, T., Friedlingstein, P., Gao, X., Gutowski, W. J., Johns, T., Krinner, G., et al.: Long-term climate change: projections, commitments and irreversibility, Cambridge University Press, pp. 1029–1136, 2013.

Curry, J. A., Schramm, J. L., and Ebert, E. E.: Sea-Ice Albedo Climate Feedback Mechanism, Journal of Climate, 8, 240–247, https://doi.org/Doi10.1175/1520-0442(1995)008⟨0240:Siacfm⟩2.0.Co;2, URL `<GotoISI>://WOS:A1995QQ91500007`, 1995.

Dai, A.: Precipitation characteristics in eighteen coupled climate models, Journal of Climate, 19, 4605–4630, 2006.

Dai, A. G.: Drought under global warming: a review, Wiley Interdisciplinary Reviews-Climate Change, 2, 45–65, https://doi.org/10.1002/wcc.81, URL `<GotoISI>://WOS:000291739500005`, 2011.

Dee, D. P., Uppala, S. M., Simmons, A. J., Berrisford, P., Poli, P., Kobayashi, S., Andrae, U., Balmaseda, M. A., Balsamo, G., Bauer, P., Bechtold, P., Beljaars, A. C. M., van de Berg, L., Bidlot, J., Bormann, N., Delsol, C., Dragani, R., Fuentes, M., Geer, A. J., Haimberger, L., Healy, S. B., Hersbach, H., Holm, E. V., Isaksen, L., Kallberg,

P., Kohler, M., Matricardi, M., McNally, A. P., Monge-Sanz, B. M., Morcrette, J. J., Park, B. K., Peubey, C., de Rosnay, P., Tavolato, C., Thepaut, J. N., and Vitart, F.: The ERA-Interim reanalysis: configuration and performance of the data assimilation system, Quarterly Journal of the Royal Meteorological Society, 137, 553–597, https://doi.org/10.1002/qj.828, URL <GotoISI>://WOS:000290450900001, 2011.

Demory, M. E., Vidale, P. L., Roberts, M. J., Berrisford, P., Strachan, J., Schiemann, R., and Mizielinski, M. S.: The role of horizontal resolution in simulating drivers of the global hydrological cycle, Climate Dynamics, 42, 2201–2225, https://doi.org/10.1007/s00382-013-1924-4, URL <GotoISI>://WOS:000334068100031, 2014.

Doi, T., Vecchi, G. A., Rosati, A. J., and Delworth, T. L.: Biases in the Atlantic ITCZ in Seasonal-Interannual Variations for a Coarse- and a High-Resolution Coupled Climate Model, Journal of Climate, 25, 5494–5511, https://doi.org/10.1175/Jcli-D-11-00360.1, URL <GotoISI>://WOS:000307793900004, 2012.

Dommenget, D.: A simple model perturbed physics study of the simulated climate sensitivity uncertainty and its relation to control climate biases, Climate Dynamics, 46, 427–447, https://doi.org/10.1007/s00382-015-2591-4, URL <GotoISI>://WOS:000370040100028https://link.springer.com/article/10.1007%2Fs00382-015-2591-4, 2016.

Dommenget, D. and Flöter, J.: Conceptual understanding of climate change with a globally resolved energy balance model, Climate Dynamics, 37, 2143–2165, https://doi.org/10.1007/s00382-011-1026-0, URL <GotoISI>://WOS:000297345800002, 2011.

Dommenget, D., Nice, K., Bayr, T., Kasang, D., Stassen, C., and Rezny, M.: The Monash Simple Climate Model experiments (MSCM-DB v1.0): an interactive database of mean climate, climate change, and scenario simulations, Geoscientific Model Development, 12, 2155–2179, https://doi.org/10.5194/gmd-12-2155-2019, URL <GotoISI>://WOS:000470255500001, 2019.

Donat, M. G., Lowry, A. L., Alexander, L. V., O'Gorman, P. A., and Maher, N.: More extreme precipitation in the world's dry and wet regions, Nature Cli-

mate Change, 6, 508–+, https://doi.org/10.1038/Nclimate2941, URL <GotoISI>:
//WOS:000375125200020, 2016.

Feng, X. B., Haines, K., and de Boisseson, E.: Coupling of surface air and sea surface
temperatures in the CERA-20C reanalysis, Quarterly Journal of the Royal Meteoro-
logical Society, 144, 195–207, https://doi.org/10.1002/qj.3194, URL <GotoISI>:
//WOS:000425645200015, 2018.

Haarsma, R. J., Roberts, M. J., Vidale, P. L., Senior, C. A., Bellucci, A., Bao, Q.,
Chang, P., Corti, S., Fuckar, N. S., Guemas, V., von Hardenberg, J., Hazeleger, W.,
Kodama, C., Koenigk, T., Leung, L. R., Lu, J., Luo, J. J., Mao, J. F., Mizielinski,
M. S., Mizuta, R., Nobre, P., Satoh, M., Scoccimarro, E., Semmler, T., Small, J.,
and von Storch, J. S.: High Resolution Model Intercomparison Project (HighResMIP
v1.0) for CMIP6, Geoscientific Model Development, 9, 4185–4208, https://doi.org/
10.5194/gmd-9-4185-2016, URL <GotoISI>://WOS:000388191000002, 2016.

Hawkins, E. and Sutton, R.: The potential to narrow uncertainty in regional climate
predictions., Bulletin of the American Meteorological Society, 90, 2009.

Haywood, A. M., Hill, D. J., Dolan, A. M., Otto-Bliesner, B. L., Bragg, F., Chan,
W. L., Chandler, M. A., Contoux, C., Dowsett, H. J., Jost, A., Kamae, Y., Lohmann,
G., Lunt, D. J., Abe-Ouchi, A., Pickering, S. J., Ramstein, G., Rosenbloom, N. A.,
Salzmann, U., Sohl, L., Stepanek, C., Ueda, H., Yan, Q., and Zhang, Z.: Large-
scale features of Pliocene climate: results from the Pliocene Model Intercomparison
Project, Climate of the Past, 9, 191–209, https://doi.org/10.5194/cp-9-191-2013,
URL <GotoISI>://WOS:000316961900012, 2013.

He, J. and Soden, B. J.: A re-examination of the projected subtropical precipitation
decline, Nature Climate Change, 7, 53–57, https://doi.org/10.1038/nclimate3157,
2016.

Held, I. M. and Soden, B. J.: Robust responses of the hydrological cycle to global
warming, Journal of Climate, 19, 5686–5699, https://doi.org/Doi10.1175/Jcli3990.1,
URL <GotoISI>://WOS:000242163800014, 2006.

James, I. N.: Introduction to circulating atmospheres, Cambridge University Press, 1995.

Kalnay, E., Kanamitsu, M., Kistler, R., Collins, W., Deaven, D., Gandin, L., Iredell, M., Saha, S., White, G., Woollen, J., Zhu, Y., Chelliah, M., Ebisuzaki, W., Higgins, W., Janowiak, J., Mo, K. C., Ropelewski, C., Wang, J., Leetmaa, A., Reynolds, R., Jenne, R., and Joseph, D.: The NCEP/NCAR 40-year reanalysis project, Bulletin of the American Meteorological Society, 77, 437–471, https://doi.org/ Doi10.1175/1520-0477(1996)077⟨0437:Tnyrp⟩2.0.Co;2, URL `<GotoISI>://WOS: A1996UG17600001`, 1996.

Kent, C., Chadwick, R., and Rowell, D. P.: Understanding Uncertainties in Future Projections of Seasonal Tropical Precipitation, Journal of Climate, 28, 4390–4413, https://doi.org/10.1175/Jcli-D-14-00613.1, URL `<GotoISI>://WOS: 000355125900005`, 2015.

Kishore, P., Ratnam, M. V., Namboothiri, S. P., Velicogna, I., Basha, G., Jiang, J. H., Igarashi, K., Rao, S. V. B., and Sivakumar, V.: Global (50 degrees S-50 degrees N) distribution of water vapor observed by COSMIC GPS RO: Comparison with GPS radiosonde, NCEP, ERA-Interim, and JRA-25 reanalysis data sets, Journal of Atmospheric and Solar-Terrestrial Physics, 73, 1849–1860, https://doi.org/ 10.1016/j.jastp.2011.04.017, URL `<GotoISI>://WOS:000294591800028`, 2011.

Knutti, R. and Sedláček, J.: Robustness and uncertainties in the new CMIP5 climate model projections, Nature Climate Change, 3, 369, 2013.

Kramer, R. J. and Soden, B. J.: The Sensitivity of the Hydrological Cycle to Internal Climate Variability versus Anthropogenic Climate Change, Journal of Climate, 29, 3661–3673, https://doi.org/10.1175/Jcli-D-15-0408.1, URL `<GotoISI>: //WOS:000375950400010`, 2016.

Lambert, F. H., Stine, A. R., Krakauer, N. Y., and Chiang, J. C.: How much will precipitation increase with global warming?, EOS, Transactions American Geophysical Union, 89, 193–194, 2008.

Li, J.-L., Lee, W.-L., Waliser, D., Stachnik, J. P., Fetzer, E., Wong, S., and Yue, Q.: Characterizing tropical Pacific water vapor and radiative biases in CMIP5 GCMs: Observation- based analyses and a snow and radiation interaction sensitivity ex-

periment, Journal of Geophysical Research, 119, 10 981–10 995, https://doi.org/ https://doi.org/10.1002/2014JD021924, 2014.

Liu, Z., Mehran, A., Phillips, T. J., and AghaKouchak, A.: Seasonal and regional biases in CMIP5 precipitation simulations, Climate Research, 60, 35–50, https://doi.org/ https://doi.org/10.3354/cr01221, 2014.

Lu, J., Vecchi, G. A., and Reichler, T.: Expansion of the Hadley cell under global warming, Geophysical Research Letters, 34, https://doi.org/10.1029/2006gl028443, URL <GotoISI>://WOS:000245186100001, 2007.

Ma, J., Xie, S. P., and Kosaka, Y.: Mechanisms for Tropical Tropospheric Circulation Change in Response to Global Warming, Journal of Climate, 25, 2979–2994, https://doi.org/10.1175/Jcli-D-11-00048.1, URL <GotoISI>://WOS:000302787300023, 2012.

Manabe, S. and Stouffer, R. J.: Sensitivity of a Global Climate Model to an Increase of Co2 Concentration in the Atmosphere, Journal of Geophysical Research-Oceans, 85, 5529–5554, https://doi.org/DOI10.1029/JC085iC10p05529, URL <GotoISI>://WOS:A1980KM84600008, 1980.

Marotzke, J., Jakob, C., Bony, S., Dirmeyer, P. A., O'Gorman, P. A., Hawkins, E., Perkins-Kirkpatrick, S., Quéré, C. L., Nowicki, S., Paulavets, K., Seneviratne, S. I., Stevens, B., and Tuma, M.: Climate research must sharpen its view, Nature Climate Change, 7, 89–91, https://doi.org/10.1038/nclimate3206, 2017.

Masson, S., Terray, P., Madec, G., Luo, J. J., Yamagata, T., and Takahashi, K.: Impact of intra-daily SST variability on ENSO characteristics in a coupled model, Climate Dynamics, 39, 681–707, https://doi.org/10.1007/s00382-011-1247-2, URL <GotoISI>://WOS:000307271200010, 2012.

Mbengue, C. and Schneider, T.: Storm-Track Shifts under Climate Change: Toward a Mechanistic Understanding Using Baroclinic Mean Available Potential Energy, Journal of the Atmospheric Sciences, 74, 93–110, https://doi.org/10.1175/Jas-D-15-0267.1, URL <GotoISI>://WOS:000392419300006, 2017.

Meehl, G. A. and Stocker, T. F.: Global Climate Projections, Climate Change 2007: The Physical Science Basis, pp. 747–845, URL <GotoISI>://WOS:000292238900012, 2007.

Meehl, G. A., Covey, C., Delworth, T., Latif, M., McAvaney, B., Mitchell, J. F. B., Stouffer, R. J., and Taylor, K. E.: The WCRP CMIP3 multimodel dataset - A new era in climate change research, Bulletin of the American Meteorological Society, 88, 1383–1394, https://doi.org/10.1175/Bams-88-9-1383, URL <GotoISI>://WOS:000250166400004, 2007.

Merlivat, L.: The dependence of bulk evaporation coefficients on air-water interfacial conditions as determined by the isotopic method, Journal of Geophysical Research, 83, 2977–2980, 1978.

Mulholland, D. P., Haines, K., Sparrow, S. N., and Wallom, D.: Climate model forecast biases assessed with a perturbed physics ensemble, Climate Dynamics, 49, 1729–1746, 2017.

Muller, C. J. and O'Gorman, P. A.: An energetic perspective on the regional response of precipitation to climate change, Nature Climate Change, 1, 266–271, https://doi.org/10.1038/Nclimate1169, URL <GotoISI>://WOS:000293853300020, 2011.

Murphy, J. M., Sexton, D. M., Barnett, D. N., Jones, G. S., Webb, M. J., Collins, M., and Stainforth, D. A.: Quantification of modelling uncertainties in a large ensemble of climate change simulations, Nature, 430, 768–772, 2004.

Neelin, J. D., Munnich, M., Su, H., Meyerson, J. E., and Holloway, C. E.: Tropical drying trends in global warming models and observations, Proceedings of the National Academy of Sciences of the United States of America, 103, 6110–6115, https://doi.org/10.1073/pnas.0601798103, URL <GotoISI>://WOS:000236999000011, 2006.

North, G. R., Cahalan, R. F., and Coakley, J. A.: Energy-Balance Climate Models, Reviews of Geophysics, 19, 91–121, https://doi.org/DOI10.1029/RG019i001p00091, URL <GotoISI>://WOS:A1981LQ32500004, 1981.

Pachauri, R. K., Allen, M. R., Barros, V. R., Broome, J., Cramer, W., Christ, R., Church, J. A., Clarke, L., Dahe, Q., Dasgupta, P., et al.: Climate change 2014: synthesis report. Contribution of Working Groups I, II and III to the fifth assessment report of the Intergovernmental Panel on Climate Change, IPCC, 2014.

Parry, M. L., Rosenzweig, C., Iglesias, A., Livermore, M., and Fischer, G.: Effects of climate change on global food production under SRES emissions and socio-economic scenarios, Global Environmental Change-Human and Policy Dimensions, 14, 53–67, https://doi.org/10.1016/j.gloenvcha.2003.10.008, URL <GotoISI>://WOS: 000189135000005, 2004.

Patz, J. A., Campbell-Lendrum, D., Holloway, T., and Foley, J. A.: Impact of regional climate change on human health, Nature, 438, 310–317, https://doi.org/10.1038/nature04188, URL <GotoISI>://WOS:000233300200039, 2005.

Pendergrass, A. G. and Gerber, E. P.: The Rain Is Askew: Two Idealized Models Relating Vertical Velocity and Precipitation Distributions in a Warming World, Journal of Climate, 29, 6445–6462, https://doi.org/10.1175/Jcli-D-16-0097.1, URL <GotoISI>://WOS:000383828300003, 2016.

Pendergrass, A. G. and Hartmann, D. L.: The Atmospheric Energy Constraint on Global-Mean Precipitation Change, Journal of Climate, 27, 757–768, https://doi.org/10.1175/Jcli-D-13-00163.1, URL <GotoISI>://WOS:000329773100016, 2014.

Petoukhov, V., Ganopolski, A., Brovkin, V., Claussen, M., Eliseev, A., Kubatzki, C., and Rahmstorf, S.: CLIMBER-2: a climate system model of intermediate complexity. Part I: model description and performance for present climate, Climate Dynamics, 16, 1–17, 1999.

Petoukhov, V., Claussen, M., Berger, A., Crucifix, M., Eby, M., Eliseev, A. V., Fichefet, T., Ganopolski, A., Goosse, H., Kamenkovich, I., Mokhov, I. I., Montoya, M., Mysak, L. A., Sokolov, A., Stone, P., Wang, Z., and Weaver, A. J.: EMIC Intercomparison Project (EMIP-CO2): comparative analysis of EMIC simulations of climate, and of equilibrium and transient responses to atmospheric CO2 doubling, Climate Dynamics, 25, 363–385, https://doi.org/10.1007/s00382-005-0042-3, URL <GotoISI>://WOS: 000232374400003, 2005.

Randall, D. A., Wood, R. A., Bony, S., Colman, R., Fichefet, T., Fyfe, J., Kattsov, V., Pitman, A., Shukla, J., Srinivasan, J., et al.: 'Climate models and their evaluation' in Climate change 2007: The physical science basis. Contribution of Working Group I to the Fourth Assessment Report of the IPCC (FAR), Cambridge University Press, 2007.

Rapti, A. S.: Spectral optical atmospheric thickness dependence on the specific humidity in the presence of continental and maritime air masses, Atmospheric Research, 78, 13–32, https://doi.org/10.1016/j.atmosres.2005.02.004, URL <GotoISI>://WOS:000233402100002, 2005.

Richter, I. and Xie, S.-P.: Muted precipitation increase in global warming simulations: A surface evaporation perspective, Journal of Geophysical Research, 113, https://doi.org/10.1029/2008jd010561, 2008.

Richter, I., Xie, S.-P., Behera, S. K., Doi, T., and Masumoto, Y.: Equatorial Atlantic variability and its relation to mean state biases in CMIP5, Climate Dynamics, 42, 171–188, 2014.

Richter, I., Doi, T., Chang, P., Zhao, X. U., Kataoka, T., Tozuka, T., Nagura, M., Oettli, P., and de Szoeke, S. P.: An overview of coupled GCM biases in the tropics, World Scientific, pp. 213–263, 2016.

Roderick, M. L., Sun, F., Lim, W. H., and Farquhar, G. D.: A general framework for understanding the response of the water cycle to global warming over land and ocean, Hydrology and Earth System Sciences, 18, 1575–1589, https://doi.org/10.5194/hess-18-1575-2014, URL <GotoISI>://WOS:000337949000003, 2014.

Sanderson, B. M., Knutti, R., Aina, T., Christensen, C., Faull, N., Frame, D., Ingram, W., Piani, C., Stainforth, D. A., Stone, D., et al.: Constraints on model response to greenhouse gas forcing and the role of subgrid-scale processes, Journal of Climate, 21, 2, 2008a.

Sanderson, B. M., Piani, C., Ingram, W., Stone, D., and Allen, M.: Towards constraining climate sensitivity by linear analysis of feedback patterns in thousands of perturbed-physics GCM simulations, Climate Dynamics, 30, 175–190, 2008b.

Sato, T., Miura, H., Satoh, M., Takayabu, Y. N., and Wang, Y. Q.: Diurnal Cycle of Precipitation in the Tropics Simulated in a Global Cloud-Resolving Model, Journal of Climate, 22, 4809–4826, https://doi.org/10.1175/2009jcli2890.1, URL <GotoISI>://WOS:000270021000006, 2009.

Seager, R., Naik, N., and Vecchi, G. A.: Thermodynamic and Dynamic Mechanisms for Large-Scale Changes in the Hydrological Cycle in Response to Global Warming, Journal of Climate, 23, 4651–4668, https://doi.org/10.1175/2010jcli3655.1, URL <GotoISI>://WOS:000281655600013, 2010.

Sellers, W.: A global climatic model based on the energy balance of the earth-atmosphere system., Journal of Applied Meteorology, 8, 392–400, 1969.

Severijns, C. and Hazeleger, W.: Optimizing parameters in an atmospheric general circulation model, Journal of climate, 18, 3527–3535, 2005.

Shaffrey, L. C., Stevens, I., Norton, W. A., Roberts, M. J., Vidale, P. L., Harle, J. D., Jrrar, A., Stevens, D. P., Woodage, M. J., Demory, M. E., Donners, J., Clark, D. B., Clayton, A., Cole, J. W., Wilson, S. S., Connolley, W. M., Davies, T. M., Iwi, A. M., Johns, T. C., King, J. C., New, A. L., Slingo, J. M., Slingo, A., Steenman-Clark, L., and Martin, G. M.: UK HiGEM: The New UK High-Resolution Global Environment Model-Model Description and Basic Evaluation, Journal of Climate, 22, 1861–1896, https://doi.org/10.1175/2008jcli2508.1, URL <GotoISI>://WOS:000266002800001, 2009.

Sniderman, J. M. K., Woodhead, J. D., Hellstrom, J., Jordan, G. J., Drysdale, R. N., Tyler, J. J., and Porch, N.: Pliocene reversal of late Neogene aridification, Proceedings of the National Academy of Sciences of the United States of America, 113, 1999–2004, https://doi.org/10.1073/pnas.1520188113, URL <GotoISI>://WOS:000370620300035, 2016.

Sniderman, J. M. K., Brown, J. R., Woodhead, J. D., King, A. D., Gillett, N. P., Tokarska, K. B., Lorbacher, K., Hellstrom, J., Drysdale, R. N., and Meinshausen, M.: Southern Hemisphere subtropical drying as a transient response to warming, Nature Climate Change, 9, 232, https://doi.org/10.1038/s41558-019-0479-8, URL <GotoISI>://WOS:000469265500022, 2019.

Stainforth, D. A., Aina, T., Christensen, C., Collins, M., Faull, N., Frame, D. J., Kettleborough, J. A., Knight, S., Martin, A., Murphy, J., et al.: Uncertainty in predictions of the climate response to rising levels of greenhouse gases, Nature, 433, 403–406, 2005.

Stanfield, R. E., Jiang, J. H., Dong, X., Xi, B., Su, H., Donner, L., Rotstayn, L., Wu, T., Cole, J., and Shindo, E.: A quantitative assessment of precipitation associated with the ITCZ in the CMIP5 GCM simulations., Climate Dynamics, 47, 1863–1880, https://doi.org/https://doi.org/10.1007/s00382-015-2937-y, 2015.

Stassen, C., Dommenget, D., and Loveday, N.: A hydrological cycle model for the Globally Resolved Energy Balance (GREB) model v1.0, Geoscientific Model Development, 12, 425–440, https://doi.org/10.5194/gmd-12-425-2019, URL <GotoISI>://WOS:000456713900001, 2019.

Stassen, C., Dommenget, D., and Chadwick, R.: Conceptual Deconstruction of the Simulated Precipitation Response to Climate Change, Climate Dynamics, submitted, 2020.

Stephens, G. L. and Ellis, T. D.: Controls of Global-Mean Precipitation Increases in Global Warming GCM Experiments, Journal of Climate, 21, 6141–6155, https://doi.org/10.1175/2008jcli2144.1, 2008.

Stephens, G. L., L'Ecuyer, T., Forbes, R., Gettelmen, A., Golaz, J.-C., Bodas-Salcedo, A., Suzuki, K., Gabriel, P., and Haynes, J.: Dreary state of precipitation in global models, Journal of Geophysical Research: Atmospheres, 115, 2010.

Taylor, K. E., Stouffer, R. J., and Meehl, G. A.: An Overview of Cmip5 and the Experiment Design, Bulletin of the American Meteorological Society, 93, 485–498, https://doi.org/10.1175/Bams-D-11-00094.1, URL <GotoISI>://WOS:000303110900004, 2012.

Trenberth, K. E., Smith, L., Qian, T., Dai, A., and Fasullo, J.: Estimates of the global water budget and its annual cycle using observational and model data, Journal of Hydrometeorology, 8, 758–769, 2007.

Vecchi, G. A. and Soden, B. J.: Global warming and the weakening of the tropical circulation, Journal of Climate, 20, 4316–4340, https://doi.org/10.1175/Jcli4258.1, URL `<GotoISI>://WOS:000249237700002`, 2007.

Vecchi, G. A., Soden, B. J., Wittenberg, A. T., Held, I. M., Leetmaa, A., and Harrison, M. J.: Weakening of tropical Pacific atmospheric circulation due to anthropogenic forcing, Nature, 441, 73–76, https://doi.org/10.1038/nature04744, URL `<GotoISI>://WOS:000237248600034`, 2006.

Wang, Z. and Myask, L. A.: A Simple Coupled Atmosphere–Ocean–Sea Ice–Land Surface Model for Climate and Paleoclimate Studies*, Journal of Climate, 13, 1150–1172, 2000.

Weaver, A. J., Eby, M., Wiebe, E. C., Bitz, C. M., Duffy, P. B., Ewen, T. L., Fanning, A. F., Holland, M. M., MacFayden, A., Matthews, H. D., Meissner, K. J., Saenko, O., Schmittner, A., Wang, H., and Yoshimori, M.: The UVic earth system climate model: Model description, climatology, and applications to past, present and future climates, Atmosphere-Ocean, 39, 361–428, 2001.

Webb, M. J., Lock, A. P., and Lambert, F. H.: Interactions between Hydrological Sensitivity, Radiative Cooling, Stability, and Low-Level Cloud Amount Feedback, Journal of Climate, 31, 1833–1850, https://doi.org/10.1175/Jcli-D-16-0895.1, URL `<GotoISI>://WOS:000427438100009`, 2018.

Weller, E., Jakob, C., and Reeder, M. J.: Understanding the Dynamic Contribution to Future Changes in Tropical Precipitation From Low-Level Convergence Lines, Geophysical Research Letters, 46, 2196–2203, https://doi.org/10.1029/2018gl080813, URL `<GotoISI>://WOS:000461855600033`, 2019.

Wentz, F. J., Ricciardulli, L., Hilburn, K., and Mears, C.: How much more rain will global warming bring?, Science, 317, 233–235, https://doi.org/10.1126/science.1140746, URL `<GotoISI>://WOS:000247968600039`, 2007.

Yang, M. M., Zhang, G. J., and Sun, D. Z.: Precipitation and Moisture in Four Leading CMIP5 Models: Biases across Large-Scale Circulation Regimes and Their Attribution to Dynamic and Thermodynamic Factors, Journal of Climate, 31,

5089–5106, https://doi.org/10.1175/Jcli-D-17-0718.1, URL <GotoISI>://WOS:000437827700008, 2018.

Yin, J. H.: A consistent poleward shift of the storm tracks in simulations of 21st century climate, Geophysical Research Letters, 32, https://doi.org/10.1029/2005gl023684, URL <GotoISI>://WOS:000232110400006, 2005.

Yin, L., Fu, R., Shevliakova, E., and Dickinson, R. E.: How well can CMIP5 simulate precipitation and its controlling processes over tropical South America?, Climate Dynamics, 41, 3127–3143, https://doi.org/https://doi.org/10.1007/s00382-012-1582-y, 2013.

Zappa, G., Ceppi, P., and Shepherd, T. G.: Time-evolving sea-surface warming patterns modulate the climate change response of subtropical precipitation over land, Proceedings of the National Academy of Sciences, 117, 4539–4545, 2020.